WRI INDIA

WORKING PAPER

Geography of hazards in India

Multi-hazard mapping and exposure to inform climate-resilient planning

Sweeta Sumant, Raj Bhagat Palanichamy, Rejeet Mathews, Harsha K., Paramjeet Chawla, and Neha Lal

CONTENTS

Executive summary 2
Introduction 3
Research design and methodology 4
Results and analysis 11
Case studies: States and cities 35
Discussion 38
Conclusion and way forward 39
Appendix A 40
Appendix B 40
Appendix C 48
Appendix D 49
Appendix E 54
Abbreviations 55
Glossary 56
Endnotes 57
References 57
Acknowledgements 62
About the authors 62
About WRI India 62

Working Papers contain preliminary research, analysis, findings, and recommendations. They are circulated to stimulate timely discussion and critical feedback and to influence ongoing debate on emerging issues.

Suggested Citation: Sumant S., R. B. Palanichamy, R. Mathews, H. K, P. Chawla, and N. Lal. 2026. "Geography of hazards in India: Multi-hazard mapping and exposure to inform climate-resilient planning." Working Paper. New Delhi: WRI India. Available online at doi.org/10.46830/wriwp.25.00044

Highlights

- In India, hazard assessments often focus on single hazards and administrative boundaries, limiting their ability to capture regions with multiple hazard occurrences and inform planning decisions.
- This working paper presents a geographic information system-based spatial framework using 14 indicators drawn from datasets across the geophysical, hydrological, meteorological, and environmental categories. The study uses hazard count to identify the number of extreme-class hazards and a multi-hazard screening score by summing harmonised ordinal classes.
- Unique national-level multi-hazard maps are developed for India to assess the country's population, built-up area, and employment exposures.
- The maps identify prominent multi-hazard prone areas along the Himalayan and sub-Himalayan regions; the eastern coast; and certain northeastern, western, and southern coastal regions of India.
- About 90 percent of India's population, built-up areas, and employment lie within hazard zones with very high to extreme rainfall, while over 80 percent are exposed to moderate-to-high heat stress.
- The national-level analysis indicates an uneven multi-hazard occurrence across India. Among the illustrative cases, Tamil Nadu shows a strong overlap of hazard exposure and Madhya Pradesh presents a lower multi-hazard screening score relative to the rest of India.

Executive summary

Background

India's hazard landscape is shaped by co-occurring and seasonally occurring hazards driven by climate variability, geographic diversity, and rapid urbanisation (Roy and Matsagar 2021). Although extreme heat, intense rainfall, flooding, drought, cyclones, landslides, seismic activity, and air pollution affect the same regions simultaneously or seasonally, assessments and planning remain targeted towards individual hazards (Kodandapani 2021; Mohanty 2020).

Therefore, nationally comparable multi-hazard evidence remains limited. Datasets differ in terms of spatial resolution, time periods, and classification. In addition, heat, lightning, groundwater stress, and air pollution are less consistently reflected in planning when compared with earthquakes, cyclones, and floods (Mahato et al. 2025).

A disconnect exists between hazard evidence and planning instruments. National frameworks, such as the National Building Code of India, Urban and Regional Development Plans Formulation and Implementation Guidelines, and Indian Standards Codes, primarily address hazards individually, while many dominant climate-related risks remain only partially recognised or absent (Mahvash Mohammadi and Barakpour 2024; Roy and Matsagar 2021). Consequently, hazard assessments rarely translate into climate-responsive development regulations, actionable zoning, building standards, emergency preparedness, nature-based solutions, or utility infrastructure protection, even in the most vulnerable areas (Intergovernmental Panel on Climate Change 2022; World Bank 2011).

Existing hazard and risk studies in India are largely organised around administrative boundaries such as districts or states, thus masking the cross-boundary impacts and regional risk corridors. India lacks statutory multi-hazard overlays comparable to those used in countries such as Chile, Japan, and the United States, where hazard maps consider impact regions and directly inform land-use regulations and building requirements (Amarnath et al. 2021).

Purpose of the working paper

Given the aforementioned research gaps, this study has two objectives. It develops a foundational national-scale, multi-hazard spatial framework that standardises diverse hazard datasets, identifying the dominant single and multiple hazard occurrences across regions, Furthermore, it quantifies the exposure of the population, built-up areas, and employment within these hazard-prone regions.

About this working paper

The methodology maps the hazard occurrences in India across four broad categories: geophysical, meteorological, hydrological, and environmental. Moreover, it develops multi-hazard overlays to identify regions where two or more hazard types converge and makes available the consolidated hazard-layer dataset. Two complementary summary measures are used: the hazard count, which identifies the number of extreme-class hazards in a region, and the hazard score, which captures the combined screening score across all classes. Then, this study quantifies how much of India's population, built-up areas, and employment fall within different hazard and multi-hazard zones at the national level. Finally, it examines illustrative cases of select states, Tamil Nadu and Madhya Pradesh, and 10 cities to illustrate hazard occurrence across diverse contexts.

Key findings

Multi-hazard overlays reveal several singular and multiple hazard-prone regions. These include the Indian Himalayan–Northeast, Indo-Gangetic and east-central, west–central and peninsular, and eastern coastal regions. The hazard count and screening score reveal different features: some areas contain several of the highest classes, whereas others accumulate moderate-to-high classes across multiple hazards.

Meteorological and hydrological hazards, particularly heat stress, extreme rainfall, drought risk, lightning, and groundwater stress, dominate national exposure. Over 80 percent of the population, built-up areas, and employment fall within the high or very-high heat-stress classes, whereas about 90 percent fall within the very-heavy or extreme-rainfall classes. Geophysical hazards, especially earthquakes and landslides, are spatially concentrated in the Himalayan and Northeast mountain systems and selected hill regions, where exposure is often very high due to terrain and landscape degradation over time. Coastal regions experience a combination of co-occurring hazards driven by cyclones, extreme rainfall, storm-related winds, and low-elevation coastal exposure.

The illustrative cases indicate differentiated hazard systems across states and cities. Tamil Nadu experiences coastal cyclones, extreme rainfall, heat, and groundwater pressure, whereas Madhya Pradesh has a lower cumulative overlap but widespread heat, drought, and rainfall exposure. Among the illustrative cities, Chennai and Greater Mumbai have dominant coastal hydrometeorological exposure; Delhi, Bengaluru, Jodhpur, and Lucknow experience heat-water-rainfall combinations; and Gangtok, Shimla, and Srinagar have seismic, landslide, and rainfall profiles.

The study also identifies employment exposure within these hazard-prone regions, but more detailed local assessment may be warranted. High employment exposure denotes employment locations where heat, flooding, water scarcity, or infrastructure failure can disrupt workers, access, utilities, and business continuity (International Labour Organization 2019).

Way forward and implications

As the way forward, this study highlights the need to strengthen the link between multi-hazard evidence and India's planning and building instruments. While seismic and wind risks are relatively well integrated into India's planning instruments such as building codes, other emerging hazards such as heat stress, lightning, groundwater stress, and co-occurring hazard interactions remain weakly reflected in spatial planning and regulation. Therefore, this study positions itself as a screening-to-action pathway. National agencies can identify hazard combinations underrepresented in the guidance, and states and cities can prioritise regions and infrastructure systems for detailed assessment. Mountain regions require seismic and geotechnical assessment, slope and drainage management, and resilient access corridors; coastal regions require integrated drainage, coastal-ecosystem protection, wind- and cyclone-resistant facilities, and evacuation systems; and inland heat-drought-groundwater regions require heat-health planning, water budgeting, recharge, and reliable services.

This study's findings support the development of geographically differentiated, multi-hazard informed planning guidelines; land-use plans; and building standards and codes as key instruments for translating hazard evidence into long-term development decisions. Additionally, the findings have implications for emergency preparedness, nature-based solutions, utility infrastructure protection, and infrastructure investment. The development of detailed state- or city-specific regulatory frameworks and implementation of roadmaps is beyond the scope of this study.

For long-term operationalisation, the proposed multi-hazard spatial framework can turn a static atlas into a continuously updated database. An open, interactive platform can facilitate screening and decision-making, whereas regulatory and project-level applications should be grounded in locally validated, site-specific evidence.

Intended users and dissemination

This working paper aims to inform multiple entities, such as the Ministry of Housing and Urban Affairs, Bureau of Indian Standards, Building Materials and Technology Promotion Council, National and State Disaster Management Authorities, state urban development departments, development authorities, urban local bodies, and infrastructure agencies. National institutions can use the presented framework to identify recurring hazard combinations that may require improved solutions, guidance, and standards. The paper can also support multiple layers of governance entities in making climate-resilient policy, planning, and investment decisions.

Introduction

Natural, climatic, and environmental hazards are considered the most significant challenges to sustainable urban development (Thomas 2017). Rising temperatures, changing rainfall patterns, sea level rise, and more frequent extreme weather events intensify the existing vulnerabilities and create new risks. The hazard risks, combined with rapid urbanisation, place cities at the centre of a growing convergence between climate risks, biodiversity loss, and socioeconomic disparities (Ahmad and Hassan 2025).

Globally, nearly 90 percent of urban growth in developing countries occurs in regions prone to floods, landslides, heatwaves, and other extreme climate events, often experienced most acutely in unplanned and informal settlements (World Bank 2020). However, urbanisation may reduce or increase vulnerability, depending on the context within which it occurs (Williams et al. 2019). Well-planned urbanisation can reduce risks through land-use control, resilient infrastructure, ecological buffers, and compliance with building standards. A poorly planned expansion can lead to the opposite. Environmental risks are among the most severe global threats (World Economic Forum 2024), and disaster frequency is estimated to rise to a staggering 560 disasters annually by 2030 (United Nations Office for Disaster Risk Reduction [UNDRR] 2022).

India reflects this increasingly complex risk landscape. According to Climate Risk Index 2025 by Germanwatch (Adil et al. 2025), India ranks sixth among the most vulnerable nations, having experienced more than 400 extreme weather events between 1993 and 2022. These disasters reflect the country's current multi-hazard risk profile, ranging from floods, cyclones, and earthquakes to heat waves, droughts, and air pollution (Alam et al. 2022). The human and economic toll is already substantial, and growing urbanisation is likely to deepen the exposure further. From 2024 to 2025, about 3,080 people died in India due to natural disasters, the highest figure in a decade (Ministry of Statistics and Programme Implementation, Government of India 2025). At the regional scale, the Asia-Pacific Disaster Report estimates annual economic losses of about US$675 billion across Asia and the Pacific, underscoring the wider economic burden of disaster risk in the region (United Nations Economics and Social Commission for Asia and the Pacific [ESCAP] 2019).

The number of Indians living in cities is expected to nearly double, from 480 million in 2020 to 951 million in 2050 (World Bank 2025), requiring major infrastructure investment while climate risks increase in severity.

Despite mounting losses to life and continued infrastructural and economic damage, disaster management plans have not kept pace with the scale and diversity of hazard risks and institutional preparedness remains inadequate. In addition, this preparedness is not reflected completely in the policy and planning processes. As of 2019, only 63 percent of districts had District Disaster Management Plans and, of these, only 32 percent of these plans were updated (Mohanty 2020).

India's approach to hazard risk management is guided by a set of national policy and planning instruments, such as the National Building Code of India (NBC),[1] standards set by the Bureau of Indian Standards (BIS),[2] Building Materials and Technology Promotion Council (BMTPC) Vulnerability Atlas of India,[3] disaster management plans,[4] and Urban and Regional Development Plans Formulation and Implementation (URDPFI)[5] guidelines.However, the treatment of these planning instruments of hazards is often fragmented, particularly concerning the complexities of multi-hazard environments in rapidly urbanising regions (G. Jain and Bazaz 2016). Variations in hazard recognition are observed in some risks, such as earthquakes and cyclones, which are well codified (i.e. in the National Building Code of India, 2016); however, other hazards, such as extreme heat, air pollution, lightning, and compound multi-hazard interactions, receive limited or no recognition. This creates inconsistencies in how hazards are integrated into planning and building processes across states and cities.

Multi-hazard assessments face challenges such as the absence of a common framework, data limitations, disciplinary silos, and difficulties in aggregating diverse hazard layers (Kappes et al. 2012; Pourghasemi et al. 2022). At the same time, international experience shows that multi-hazard overlays can inform planning and regulation in countries such as Chile, Japan, and the United States (Herrmann Lunecke 2015; Raduszynski and Numada 2023).

This working paper provides an evidence base for multi-hazard informed planning. It also addresses the mentioned gap by documenting the development of each hazard dataset, including its source link, spatial and temporal resolutions, processing steps, classification rationale, and limitations. It also explains the overlay methods used to generate the multi-hazard outputs while recognising that these do not replace detailed local assessments.

Research design and methodology

This mapping approach aims to identify where hazards occur individually or co-occur and where people, built-up areas, and employment are exposed within hazard-prone geographical regions.

Research question

The study aims to answer the following research questions:

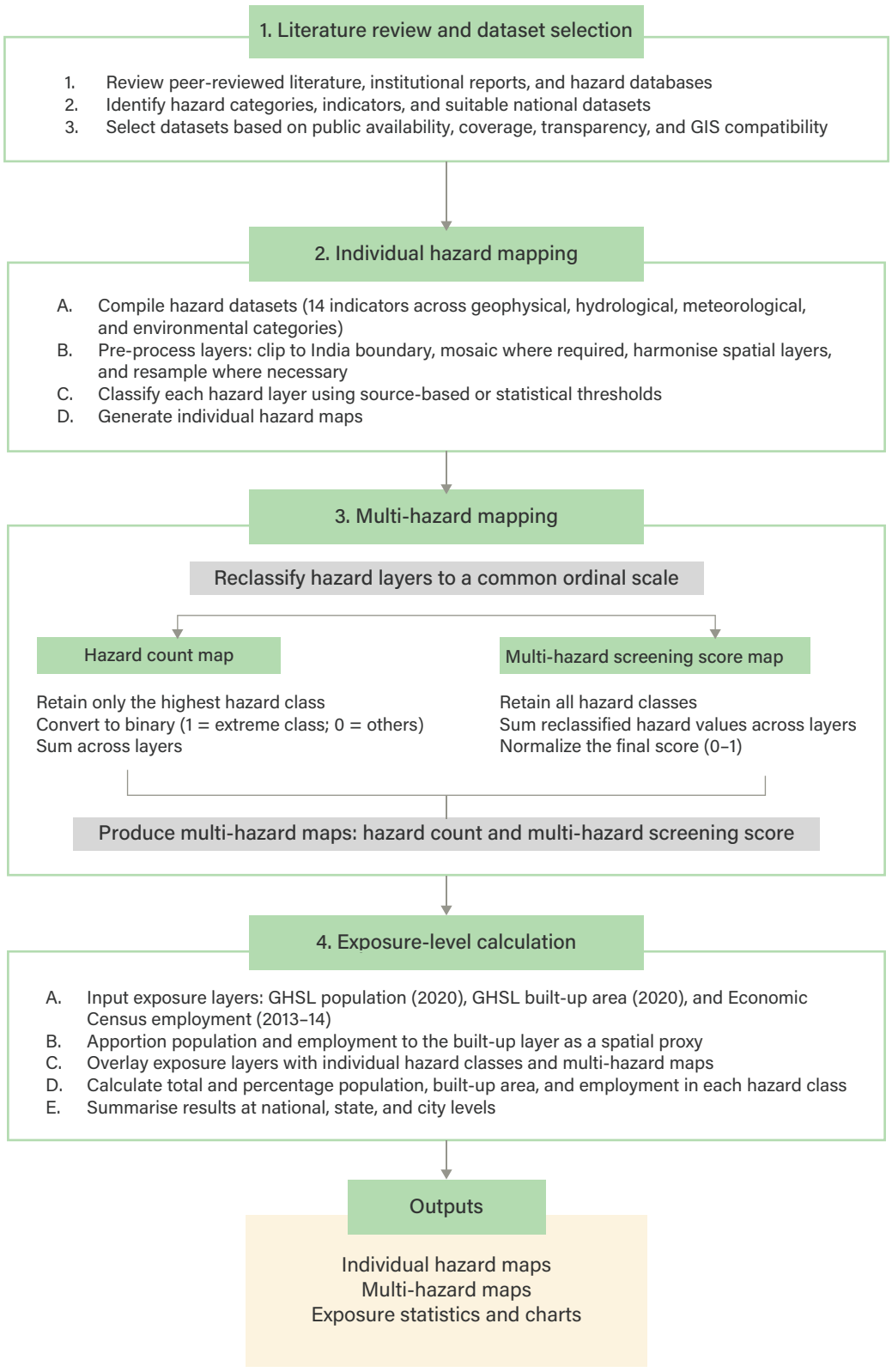
- Which types of hazards (hydrological, geophysical, environmental, or meteorological) dominate across the regions in India?
- Where do two or more extreme hazards coincide spatially, indicating areas of multi-hazard occurrence?
- What proportion of India's population, built-up areas, and employment lie within hazard zones at the national level as well as in selected illustrative cases at the state and city levels?

Research methodology

The following steps were taken to address the research questions (see Figure 1):

- **Literature review and secondary datasets:** The literature review focused on peer-reviewed research, institutional reports, and hazard databases on multi-hazard assessment, spatial overlay, exposure, climate risk, planning, and building instruments. The review followed the thematic, inclusion, and exclusion criteria described in Appendix A.
- **Individual hazard mapping:** The study selected the most appropriate indicators and datasets for national-scale analysis based on public availability, spatial coverage, methodological transparency, and compatibility with geographic information system (GIS) overlays. The details of the indicator selection are presented in Appendix B.
- **Multi-hazard mapping:** Reclassified hazard layers were overlaid to create two outputs: a hazard count showing the overlap of extreme hazard classes and a multi-hazard screening score using all classes.
- **Descriptive statistics of exposure level in hazard-prone zones:** These statistics included a descriptive summary of demographic and economic characteristics of the identified hazard zones.

Figure 1 | **Methodological workflow for individual hazard mapping, multi-hazard mapping, and exposure analysis**



Notes: GIS: geographic information system; GHSL: Global Human Settlement Layer.

Source: Authors' analysis.

Data sources for individual hazard mapping and selection criteria

Indicator selection was based on a review of national hazard and climate-risk frameworks, including the BMTPC Vulnerability Atlas of India, National Disaster Management Plan (NDMP), and India Meteorological Department (IMD) Climate Hazards and Vulnerability Atlas of India (CHVA), as well as recent climate-risk assessments for India (BMTPC 2019; Council on Energy, Environment and Water [CEEW] 2021; Department of Science and Technology et al. 2024; IMD 2021; National Disaster Management Authority [NDMA] 2019). Accordingly, the paper identified earthquakes, floods, cyclones, droughts, extreme rainfall, heat and cold waves, landslides, lightning, and wind-related hazards as nationally relevant concerns. Air pollution and groundwater stress were included because they influence health, settlement-level exposure, and long-term urban resilience.

The datasets were then selected based on four criteria: public availability and open accessibility, adequate spatial resolution for national-scale analysis, methodological transparency and credibility, and compatibility with GIS-based classification and overlay analyses.

Hazards with highly localised, rapidly changing, event-based, or non-comparable datasets, such as industrial and chemical accidents, urban fires, epidemics, fog, hailstorms, and dust storms, were excluded from this national baseline. Glacial lake outburts, floods, and tsunamis were also excluded because the available national data comprise inventories or scenario-specific outputs rather than spatially continuous hazard layers comparable with other indicators (Indian National Centre for Ocean Information Services n.d.; National Remote Sensing Centre 2023). Table 1 presents the 14 hazard indicators across 4 thematic categories: geophysical, hydrological, meteorological, and environmental.

The detailed data, selection rationale, dataset sources, and dataset-specific limitations are provided in Appendix B.

Table 1 | **The 14 hazard indicators across 4 thematic categories: geophysical, hydrological, meteorological, and environmental**

HAZARD CATEGORY	HAZARD	DATA SOURCES	UNIT	TEMPORAL SCALE	SCALE OR RESOLUTION
Geophysical	Seismic zone	Bureau of Indian Standards	No unit	Static map	Regional scale
	Landslide	National Aeronautics and Space Administration (NASA), Global Landslide Susceptibility Map	No unit	Static map	~1 kilometre (km)
	Coastal flooding	Advanced Land Observing Satellite (ALOS) Global Digital Surface Model and ALOS World 3D – 30 metres (m), Alaska Satellite Facility	Metres above mean sea level	Static	30 m
Hydrological	Hydrological Drought	World Resources Institute (WRI) Aqueduct water-risk dataset	No unit	2000–2014	Basin level
	Groundwater stress (stage of groundwater extraction)	Central Ground Water Board, Water Resources Information System (2017, 2020)	Percentage stage of groundwater extraction	2017 and 2020	Block-level administrative data
	Riverine flood	Joint Research Centre and Copernicus Emergency Management Service's Global Flood Awareness System, representing a 100-year return period flood-hazard layer	Metres of modelled inundation depth	Static map	~90 m

Notes: ERA5: ECMWF Reanalysis version 5; HEAT: Human thermal comfort; WRI: World Resources Institute.
Source: Authors' compilation based on the literature review and collation of data sources.

Table 1 | **The 14 hazard indicators across 4 thematic categories: geophysical, hydrological, meteorological, and environmental (cont.)**

HAZARD CATEGORY	HAZARD	DATA SOURCES	UNIT	TEMPORAL SCALE	SCALE OR RESOLUTION
Meteorological	Meteorological drought	Gridded rainfall dataset of the India Meteorological Department (IMD)	No unit	Daily: 1985–2020	0.25°
	Extreme rainfall	IMD (2000–2021)	Millimetre	Daily: 2000–2021	0.25°
	Heat stress	ERA5-HEAT and Universal Thermal Climate Index and European Centre for Medium-Range Weather Forecasts (ECMWF)	No unit	Hourly: 1991–2021	0.25°
	Cold stress	ERA5-HEAT and ECMWF	No unit	Hourly: 1991–2021	0.25°
	Lightning	NASA Global Hydrometeorology Resource Centre's Lightning Imaging Sensor–Optical Transient Detector High Resolution Full Climatology Combined Flash Rate	Flashes per km square per year	Monthly: 1995–2014	0.5°
	Extreme wind	ECMWF ERA5 (2000–2024)	Metres per second	Hourly: 2000–2024	0.25°
	Cyclone	IMD E-Atlas (1891–2020)	Count and number of cyclone-track buffer intersections	1891–2020	National
Environmental	Air quality (particulate matter 2.5)	Atmospheric Composition Analysis Group, Washington University (1998–2022)	Micrograms per cubic meter	Monthly: 1998–2022	~1 km

Notes: ERA5: ECMWF Reanalysis version 5; HEAT: Human thermal comfort; WRI: World Resources Institute.
Source: Authors' compilation based on the literature review and collation of data sources.

Data processing and classification

For each dataset, raw data were first processed and harmonised. The processing steps included clipping, mosaicking as required, and spatial harmonisation to a common analysis grid. Resampling was performed to enable a raster overlay. However, this neither involved statistical or physical downscaling nor added spatial information beyond the native resolution of each source dataset. This was followed by classification as per the hazard categorisation classes provided by the original data sources; statistical breaks were used only where necessary and are documented in Appendix B. Class 5 represents the extreme category defined for each indicator. For all hazards indicated in Table 1, Class 5 represents the highest category for an indicator, rather than an equivalent recurrence probability or physical intensity across all hazards. The classification method and threshold basis for each indicator are presented in Appendix B.

GEOPHYSICAL HAZARDS

- **Seismic zone:** Seismic zone was derived from the BIS seismic zonation map, which classifies India into Zones II–V. Zone II represents the lowest hazard level, and Zone V corresponds to the highest. These zones were adopted according to Indian Standard (IS) 1893 (BIS 2016; BMTPC 2019).
- **Landslide:** Landslide susceptibility data were obtained from the National Aeronautics and Space Administration (NASA) global landslide susceptibility datasets, which is based on terrain and conditioning factors, such as slope, lithology, distance to faults and roads, and forest loss (Stanley and Kirschbaum 2017). The raw raster dataset was clipped to the study area and classified into hazard classes following the classification provided by the original dataset: Class 1 = very low; Class 2 = low; Class 3 = moderate; Class 4 = high; and Class 5 = very high.

- **Coastal flooding:** Coastal flooding was represented using digital elevation data obtained from the Alaska Satellite Facility (digital surface model, 30-metre [m] resolution). Raw elevation data were clipped to coastal states and analysed using an elevation-based approach. Areas lying 0–10 m above the mean sea level were identified as zones potentially susceptible to high sea level rise and storm surges. The highest elevation was taken based on the Odisha Super Cyclone as the most extreme event, which had the highest causality related to storm surge in India. The classes had elevations of <1 m, 1–2 m, 2–5 m, 5–10 m and >10 m based on the histogram.

HYDROLOGICAL HAZARDS

- **Hydrological drought:** Drought hazard was derived from a non-parametric analysis of historical precipitation deficits at the 0.5-degree resolution; drought exposure was based on a non-parametric aggregation of gridded indicators of population and livestock densities, crop cover, and water stress; and drought vulnerability was computed as the arithmetic composite of high-level factors of social, economic, and infrastructural indicators, collected at both the national and sub-national levels. The global data layer was clipped to the Indian boundary and symbolised using the same classes as the original global data (World Resources Institute [WRI] Aqueduct). Hazard risk was categorised (based on the drought score) as 0 (low), 1–2 (low-medium), 2–3 (medium), 3–4 (medium-high), or 4–5 (high).
- **Groundwater stress:** Groundwater stress was assessed using the stage of groundwater extraction data from the Water Resources Information System (WRIS). The stage of groundwater development compares gross groundwater extraction and annual extractable groundwater resources and is expressed as a percentage:

  Stage of groundwater extraction (percent) = [existing gross groundwater extraction (volume) × 100] / annual extractable groundwater resource (volume)

  Classes were determined according to the Central Ground Water Board's (CGWB) groundwater assessment methodology and categorised as safe, semi-critical, critical, over-exploited, and saline.
- **Riverine flood:** Riverine flood hazards were derived from the Global River Flood Hazard Maps v2.1 (2024) of the Joint Research Centre and Copernicus Emergency Management Service's Global Flood Awareness System. These maps represent a 100-year return period flood event. Reanalysis hydrographs of the Global Flood Awareness System and European Flood Awareness System were used as inputs to a two-dimensional hydraulic inundation model, and the simulated maximum flood-depth domains for several return periods were mosaicked into gridded layers. The 100-year layer was clipped to India and classified using a histogram and statistical review. Classes were categorised as 0.1–1 m, 1–2 m, 2–3 m, 3–5 m, and >5 m.

METEOROLOGICAL HAZARDS

- **Meteorological drought:** The IMD 0.25-degree rainfall data for 1985–2020 were used in this study. Annual rainfall was calculated for each pixel and year. The baseline was defined as the mean annual rainfall of 36 years. The deficiency percentage was calculated as follows:

  Deficiency percentage = [(baseline rainfall – annual rainfall) / baseline rainfall] × 100

  Pixels with deficiency percentage of ≥26 percent were treated as drought, following IMD's meteorological-drought definition: drought frequency = drought years / 36. Classes were categorised as 0–0.05, 0.05–0.1, 0.1–0.2, 0.2–0.33, and >0.33 (no unit).
- **Extreme rainfall:** The maximum daily rainfall in each pixel for each year during 2000–21 was calculated to obtain a yearly raster layer representing the maximum daily rainfall within each year. Then, the maximum of the yearly rasters was calculated to obtain the final output, which was visualised using quantum GIS (QGIS). Accordingly, the map shows the maximum annual rainfall for 2000–21. Processing was performed using Python.

  The visualisation categories included extreme rainfall ≥ 204.5 millimetres (mm); very-heavy rainfall = 115.6–204.4 mm; heavy rainfall = 64.5–115.5 mm; moderate rainfall = 15.6–64.4 mm; and light rainfall ≤ 15.5 mm.
- **Heat stress:** Universal Thermal Climate Index (UTCI) data for 1991–2021 were downloaded. The units were converted from Kelvin to degree Celsius. The daily maximum UTCI was calculated. The total number of days with maximum UTCI falling under each heat stress category was then computed and exported as a raster. The total number of days with strong to extreme heat stress was computed.

  The frequency of heat stress was calculated as follows:

  Total number of days with daily maximum UTCI in the specified category / total number of days

  Processing was performed in Python, and the final layer was visualised using QGIS. An equal-interval classification was adopted. The visualisation categories included 0–0.2, 0.2–0.4, 0.4–0.6, 0.6–0.8 and 0.8–1 (no unit)

- **Cold stress:** Daily minimum UTCI was calculated after conversion to degree Celsius. Days with moderate, strong, very strong, and extreme cold stress were counted. Cold-stress frequency was calculated as follows:

  Number of cold-stress days / total number of days.

  The classes were determined based on the frequency of events. The visualisation categories included 0–0.05, 0.05–0.1, 0.1–0.2, 0.2–0.33, and >0.33 (no unit).

- **Lightning:** High Resolution Full Climatology Combined Flash Rate is the product of the Lightning Imaging Sensor–Optical Transient Detector gridded climatology dataset. This yielded the global mean annual flash rate. The raw data were downloaded, processed, and clipped to the Indian boundary. They were classified using an equal-interval classification, and the hazard-risk categories were 0–5, 5–10, 10–15, 15–20, and >20 (flashes/kilometre squared (km^2)/year).

- **Cyclone**: Cyclone incidence was determined using the IMD E-Atlas cyclone files for intensity categories (depression, deep depression, cyclonic storm, and severe cyclonic storm) for 1891–2020. Rasters were geocoded, converted to polylines in Python, cleaned, buffered by 100 kilometres (km), assigned a value of 1, and summed in the Google Earth Engine (GEE) to count the cyclone-track buffers at each location. The classes were 0, 1–3, 3–8, 8–15, and >15 (cyclone counts). Zero incidence was treated as the lowest harmonic class.

- **Extreme wind:** Instantaneous wind gust data from the European Centre for Medium-range Weather Forecasts Reanalysis version 5 was imported into the GEE, and the maximum annual wind speed was calculated and used to represent extreme wind hazard. The resulting raster was then exported for further analysis. Pixels with a frequency greater than 25 percent were treated as data errors and removed.

  Classes were determined on the basis of pretty breaks.

  The hazard categories included ≤20, 20–25, 25–30, 30–35, and 35–50 metres per second.

ENVIRONMENTAL STRESS HAZARD: AIR QUALITY

Air quality was represented using the monthly ground-level concentration estimates of particulate matter with a diameter of 2.5 micrometres or smaller ($PM_{2.5}$) (Atmospheric Composition Analysis Group, Washington University) (Hofste et al. 2019) at 0.01° (~1 km) resolution. For each year, the maximum monthly $PM_{2.5}$ concentration was identified for each pixel; the final layer was the mean of these annual maximum concentrations. Values were concentrations in micrograms per cubic metre, not Air Quality Index scores. Following the US Environmental Protection Agency's 24-hour $PM_{2.5}$ concentration breakpoints, air pollution was classified as good = 0–9.0; moderate = 9.1–35.4; unhealthy for sensitive groups = 35.5–55.4; unhealthy = 55.5–125.4; and very unhealthy = 125.5–225.4, with the unit being micrograms per cubic metre.

Spatial framework for multi-hazard mapping

To identify locations where multiple hazards occur, two multi-hazard maps were developed for the hazard count and multi-hazard screening score.

HAZARD COUNT MAP

This map represents the number of hazard indicators classified into extreme categories that spatially overlap within a given spatial unit. The steps were as follows:

- **Step 1:** From each reclassified hazard raster, only the highest class (Class 5) was retained to identify areas exposed to the most extreme form of each hazard.
- **Step 2:** The reclassified hazard raster were converted into a binary raster, where pixels with a value of 5 were assigned a value of 1 and all other pixels were assigned a value of 0.
- **Step 3:** These binary rasters were then summed pixelwise, using the GEE.
- **Step 4:** The resulting raster represents the number of hazards reaching the extreme class at the same location. Higher values indicate the overlap of a greater number of extreme hazards.
- **Step 5:** In the mapping of 14 individual hazards, the observed hazard count ranged from 0 to 7, where 0 indicated no extreme hazard overlap and 7 indicated an overlap of 7 extreme hazards.

MULTI-HAZARD SCREENING SCORE

The multi-hazard screening score combines all indicator classes according to their classification for spatial comparison but does not imply that the class thresholds are equivalent across indicators. The screening score is calculated using the following steps:

- **Step 1:** Fully reclassified rasters (Classes 1–5) were retained rather than converted into binary layers.
- **Step 2:** The reclassified hazard rasters were summed pixel-wise, using GEE.
- **Step 3:** Each indicator was assigned an equal weight after selection based on national relevance, data availability, transparency, and spatial compatibility. This provided a simple and reproducible screening approach although the

domains with more indicators contributed more to the overall score. The details are included in Appendix C.

- **Step 4:** The resulting value for each pixel represents the cumulative screening score, which captures both the number of hazards present and their relative classes. For example, if a location records Class 2 for landslides, Class 4 for cyclones, and Class 5 for earthquakes, its screening score is 11. Ordinal values were added only after harmonisation: Class 4 was not twice Class 2, and the score did not model physical interaction, cascading effects, timing, vulnerability, or losses (OECD et al. 2008)
- **Step 5:** The observed multi-hazard screening score ranged from 10 to 54. This range was not predefined or normalised; it emerged directly from the sum of the reclassified hazard values across all hazard layers. Thus, 10 represented the lowest observed cumulative screening score in the study area, whereas 54 represented the highest.

MULTI-HAZARD SCREENING SCORE STANDARDISATION

The raw multi-hazard screening score was calculated by summing the reclassified hazard class values across all hazard layers for each pixel. Because the observed raw scores ranged from 10 to 54, the scores were standardised using the minimum-maximum normalisation method to bring all values onto a common 0–1 scale. The standardised multi-hazard screening score was calculated as follows:

$$\textit{Normalised multi-hazard screening score} = \frac{X - X_{\min}}{X_{\max} - X_{\min}}$$

where X is the raw multi-hazard score for each pixel and X_{min} = 10 and X_{max} = 54. A value closer to 0 indicates a lower cumulative screening score, whereas a value closer to 1 indicates a higher cumulative screening score within the observed national range.

MULTI-HAZARD EXPOSURE

To calculate the exposure at the national, state, and city levels, the following steps were taken using the data sources listed in Table 2:

- **Built-up statistics:** The total built-up area within each hazard category was calculated using the Global Human Settlement Layer (GHSL) Built Settlement data for 2020. Processing was performed using GEE.
- **Apportionment of population data (GHSL 2020):** GHS-Population data were calculated at the town and village level based on the Census 2011 boundaries. It was then redistributed (apportioned) geographically into grid cells using the physical distribution of the GHS-Built Settlement layer as a spatial proxy, ensuring that people are assigned to areas where buildings and infrastructure exist rather than spreading them uniformly across empty geographic zones. Analysis was performed using the GEE.
- **Employment exposure estimated using the Sixth Economic Census 2013–14:** The estimation excluded crop production, plantations, public administration, defence, compulsory social security, and several informal or household-based occupations. Therefore, this layer was interpreted as an estimate of employment within built-up areas rather than of total livelihoods (Mathews et al. 2023). First, the total amount of employment in each town or village was divided by the total GHSL built-up area in that town or village to calculate employment per unit of the built-up area. This ratio was then multiplied by the GHSL Built Settlement 2010 pixel value, which represents the amount of built-up area in each grid cell. This produced an estimate of total employment per cell layer. As both the population and employment layers are spatially apportioned using the GHSL built-up area information, they are not fully independent spatial measures and similarities in their exposure patterns may partly reflect this shared spatial proxy.
- **National-level statistics:** The apportioned population layer, GHSL Built Settlement Layer 2020, and apportioned employment layer were imported into GEE along with all the reclassified hazard rasters. Using zonal statistics, the total population, total built-up area, and total employment within each hazard category (1–5) were calculated for each hazard indicator. These values were exported as tables, and percentages were calculated. The percentages represent the proportion of the total population, built-up area, and employment falling within each hazard category (including the extreme hazard category, where applicable), calculated relative to the corresponding national totals. These values were then visualised through stacked bar charts to show how the population, built-up areas, and employment are distributed nationally across different hazard classes.

Table 2 | **Exposure-level calculation**

S. NO.	INDICATOR	METHODOLOGY	SOURCE	PERIOD	SCALE
1	Population	The total population and percentage of population in each hazard zones were calculated.	GHSL[a]	2020	100 metres
2	Built-up	The total built-up area and percentage of built-up area in each hazard zone were calculated.	GHSL[a]	2020	100 metres
3	Employment	The total employment and percentage of employment falling under each hazard category were calculated.	Sixth Economic Census 2013–14[b]	2013–14	State-level

Note: GHSL: Global Human Settlement Layer a. Copernicus n.d., b. Ministry of Statistics and Programme Implementation, Government of India 2019.
Sources: Author's compilation based on literature review and a collation of data sources.

ILLUSTRATIVE CASE STUDY APPROACH

Tamil Nadu and Madhya Pradesh were selected, based on results of the hazard count and multi-hazard score, to examine the differences in hazard composition corresponding with exposure patterns across regional contexts. In addition, 10 cities—Bengaluru, Chennai, Delhi, Gangtok, Jodhpur, Kolkata, Lucknow, Mumbai, Shimla, Srinagar —were selected as illustrative cases across different parts of India to assess how multi-hazard conditions intersect with the concentrations of population, built-up area, and employment. These city cases were chosen to reflect variations in geography, climatic settings, urbanisation patterns, and hazard profiles, and they were used to demonstrate the framework's applicability across diverse spatial contexts.

To define the cities' geographic limits, we used the Contiguously Built Urban Agglomeration (CBUA) boundaries (Sebastian et al. 2026). Within each CBUA boundary, percentages of the built-up area, apportioned population, and apportioned employment corresponding to each hazard class (1–5) were computed using the same zonal statistical approach. Similarly, charts were produced to show the exposure levels.

METHODOLOGY LIMITATIONS AND CAVEATS

The methodology proposed in this study has limitations pertaining to data sources, conceptual and classification comparability of indicators, and spatial and temporal resolution of source datasets. Second, caveats and limitations apply to the multi-hazard screening score in terms of construction, weighting, and normalisation. Moreover, a few contingencies exist pertaining to the framework's scale and intended use, validation against observed disaster impacts, interpretation of spatial co-location and exposure, and selection and use of illustrative state and city cases. Third, there are limitations related to calculation of the screening score. Finally, in this working paper, co-occurrence refers to only different hazard indicators occurring in the same area. Compound or concurrent hazards occur together or through connected drivers; cascading hazards involve one event triggering another hazard or infrastructure failure; and sequential hazards occur when an earlier event changes the vulnerability to a later event (Gill and Malamud 2016; Zscheischler et al. 2018). These distinctions are important because the overlays identify potential combinations for investigation but do not model event dependence, temporal sequencing, or infrastructure failure. These methodological limitations are detailed in Appendix C.

Results and analysis

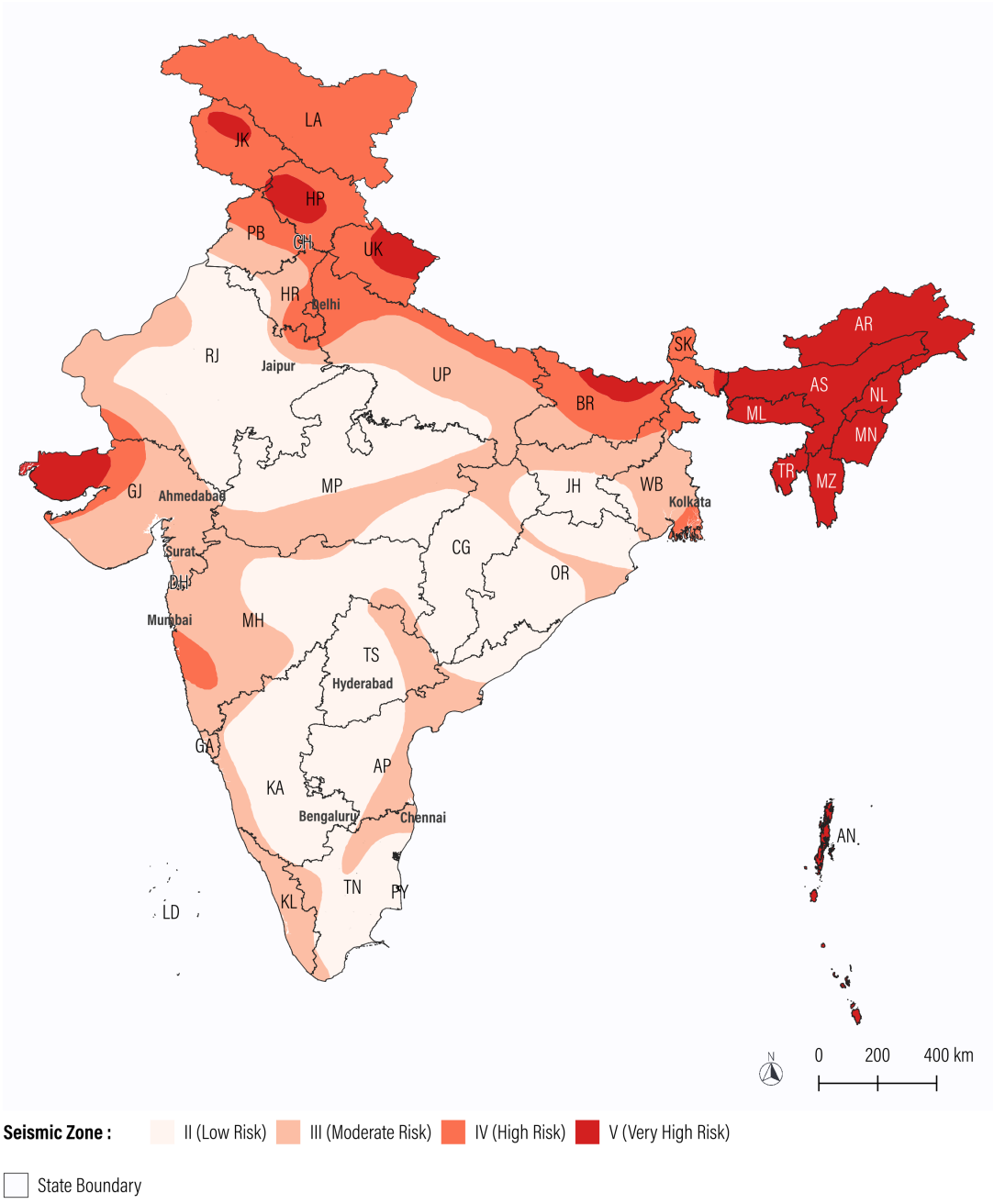
This section first analyses each hazard individually, followed by an explanation of the multi-hazard overlaps. Next, the findings are interpreted in relation to the exposure of the population, settlements, and infrastructure within hazard-prone areas.

Single-hazard occurrences

Many hazard zones in India, such as the Himalayan seismic and landslide belt, are well documented. However, previous research does not always readily provide comparable spatial maps across multiple hazards. Therefore, the mapping exercise in this study contributes by translating diverse hazard datasets into a common GIS-based spatial framework, which allows individual hazards to be compared, overlaid, and interpreted together. Mapped patterns that align with previous studies helped validate the selected datasets' suitability for a national-scale assessment. The harmonised layers provided the basis for developing hazard-count maps, multi-hazard screening score maps, and exposure estimates for the population, built-up areas, and economic activities.

Studies have shown that approximately 0.43 million km^2 (12.6 percent) of India's land area is susceptible to landslides (Singh et al. 2025). Furthermore, a significant proportion of the country, approximately one-fourth, is classified as a flood, landslide, or earthquake zone, underscoring the widespread nature of these geophysical threats (Sarif et al. 2024).

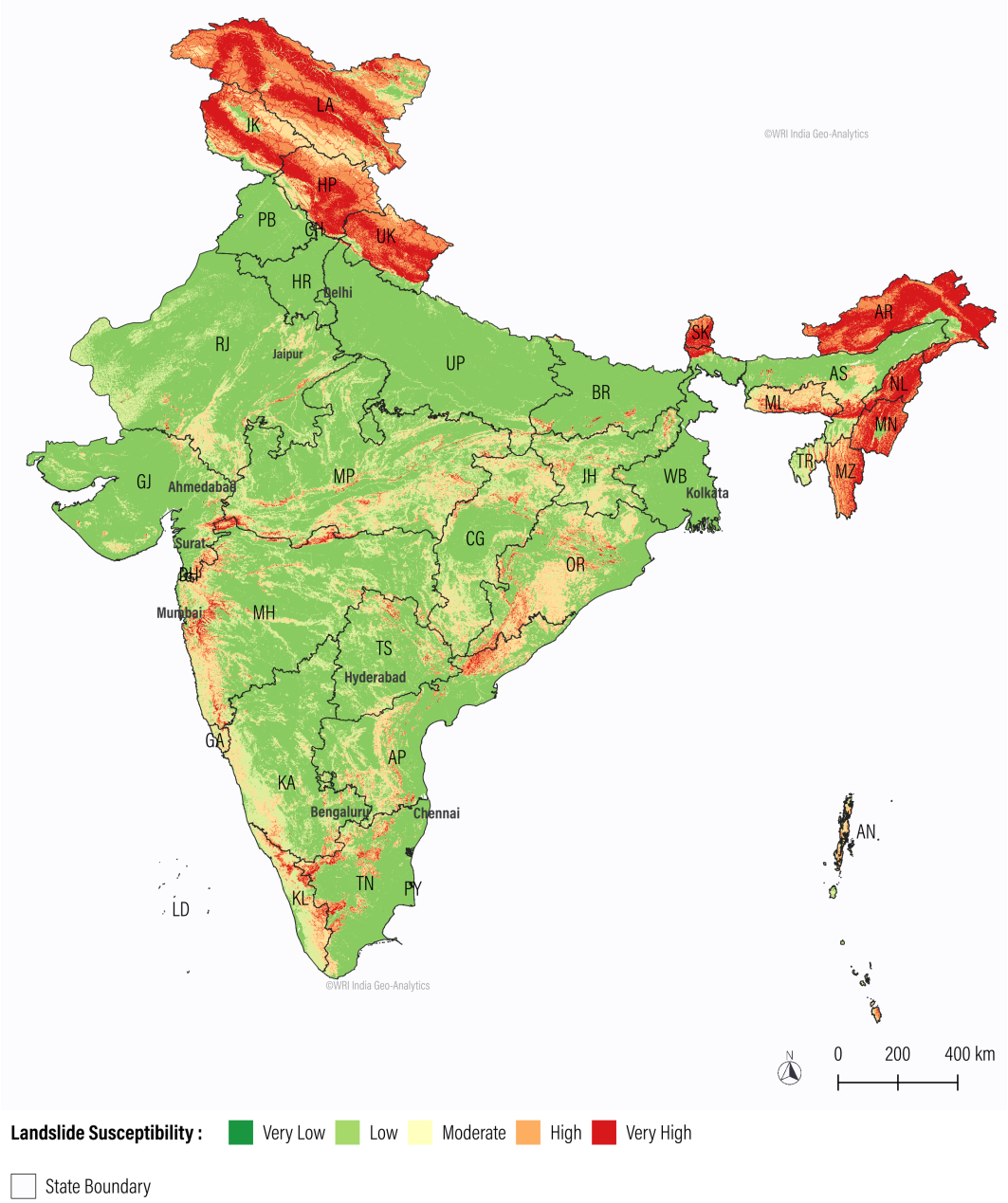
Figure 2 | **Seismic zone**



Source: Processed and visualised by the authors, using the Bureau of Indian Standards seismic zonation map

Disclaimer: This map is for illustrative purpose and does not imply the expression of any opinion on the part of WRI India, concerning legal status of any country or territory or concerning the delimitation of frontiers or boundaries.

Figure 3 | **Landslide**



Source: Processed and visualised by the authors, using the National Aeronautics and Space Administration's Global Landslide Susceptibility Map.

Disclaimer: This map is for illustrative purpose and does not imply the expression of any opinion on the part of WRI India, concerning legal status of any country or territory or concerning the delimitation of frontiers or boundaries.

SEISMIC ZONE

The seismic hazard distribution in India, as delineated by the BIS (IS 1893), reveals clear regional concentration patterns associated with active tectonic settings (Roy and Matsagar 2021). The broader literature points to the Himalayan arc, the northeastern region, and parts of western India as the country's principal zones of seismic risk (Agrawal et al. 2021). The results are consistent with this pattern.

Figure 2 shows the seismic hazards in Zones IV and V, largely along the Himalayan arc and northeastern region, reflecting the active tectonic boundary between the Indian and Eurasian plates. Zone V includes most of the northeastern states—Arunachal Pradesh, Assam, Nagaland, Manipur, Mizoram, Tripura, and Meghalaya—as well as parts of Jammu & Kashmir, Ladakh, Himachal Pradesh, Uttarakhand, northern Bihar, and northern West Bengal. Zone IV (high risk) extends across the Himalayan foothills and the adjoining Indo-Gangetic Plains, covering parts of Punjab, Haryana, Delhi, northern Uttar Pradesh, Bihar, West Bengal, and sections of Gujarat.

LANDSLIDE

Figure 3 shows that severe landslide susceptibility is concentrated in the Himalayan and northeastern hill states, including Jammu & Kashmir, Ladakh, Himachal Pradesh, Uttarakhand, Sikkim, Arunachal Pradesh, Assam (northern and hill regions), Nagaland, Manipur, Mizoram, Meghalaya, and Tripura. Moreover, it is particularly concentrated in parts of western Maharashtra, Goa, coastal and western Karnataka, Kerala, western Tamil Nadu, eastern Odisha, and eastern Andhra Pradesh.

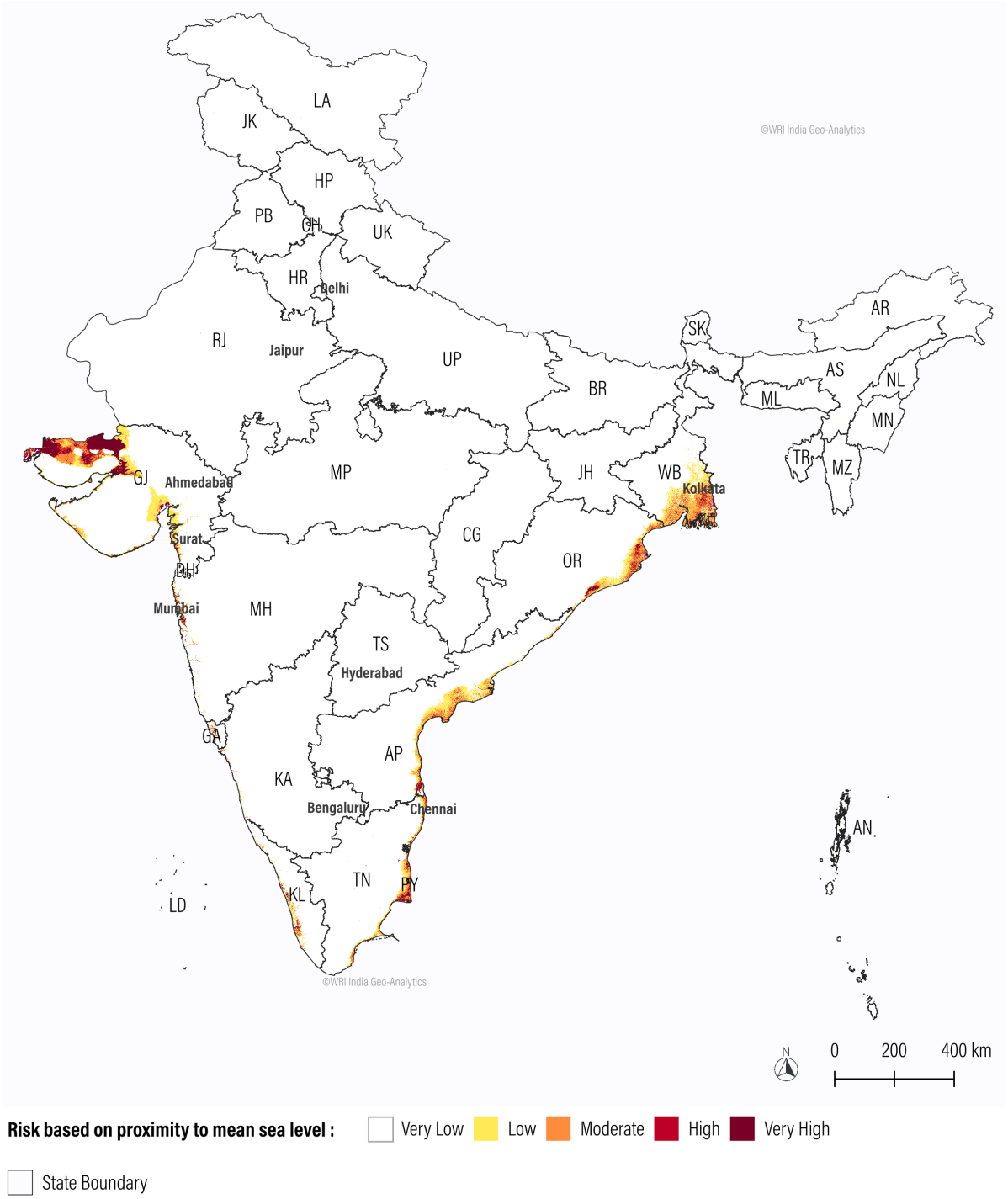
These patterns align with studies linking landslide vulnerability in the Himalayas and the Northeast to steep slopes, fragile geology, and heavy monsoon rainfall (Khan et al. 2025) and in the Western Ghats to slope instability, road construction, mining, and land-use change (Joshi et al. 2025; Khan et al. 2025).

COASTAL FLOODING

Figure 4 shows that low-lying coastal areas, particularly areas below 5 m above the mean sea level, are concentrated along western Gujarat, including the Kachchh and Saurashtra coasts; southern Gujarat; coastal areas of Maharashtra, Goa, Karnataka, Kerala, Tamil Nadu, Andhra Pradesh, and Odisha; and southern and eastern West Bengal, including the Sundarbans. Very low-lying zones also lie in parts of the Andaman and Nicobar Islands.

Previous studies identify India's low-lying coastal zones as highly vulnerable, coinciding with cyclonic activity, storm surges, and sea level rise (Sahoo and Bhaskaran 2018; Santra et al. 2025). Deltaic regions may also be affected by subsidence, sediment dynamics, and repeated cyclonic exposure although these processes are not directly modelled in the elevation dataset.

Figure 4 | **Coastal flooding**



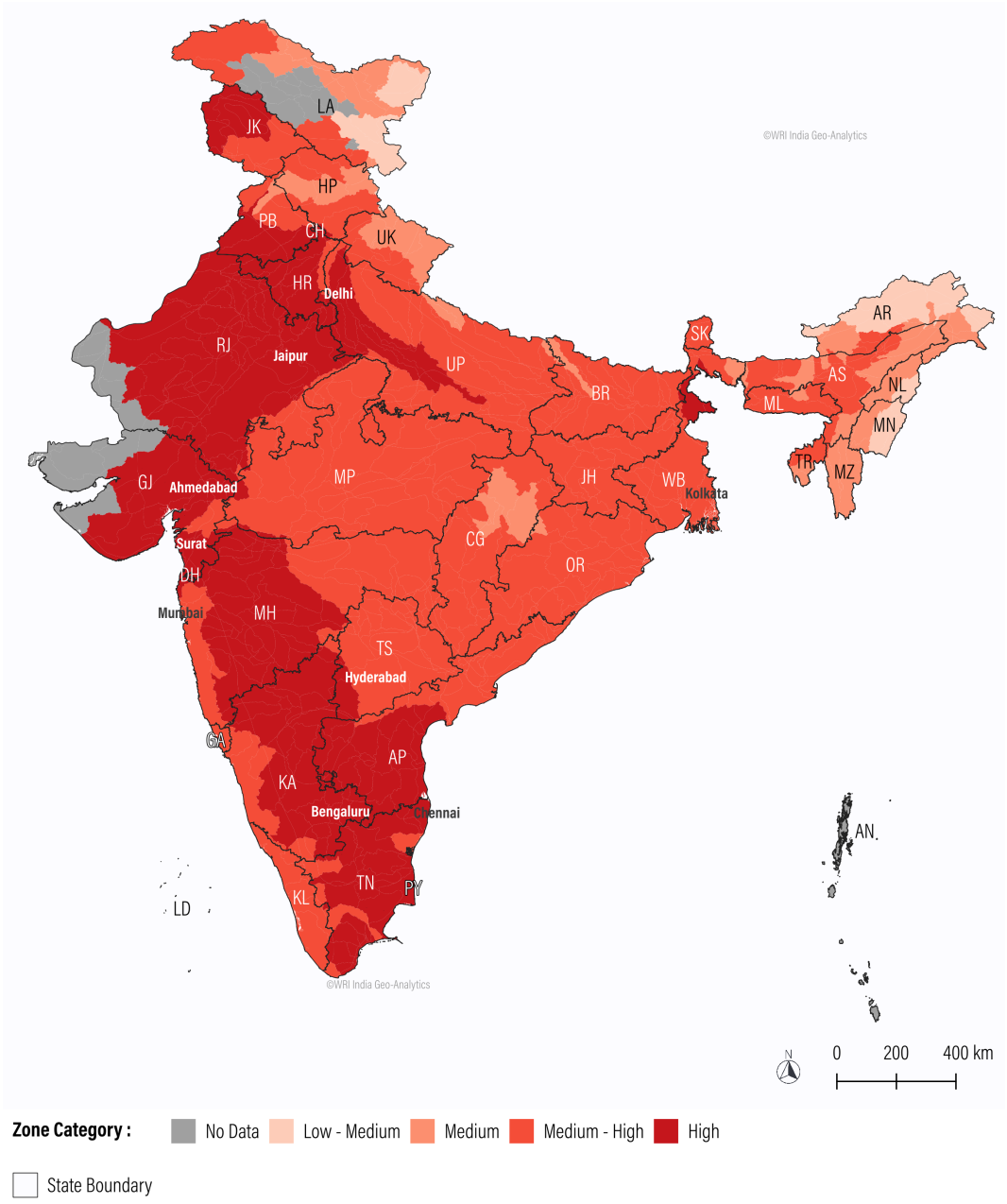
Source: Processed and visualised by the authors using the Advanced Land Observing Satellite Phased Array Type L-Band Synthetic Aperture Radar Digital Surface Model of the Alaska Satellite Facility.

Disclaimer: This map is for illustrative purpose and does not imply the expression of any opinion on the part of WRI India, concerning legal status of any country or territory or concerning the delimitation of frontiers or boundaries.

HYDROLOGICAL HAZARDS

The hydrological hazard layers revealed a complex water-risk landscape shaped by basin hydrology, monsoon variability, and extraction pressure. Existing studies have shown that the Indian eastern coast is particularly susceptible to compound coastal extremes, including concurrent storm surges and rainfall events driven by low-pressure systems originating in the Bay of Bengal during the monsoon and post-monsoon seasons (Dutta et al. 2025).

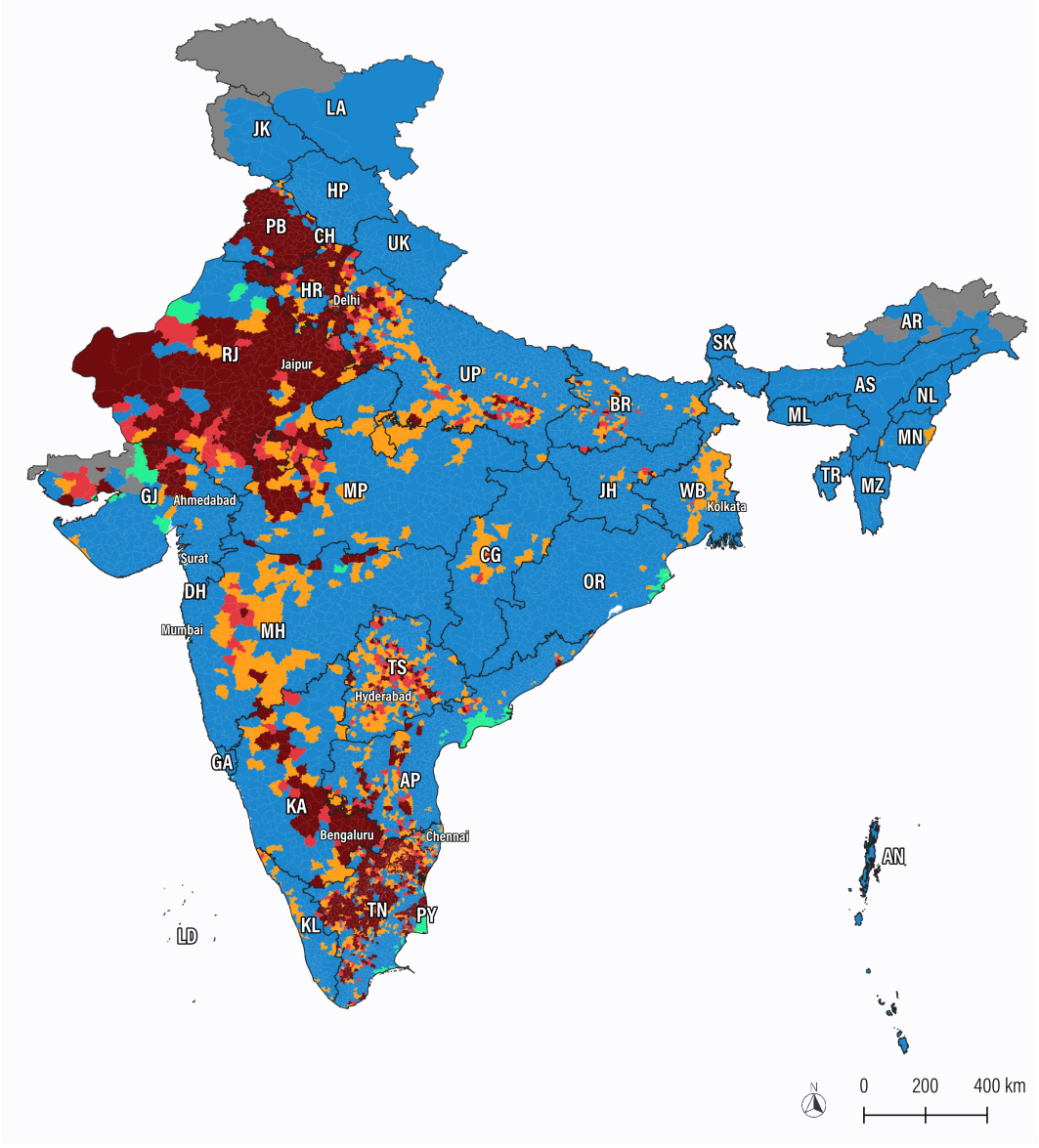
Figure 5 | **Drought**



Source: Processed and visualised by authors based on the drought risk identified by World Resource Institute's Aqueduct.

Disclaimer: This map is for illustrative purpose and does not imply the expression of any opinion on the part of WRI India, concerning legal status of any country or territory or concerning the delimitation of frontiers or boundaries.

Figure 6 | **Groundwater stress**



Source: Processed and visualised by authors based on the groundwater assessment by the Central Ground Water Board and India Water Resources Information System.

Disclaimer: This map is for illustrative purpose and does not imply the expression of any opinion on the part of WRI India, concerning legal status of any country or territory or concerning the delimitation of frontiers or boundaries.

HYDROLOGICAL DROUGHT

The WRI Aqueduct drought-risk dataset shows the highest risk across Rajasthan and Gujarat and parts of Maharashtra, Karnataka, and Tamil Nadu (Figure 5). This is driven by recurrent meteorological droughts, high water demand for agricultural and urban areas, and, often unsustainable groundwater abstraction rates, which lead to depleted reservoirs and reduced surface water flow (S.K. Jain et al. 2025). Despite occasional snowfall, drought-prone regions in Jammu & Kashmir receive very low annual precipitation and have limited surface water retention, short growing seasons, and high climatic variability (Ul Zaman and Pandit 2023). Moreover, high drought risk extends across central Uttar Pradesh, southern Bihar, Jharkhand, and Chhattisgarh, where seasonal rainfall variability and inadequate water management infrastructure contribute to chronic water scarcity (Chuphal et al. 2024). The drought risk map in Figure 4(a) presents similar results.

GROUNDWATER STRESS

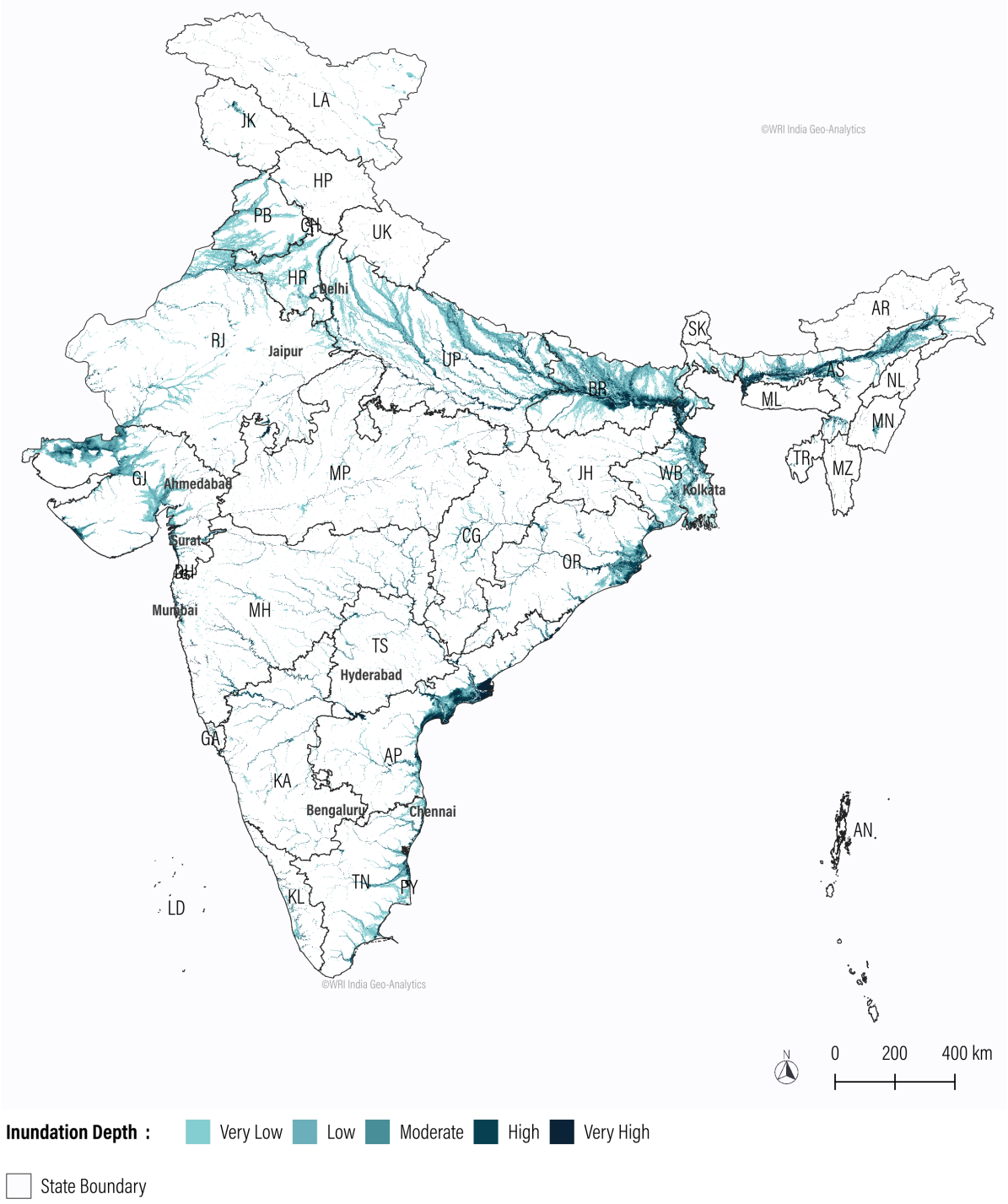
Northwestern India is a major groundwater stress hotspot owing to intensive agriculture, high extraction, and limited surface water availability, along with overexploited pockets in western and peninsular India driven by irrigation demand and constrained recharge (Mahato et al. 2025; Pandey et al. 2022; Rawat et al. 2022). This pattern is consistent with our results, as reflected in the map in Figure 6. The map shows extensive overexploited and critical blocks concentrated in Punjab, Haryana, Delhi, and western Uttar Pradesh, with additional clusters in Rajasthan and Gujarat. Strong groundwater stress is also observed across peninsular India, particularly in Maharashtra, northern Karnataka, Telangana, Andhra Pradesh, and large parts of Tamil Nadu.

RIVERINE FLOOD

The map in Figure 7 shows that the riverine flood hazard is most pronounced along the Ganga Basin, particularly across eastern Uttar Pradesh, Bihar, and southern and central West Bengal. Here, the extensive low-lying alluvial plains, high monsoonal discharge, and sediment-laden river systems contribute to deep and widespread inundation (Roy and Matsagar 2021). Southern flood-prone corridors are visible along the Godavari Basin (Maharashtra and Telangana), Krishna Basin (Karnataka and Andhra Pradesh), and Cauvery Basin (Karnataka and Tamil Nadu), as well as stretches of the Mahanadi in Odisha.

The riverine-flood layer map also indicates flood-prone corridors in the Brahmaputra Basin in Assam and parts of coastal Odisha. This aligns with studies linking flood risk in these regions to heavy monsoon rainfall, storm-surge interactions during cyclonic events, and embankment breaches (Ranjan and Karmakar 2024). In western India, localised but notable inundation appears along parts of coastal Gujarat, influenced by basin-scale runoff and estuarine backwater effects (Ray et al. 2021).

Figure 7 | **Riverine flood**



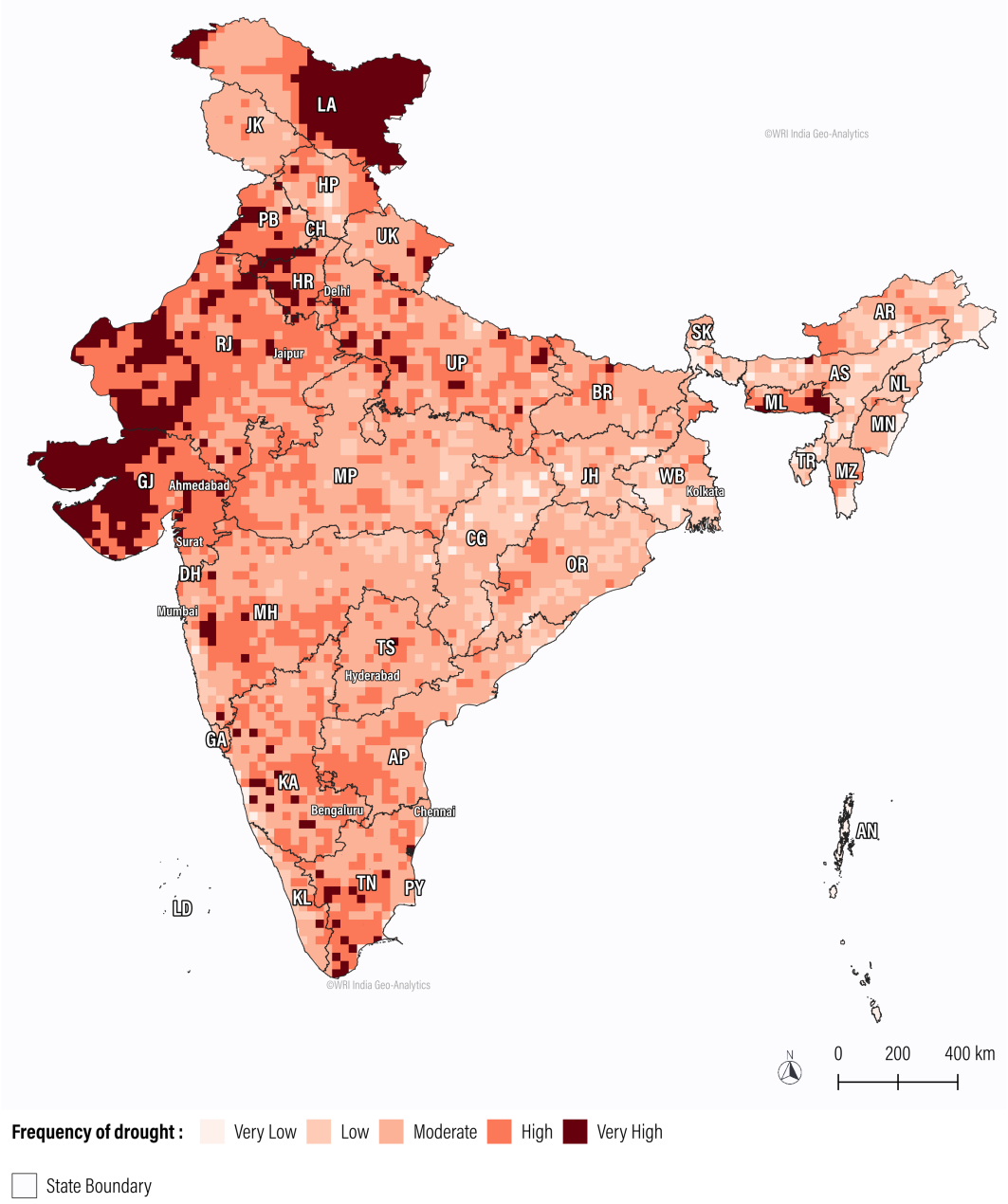
Source: Processed and visualised by authors, using the Joint Research Centre and Copernicus Emergency Management Service's Global Flood Awareness System's flood inundation maps for the 100-year return period.

Disclaimer: This map is for illustrative purpose and does not imply the expression of any opinion on the part of WRI India, concerning legal status of any country or territory or concerning the delimitation of frontiers or boundaries.

Meteorological hazards

Meteorological hazards show spatially extensive extreme weather patterns shaped by India's monsoon climate, heat regime, coastal systems, and mountainous topography. Studies indicate that approximately 12 percent of India's land area is susceptible to floods and river erosion (Roy and Matsagar 2021) and thermal stress events increasingly pose public health risks (Prasad et al. 2023).

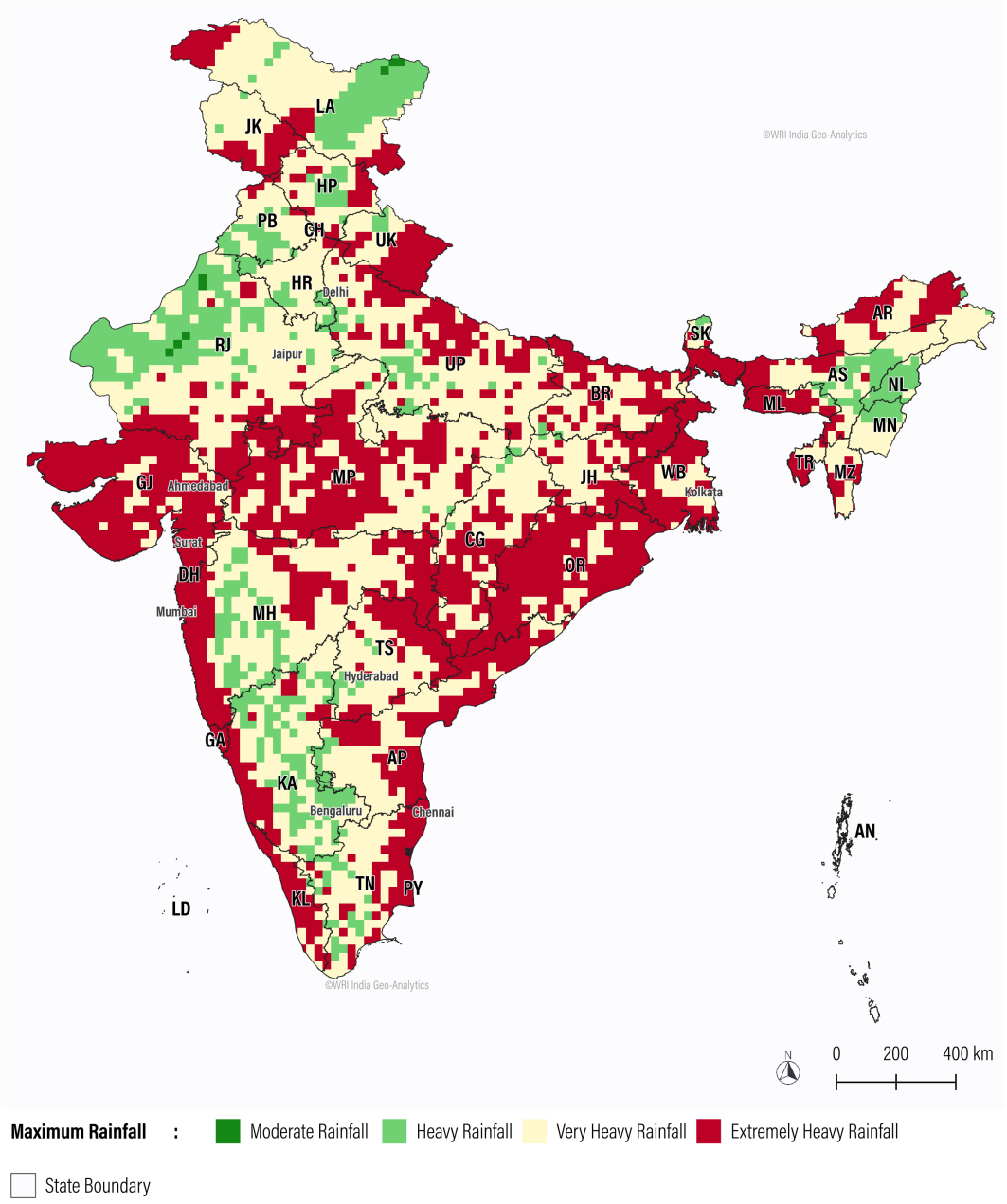
Figure 8 | **Meteorological drought**



Source: Processed and visualised by the authors, using the India Meteorological Department's gridded rainfall data for 1985–2020.

Disclaimer: This map is for illustrative purpose and does not imply the expression of any opinion on the part of WRI India, concerning legal status of any country or territory or concerning the delimitation of frontiers or boundaries.

Figure 9 | **Extreme precipitation**



Source: Processed and visualised by the authors, using the India Meteorological Department's gridded rainfall data for 2000–21.

Disclaimer: This map is for illustrative purpose and does not imply the expression of any opinion on the part of WRI India, concerning legal status of any country or territory or concerning the delimitation of frontiers or boundaries.

METEOROLOGICAL DROUGHT

Figure 8 shows that the highest meteorological drought probability is concentrated in western Rajasthan and Gujarat, which form the country's most prominent hotspots. Additional high-probability regions appear in parts of Punjab, Haryana, and the northwestern plains. Moreover, moderate drought probability extends across much of peninsular and central India, including parts of Maharashtra, Karnataka, Telangana, Andhra Pradesh, Tamil Nadu, and Madhya Pradesh. Furthermore, lower-to-moderate drought probability is visible across several parts of northern and eastern India, indicating that meteorological drought is spatially widespread although its intensity is the strongest in the arid and semiarid western regions.

EXTREME PRECIPITATION

The western coast, eastern India, and parts of peninsular India are major zones of extreme precipitation because of monsoonal troughs, cyclonic systems, and strong orographic effects along the Western Ghats (Dash et al. 2024; Dutta et al. 2025; Singh et al. 2025). This is in line with findings from the literature indicating that parts of Andhra Pradesh and Tamil Nadu also experience intense rainfall linked to monsoon variability and northeast monsoon systems (Shahi and Rai 2023).

Figure 9 shows a broader pattern of precipitation. High concentrations are observed across eastern Rajasthan, Madhya Pradesh, Chhattisgarh, Maharashtra, Telangana, Andhra Pradesh, Karnataka, Tamil Nadu, and parts of Odisha, Jharkhand, Bihar, eastern Uttar Pradesh, and Assam. Strong concentrations are also evident along the western coast, particularly in coastal Gujarat, coastal Maharashtra, Goa, coastal Karnataka, and Kerala. Overall, the map indicates that extreme precipitation is spatially extensive across India.

HEAT STRESS

The most frequent extreme heat-stress conditions appear in western Rajasthan, Gujarat (particularly the western and northern parts), and parts of southwestern Haryana and Delhi, as per the previous literature (Debnath et al. 2023; Kalaiarasi et al. 2023; Ranjan and Karmakar 2024). These regions experience prolonged periods of intense heat that often exceed critical physiological thresholds, particularly impacting vulnerable populations and agricultural productivity, as reported in previous studies listed.

This pattern is consistent with the results (Figure 10), which show that strong-to-extreme heat stress extends across a much larger area. The highest frequency is concentrated in western and northwestern India, including Rajasthan and Gujarat, but high values are also spread across the Indo-Gangetic Plain, central India, and much of peninsular India. High heat stress frequency is observed in Punjab, Haryana, Delhi, Uttar Pradesh, Madhya Pradesh, Chhattisgarh, Jharkhand, Bihar, West Bengal, Maharashtra, Telangana, Andhra Pradesh, Karnataka, Tamil Nadu, and parts of Kerala. Elevated values also occur in parts of the Northeast. Therefore, heat stress is one of the most spatially extensive hazards in India.

COLD STRESS

The Himalayan region is identified as India's most intense cold-stress zone because of high-altitude exposure, severe winter temperatures, and snowfall-related conditions (Kumar and Chakraborty 2025). The analysis shows that cold stress is concentrated mainly in the Himalayan and adjoining northern belts, with the highest intensity in Ladakh, Jammu & Kashmir, Himachal Pradesh, and Uttarakhand, and lower-intensity extension into parts of Punjab, Haryana, Delhi, and the upper Gangetic Plain. Isolated high-altitude pockets are also observed in Arunachal Pradesh and Sikkim (Figure 11).

LIGHTNING FLASH RATE

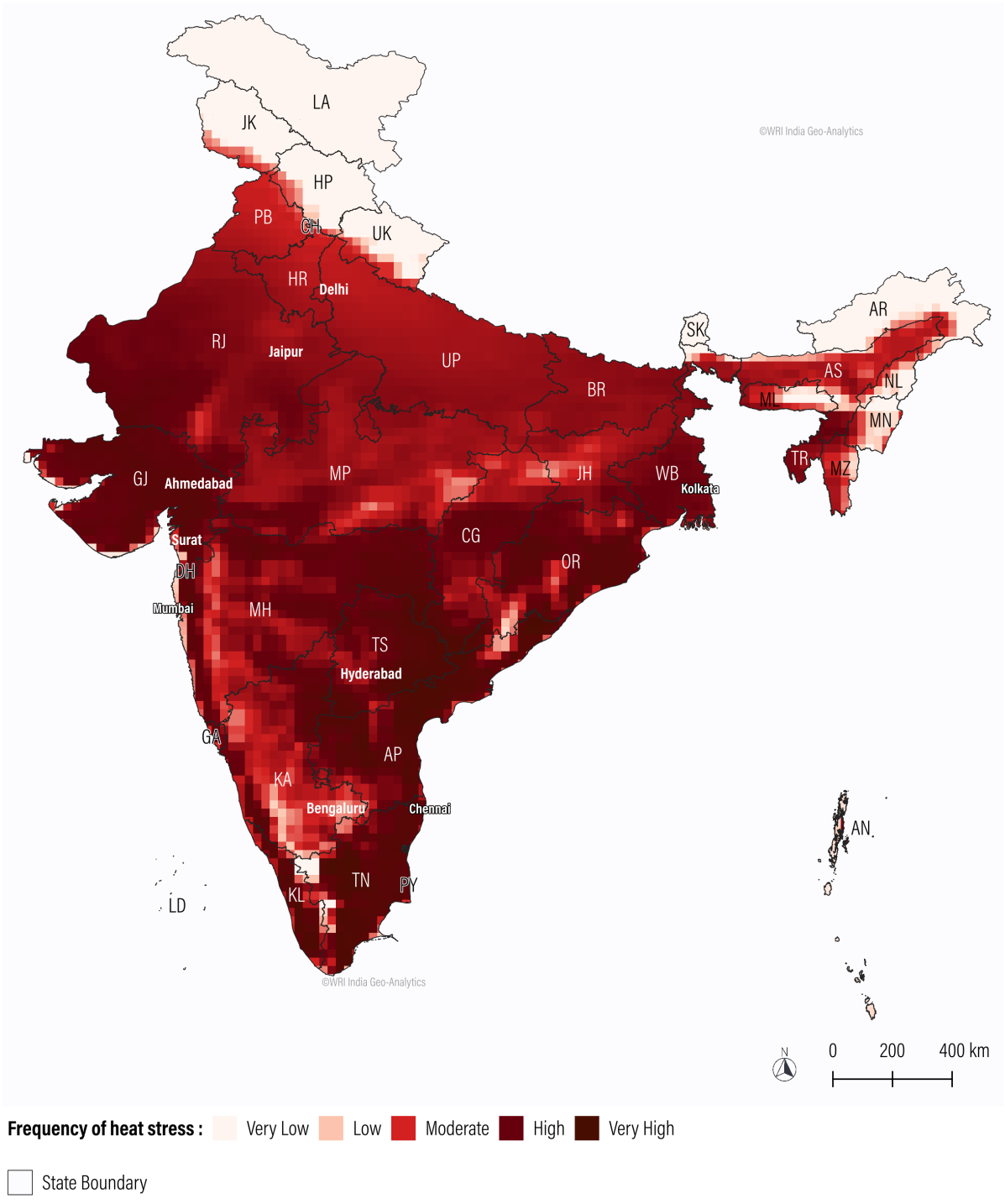
Eastern and northeastern India are major lightning-prone regions because of moist air inflow from the Bay of Bengal, strong convective instability, and monsoonal atmospheric dynamics that support frequent thunderstorm activity (Chakraborty et al. 2021; Ranjan and Karmakar 2024). Our results show high flash densities from the Himalayan foothills and northern plains into eastern India and the Northeast, especially Uttarakhand, Uttar Pradesh, Bihar, Jharkhand, West Bengal, Odisha, Assam, Meghalaya, and adjoining states (see Figure 12). Moderate-to-high rates also appear in Chhattisgarh, coastal Andhra Pradesh, southern Tamil Nadu, and Kerala.

CYCLONE

According to the literature, the coast of Bay of Bengal is India's most cyclone-prone region because of high cyclogenesis, warmer sea surface temperatures, and coastal configurations that direct cyclonic systems towards the eastern shoreline (Bandyopadhyay et al. 2021; Hussain et al. 2024).

Figure 13 shows the highest cyclone frequency from 1891 to 2020 along the coasts of West Bengal, particularly the Sundarbans, and Odisha. The high frequency extends along coastal Andhra Pradesh and northern Tamil Nadu. On the west coast, lower but notable cyclone occurrences appear in southern and western Gujarat, including Kachchh and Saurashtra.

Figure 10 | **Heat stress**

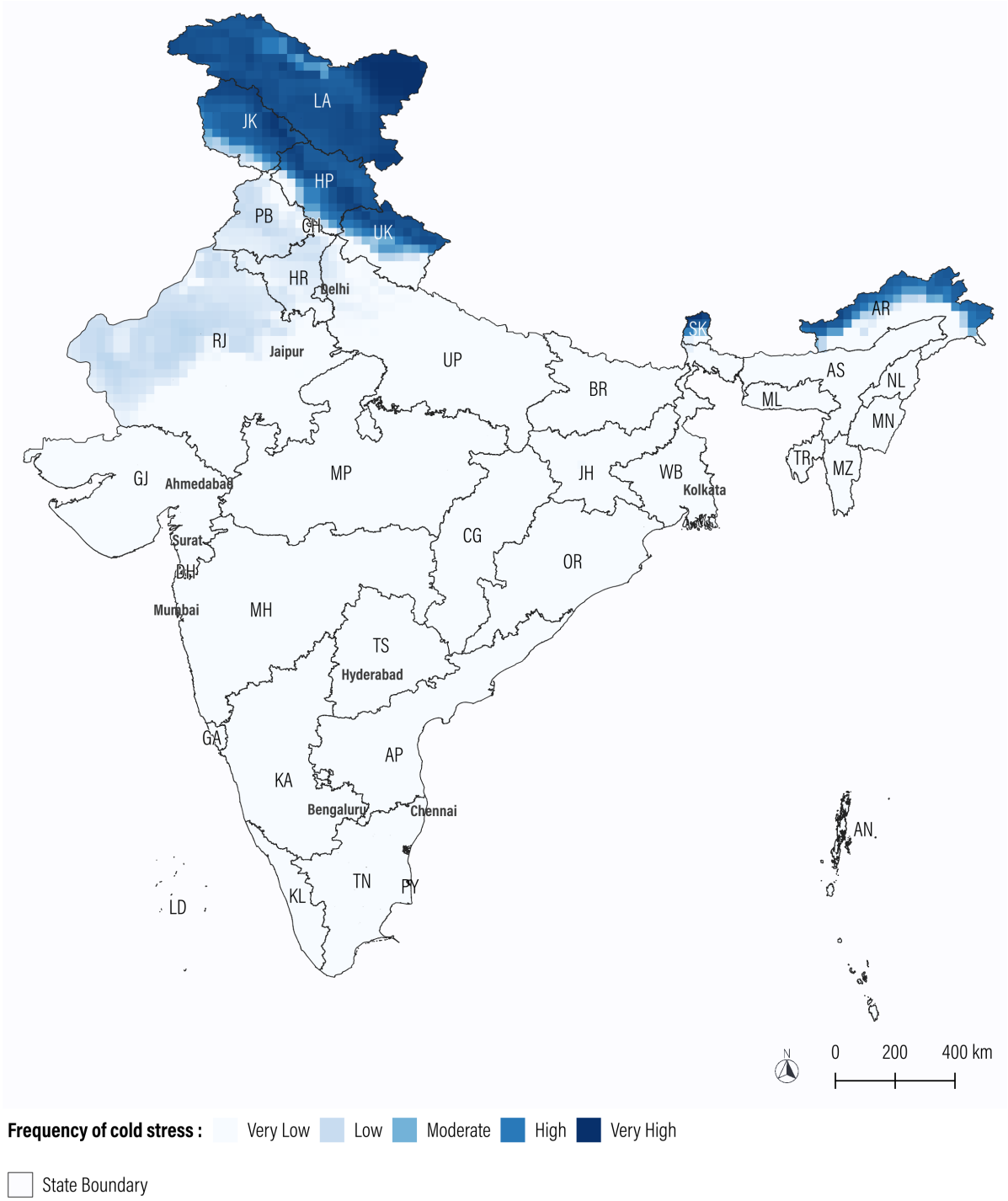


Notes: ECMWF: European Centre for Medium-Range Weather Forecasts; ERA5: ECMWF Reanalysis version 5; HEAT: Human thermal comfort.

Source: Processed and visualised by authors, using data from ERA5-HEAT and ECMWF Universal Thermal Climate Index for 1991–2021.

Disclaimer: This map is for illustrative purpose and does not imply the expression of any opinion on the part of WRI India, concerning legal status of any country or territory or concerning the delimitation of frontiers or boundaries.

Figure 11 | **Cold stress**

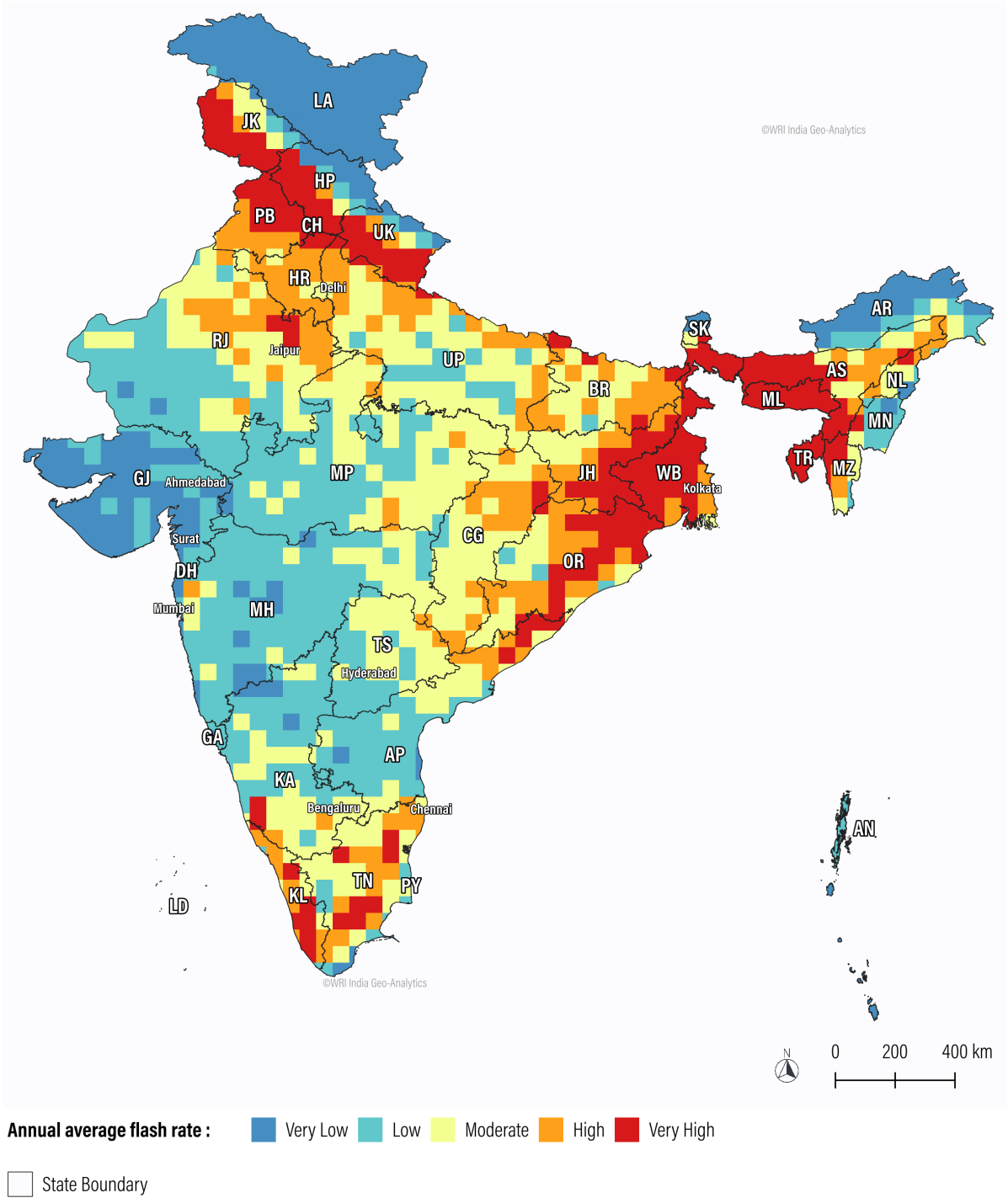


Notes: ECMWF: European Centre for Medium-Range Weather Forecasts; ERA5: ECMWF Reanalysis version 5; HEAT: Human thermal comfort.

Source: Processed and visualised by authors, using data from ERA5-HEAT and ECMWF Universal Thermal Climate Index for 1991–2021.

Disclaimer: This map is for illustrative purpose and does not imply the expression of any opinion on the part of WRI India, concerning legal status of any country or territory or concerning the delimitation of frontiers or boundaries.

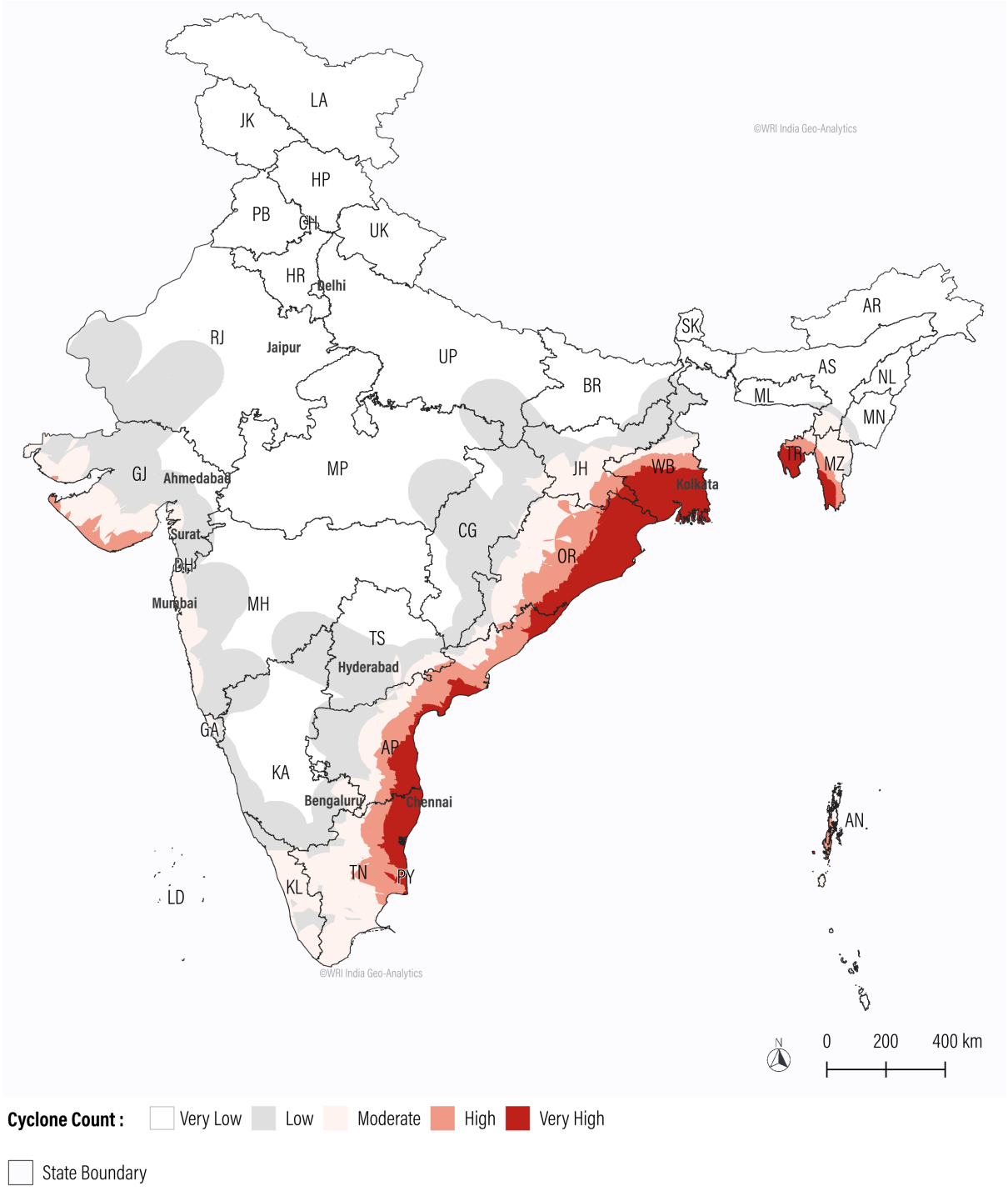
Figure 12 | **Lightning**



Source: Processed and visualised by authors, using the National Aeronautics and Space Administration, Global Hydrometeorology Resource Center's Lightning Imaging Sensor–Optical Transient Detector lightning climatology (1995–2014).

Disclaimer: This map is for illustrative purpose and does not imply the expression of any opinion on the part of WRI India, concerning legal status of any country or territory or concerning the delimitation of frontiers or boundaries.

Figure 13 | **Cyclone**



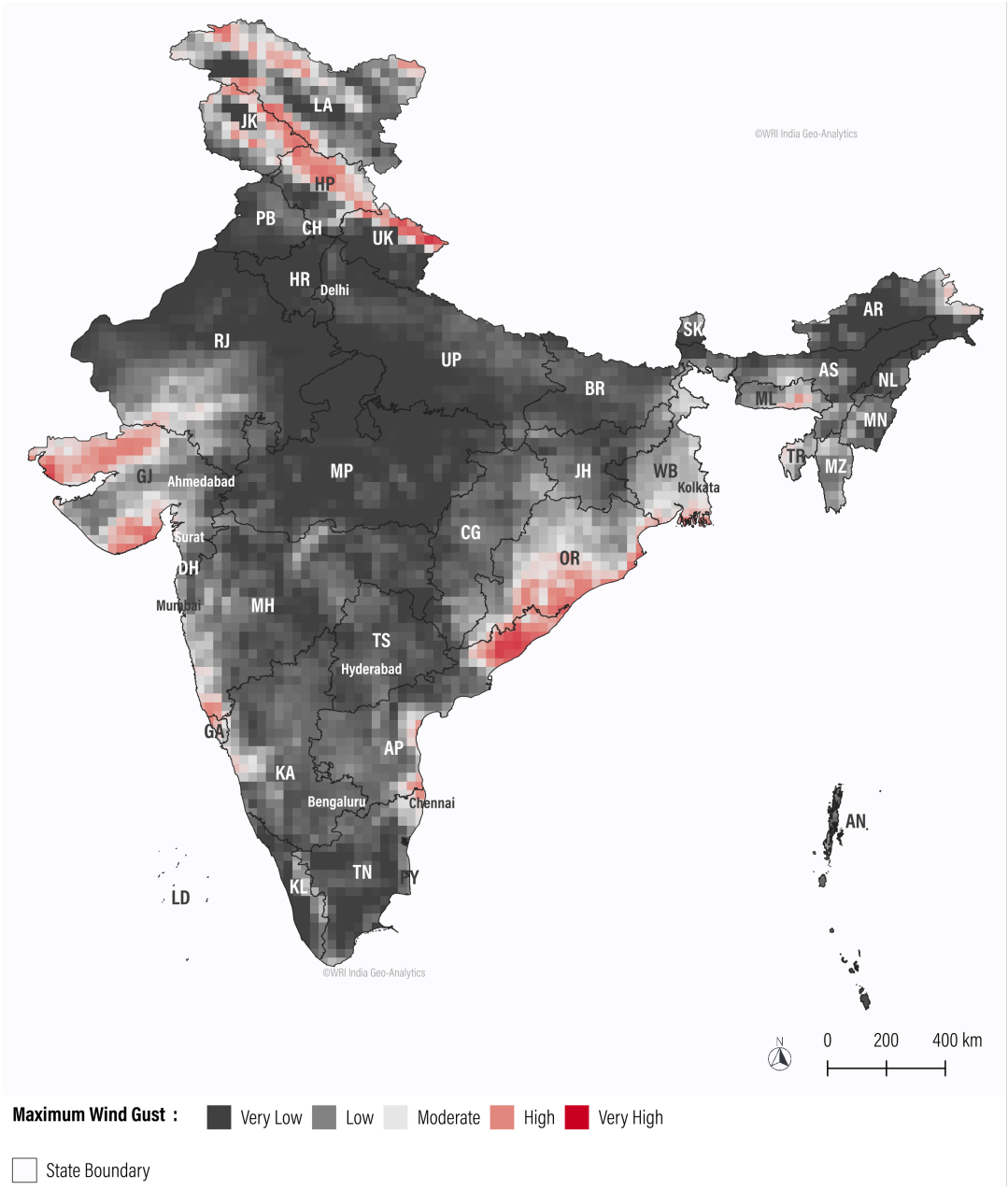
Source: Processed and visualised by authors, using the India Meteorological Department's Cyclone E-Atlas (1891–2020).

Disclaimer: This map is for illustrative purpose and does not imply the expression of any opinion on the part of WRI India, concerning legal status of any country or territory or concerning the delimitation of frontiers or boundaries.

EXTREME WIND

Previous studies show that India's eastern coast is a major extreme-wind corridor because of recurrent cyclonic activity from the Bay of Bengal. They also highlight the exposure along parts of the western coast and selected mountain regions shaped by topography and atmospheric systems (Kantamaneni et al. 2022; Ranjan and Karmakar 2024). Figure 14 shows that the highest wind gust classes are concentrated along parts of coastal Odisha, southern West Bengal, coastal Andhra Pradesh, and Tamil Nadu, with additional pockets in Gujarat, coastal Maharashtra, the western Himalayas, the Northeast, and the Andaman and Nicobar Islands. Overall, extreme wind exposure is concentrated along cyclone-prone coasts and high-relief mountain regions.

Figure 14 | **Extreme wind**

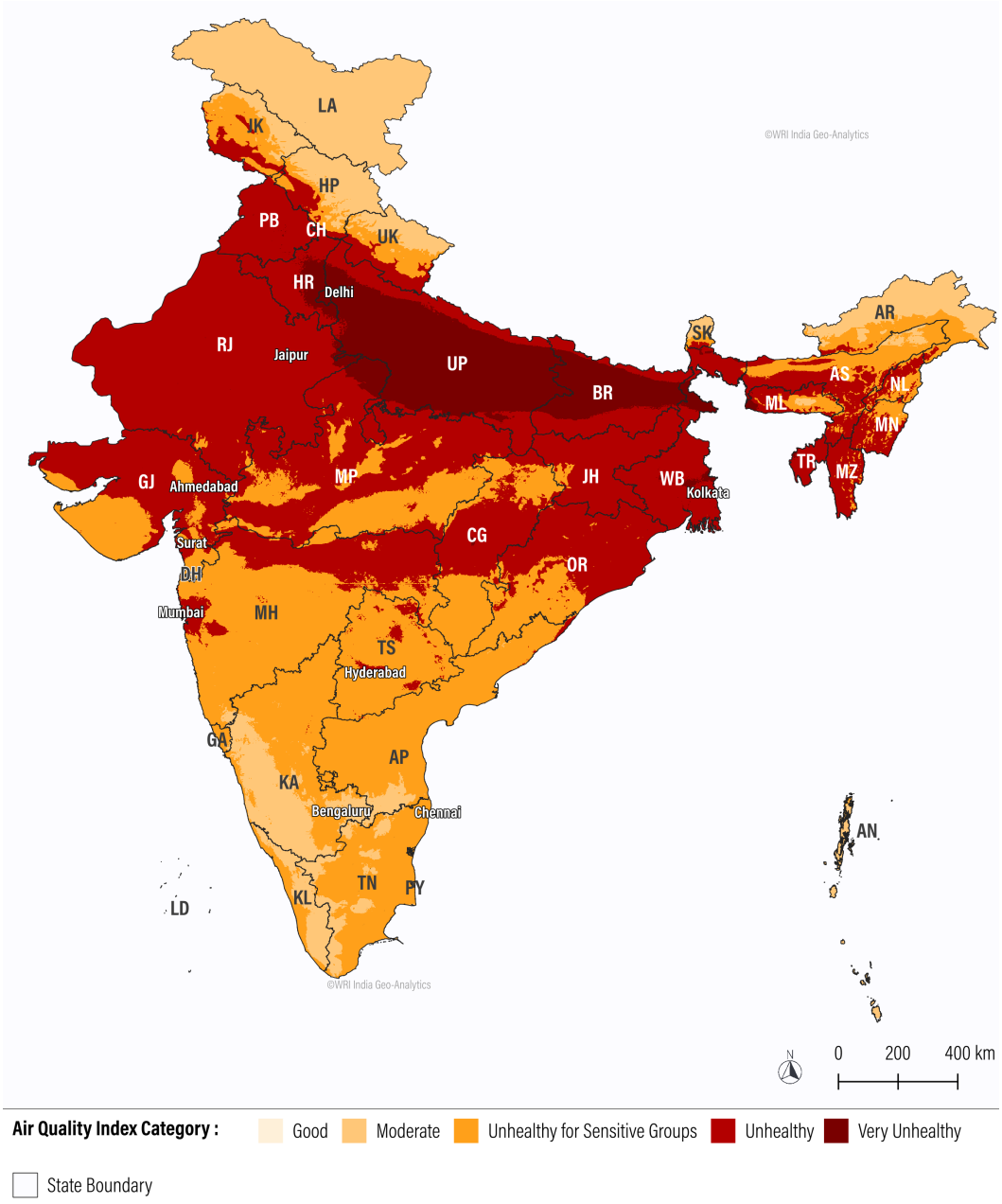


Notes: ECMWF: European Centre for Medium-Range Weather Forecasts; ERA5: ECMWF Reanalysis version 5.

Source: Processed and visualised by authors, using ECMWF ERA5 wind gust data (2000–24).

Disclaimer: This map is for illustrative purpose and does not imply the expression of any opinion on the part of WRI India, concerning legal status of any country or territory or concerning the delimitation of frontiers or boundaries.

Figure 15 | **Air quality**



Notes: $PM_{2.5}$: particulate matter finer than 2.5 micrometres in diameter.

Source: Processed and visualised by authors, using the surface $PM_{2.5}$ dataset of the Atmospheric Composition Analysis Group, Washington University (1998–2022).

Disclaimer: This map is for illustrative purpose and does not imply the expression of any opinion on the part of WRI India, concerning legal status of any country or territory or concerning the delimitation of frontiers or boundaries.

Environmental hazards

Air pollution can be measured using several pollutants including $PM_{2.5}$, PM_{10}, sulphur dioxide, nitrogen dioxide, and ozone. In this study, air pollution was represented specifically by $PM_{2.5}$ concentration because nationally comparable gridded $PM_{2.5}$, data were available for the study period. Previous studies have shown that $PM_{2.5}$ concentrations are higher in regions with dense populations, transport emissions, industrial activity, and agricultural burning, particularly in the Indo-Gangetic Plain (Mani et al. 2021).

AIR QUALITY

Figure 15 shows a broad unhealthy-to-very-unhealthy $PM_{2.5}$ belt across Punjab, Haryana, Delhi, Uttar Pradesh, Bihar, and West Bengal, with severe concentrations across much of the northern plain. Elevated concentrations extend into Rajasthan, Madhya Pradesh, Jharkhand, Chhattisgarh, Gujarat, and Maharashtra, along with a corridor across Assam, Meghalaya, Tripura, and the adjoining northeastern states. This pattern aligns with the literature on pollutant build-up in the Indo-Gangetic Plain and parts of central, western, and northeastern India (Mishra and Verma 2024).

Multi-hazard maps: National level

The individual hazard layers establish the structural foundation of India's hazard geography. However, these hazards do not operate in isolation. The same regions that experience extreme rainfall also face drought; regions under recurrent heat stress often overlap with groundwater depletion; and tectonically active mountains coincide with landslide-prone slopes and intense precipitation.

The multi-hazard maps integrate 14 layers and show the point of convergence of different hazards. They help move from individual hazard assessments to a multi-hazard view to assess the compounding risks.

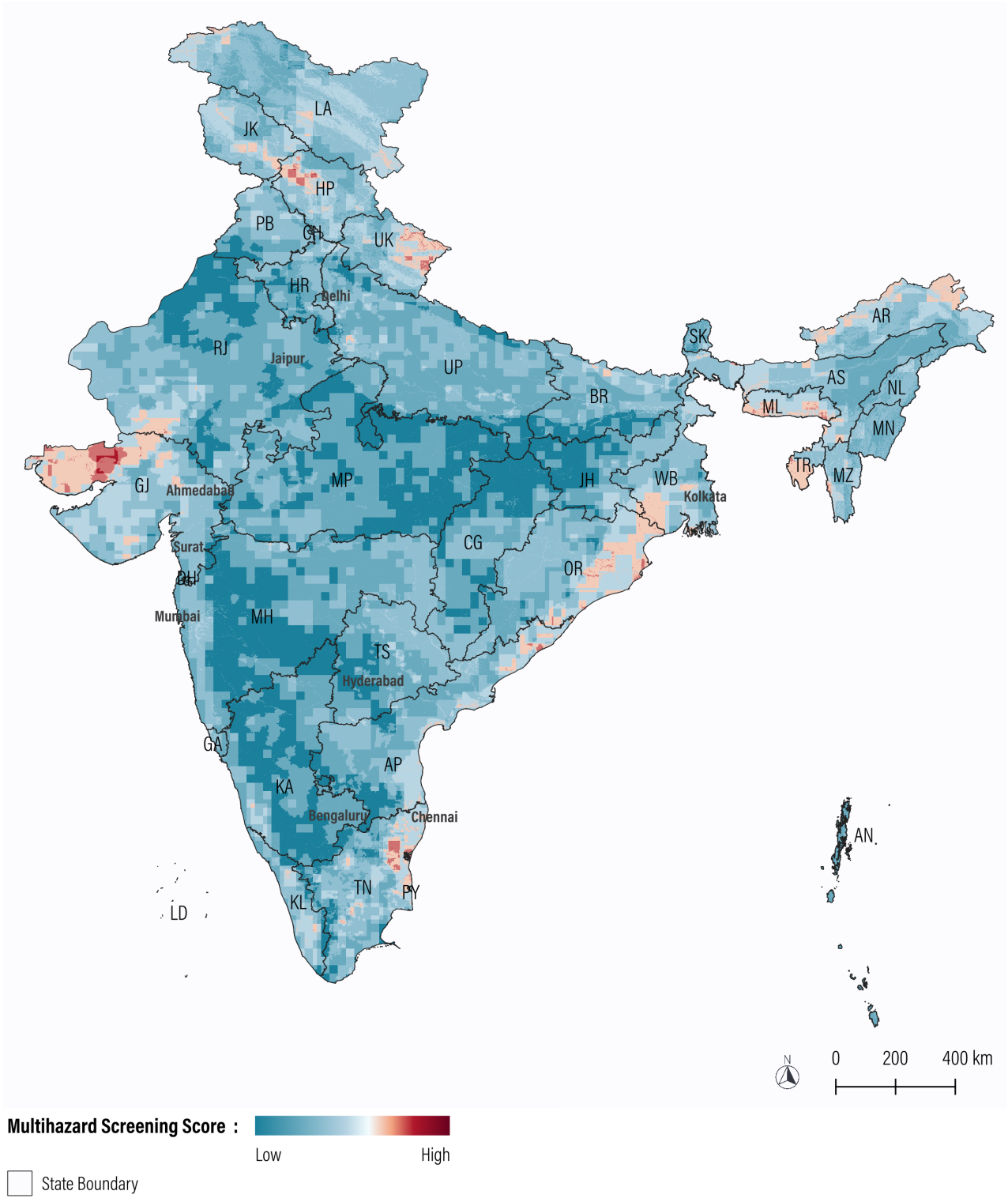
National-level hazard count: Number of extreme hazards affecting each area

The hazard count map (Figure 16(a)) shows, for the analysis unit, the number of hazards occurring in their most extreme classes. Higher hazard counts are concentrated in parts of Jammu & Kashmir, Himachal Pradesh, and Uttarakhand and across parts of Assam, Arunachal Pradesh, Meghalaya, and Tripura. Additional hotspots appear in northern Gujarat and along the eastern coast, especially in Odisha and Andhra Pradesh, indicating where multiple extreme hazards spatially coincide, contingent on data limitations.

The Himalayan regions experience interactions with several hazards, such as landslide susceptibility, earthquakes, intense precipitation, and convective storms (Pathak et al. 2025)). These hazards often reinforce one another, with rainfall triggering landslides and floods and seismic activity heightening geological instability (Rusk et al. 2022). Similarly, the literature points to the Northeast as a region where high rainfall, flooding, lightning, and seismic exposure frequently coincide and to pockets of northern Gujarat, Odisha, and Andhra Pradesh as coastal zones where cyclones, storm surges, coastal erosion, sea level rise, and intense precipitation combine to produce compound risks (Ranjan and Karmakar 2024). The Indo-Gangetic Plain is also recognised as a region of layered hydrological and climatic stress, experiencing floods, droughts, heat waves, and poor air quality (Kalaiarasi et al. 2023). This pattern is broadly consistent with our hazard count map.

Figure 16 | **Multi-hazard maps: (a) hazard count and (b) hazard screening score**

(A) EXTREME HAZARD COUNT

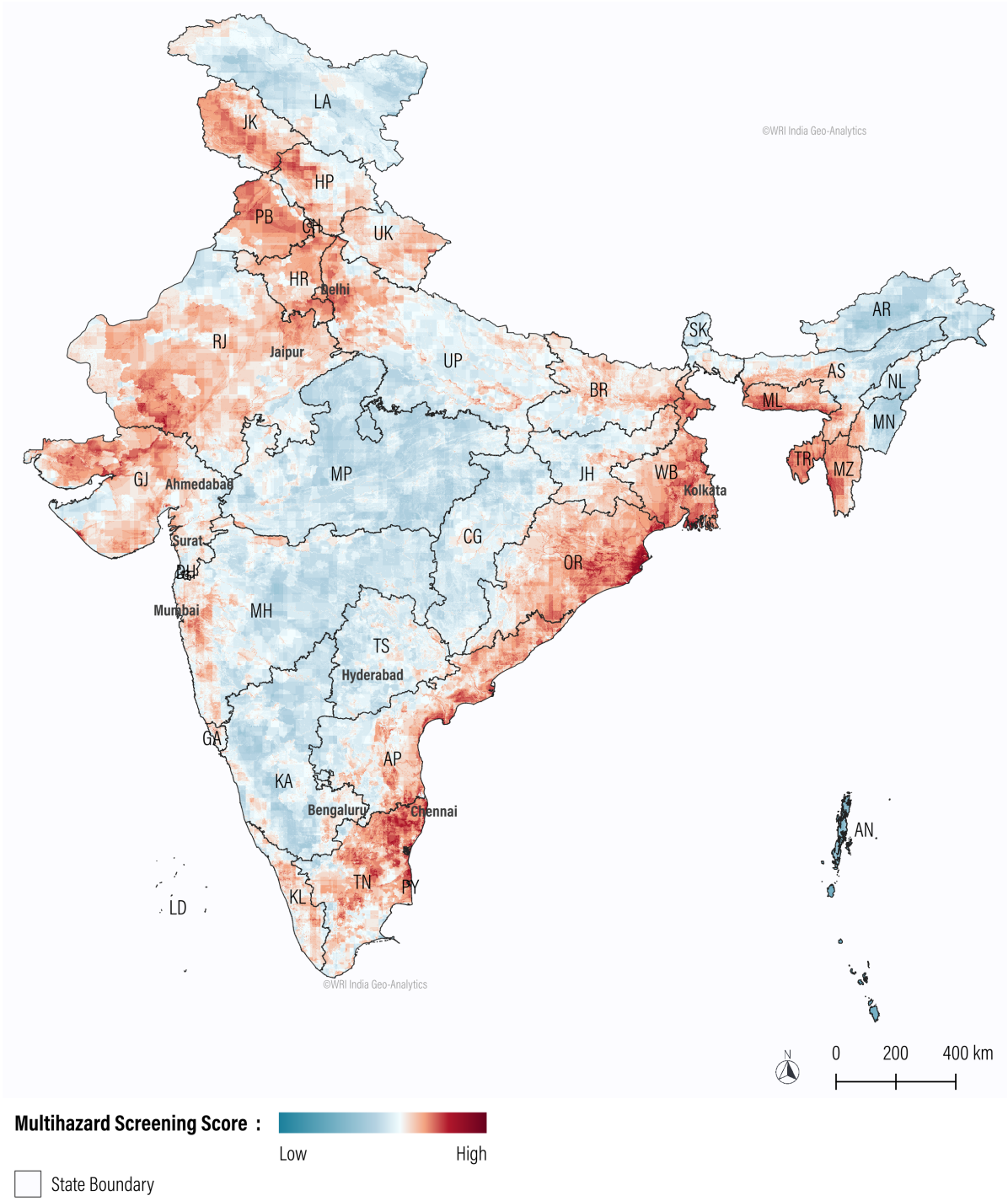


Source: Authors' analysis.

Disclaimer: This map is for illustrative purpose and does not imply the expression of any opinion on the part of WRI India, concerning legal status of any country or territory or concerning the delimitation of frontiers or boundaries.

Figure 16 | **Multi-hazard maps: (a) hazard count and (b) hazard screening score (cont.)**

(B) MULTIHAZARD SCORE



Source: Authors' analysis.

Disclaimer: This map is for illustrative purpose and does not imply the expression of any opinion on the part of WRI India, concerning legal status of any country or territory or concerning the delimitation of frontiers or boundaries.

National-level multi-hazard score: Cumulative screening score of all classes

The multi-hazard score captures the composite screening score across all hazard classes, not only the extreme class. Scores ranging from approximately 10 (lower score) to 54 (highest score) were standardised to obtain indices from 0 to 1. Figure 16(b) shows that the highest scores are concentrated in parts of the northwestern Himalayan region, particularly Jammu & Kashmir, Himachal Pradesh, and Uttarakhand, where strong seismic exposure intersects with landslide susceptibility, extreme precipitation, and convective hazards. Higher scores are also obtained for Punjab, Haryana, Delhi, and adjoining parts of Uttar Pradesh, where overlapping heat stress, flooding, air pollution, and drought risk converge, exacerbating the vulnerability of agricultural systems and dense urban populations (Sahana and Mondal 2023). Similar scores are visible across West Bengal and the eastern coastal regions of Odisha, Andhra Pradesh, and Tamil Nadu, where cyclones, extreme rainfall, flooding, and wind events combine seasonally during the post-monsoon cyclone period (Boragapu et al. 2023; Ranjan and Karmakar 2024). Parts of the northeastern states, particularly Assam, Meghalaya, Tripura, and Mizoram, experience high rainfall, flooding, and seismic exposure.

Hazard counts and screening scores should be considered together. The count map identifies locations where multiple hazards reach the extreme class. The screening score map captures cumulative occurrences across all classes. Thus, some regions, including parts of eastern India, may have lower extreme hazard counts but higher screening scores because several hazards occur at moderate-to-high levels. For decision-makers, the count map helps identify overlapping extreme hazards, whereas the score map supports broader planning, infrastructure prioritisation, and long-term risk-reduction investment.

In the next section, we quantify the exposure levels of these multi-hazard layers using data on population, built-up areas, and employment.

Exposure at the national scale: Population, built-up area, and employment in hazard zones

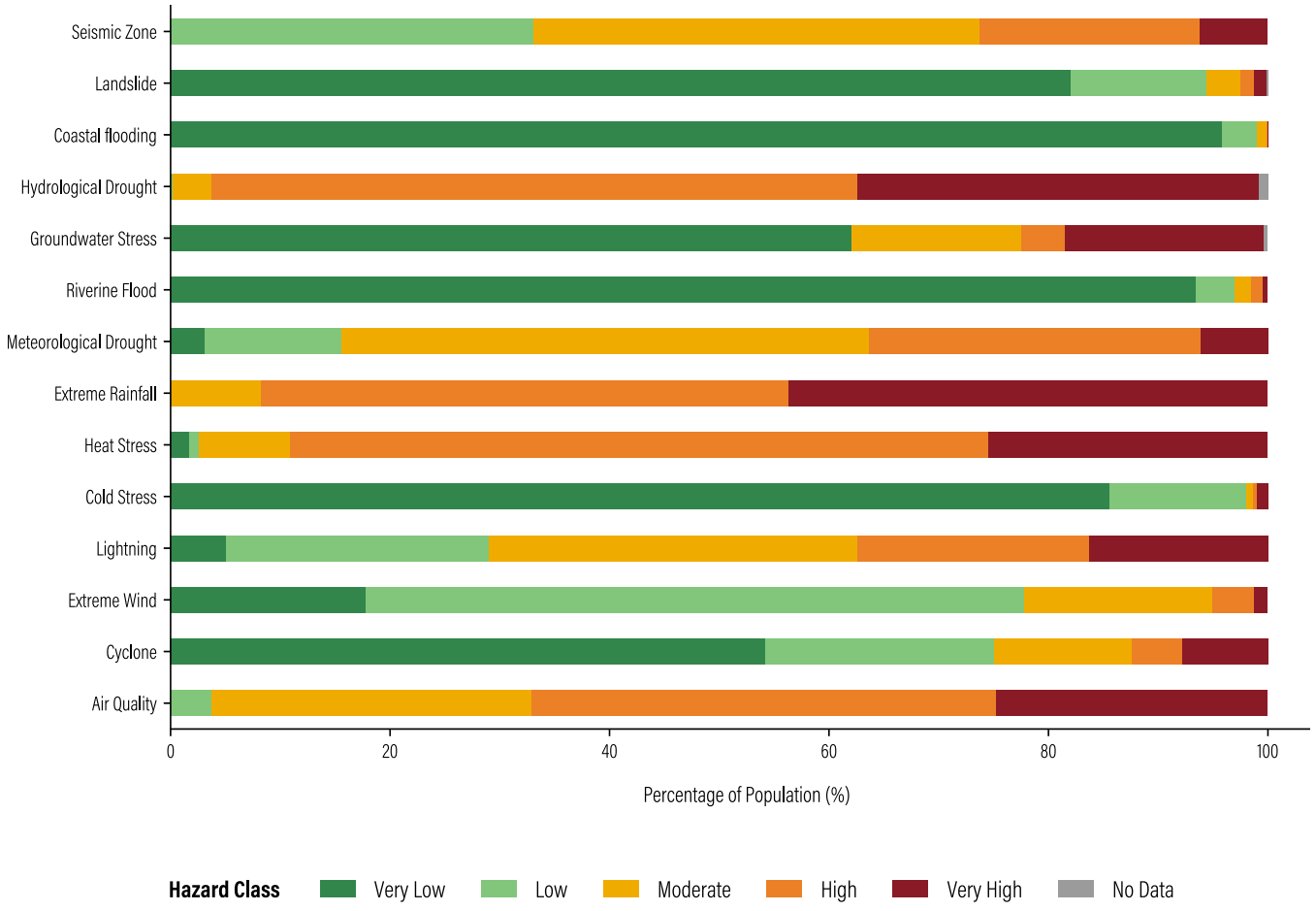
The exposure percentages reported in this section were calculated separately for each hazard and are not mutually exclusive across hazards. Therefore, the same population, built-up area, or employment location may be exposed to more than one hazard and the percentages across different hazards should not be summed.

Figure 17 shows the national distribution of population across hazard classes.

The key takeaways are as follows:

- **Extreme rainfall:** Over 90 percent of India's population live in high or very high extreme rainfall areas.
- **Hydrological drought:** Over 90 percent of India's population live in high or very high drought areas.
- **Heat stress:** Over 80 percent of India's population lives in areas with high or very-high heat-stress areas.
- **Air quality:** About 70 percent of India's population is exposed to high or very high poor air quality.
- **Lightning:** About 40 percent of India's population live in high or very-high lightning zones.

Figure 17 | **National population exposure to different hazards by percentage**



Source: Authors' analysis.

Figure 18 shows the national distribution of built-up areas across hazard classes.

The largest exposures for built-up areas are as follows:

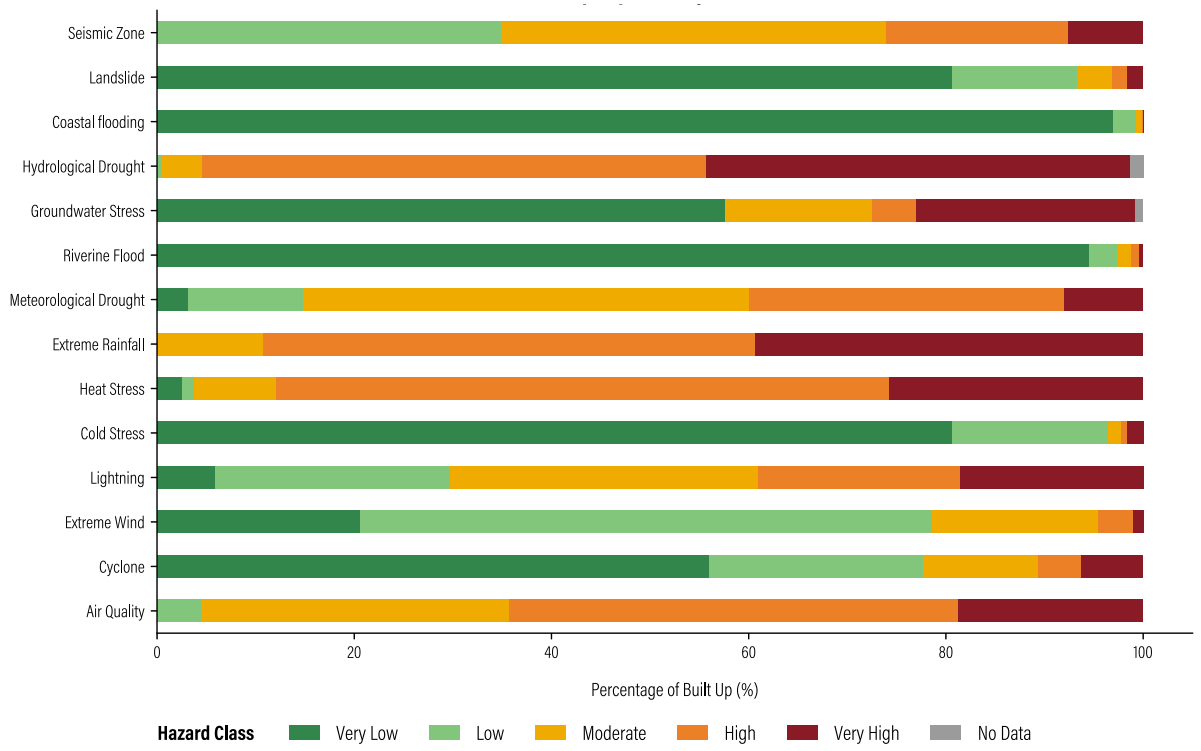
- **Extreme rainfall:** About 90 percent of built-up areas are located in high or very high extreme rainfall areas.
- **Hydrological drought:** More than 90 percent of built-up areas fall within high or very-high drought-risk areas.
- **Heat stress:** Over 80 percent of built-up areas lie within high-to-very-high heat-stress areas.
- **Air quality:** More than 60 percent of the built-up areas lie in high or very high poor air quality areas.
- **Lightning:** Nearly 40 percent of built-up areas lie in high- and very-high lightning-frequency areas.

Figure 19 shows the national distribution of employment across hazard classes.

The largest exposures for employment are as follows:

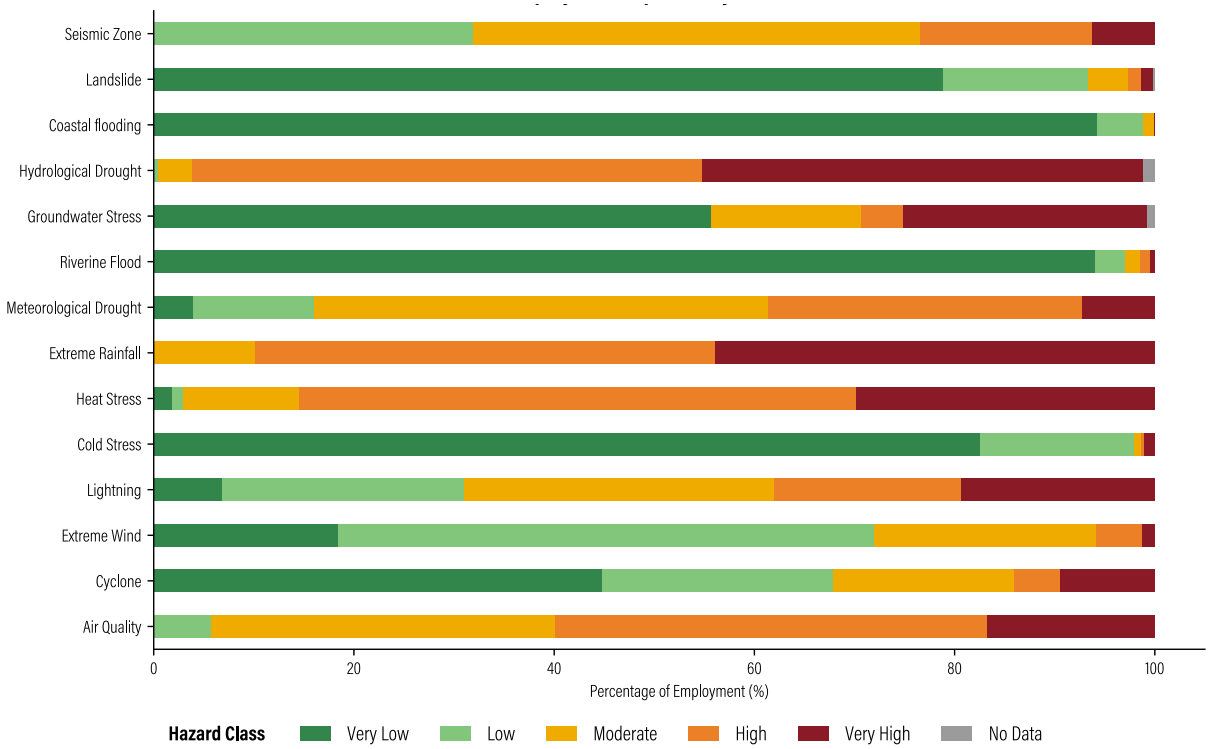
- **Extreme rainfall:** About 90 percent of employment falls within high or very high extreme heavy rainfall areas.
- **Hydrological drought:** More than 90 percent of employment falls in high or very high drought-risk areas.
- **Heat stress:** Over 80 percent of employment is in high-to-very-high heat-stress areas.
- **Air quality:** About 60 percent of employment lies in high or very high poor air quality areas.
- **Lightning:** About 40 percent of employment falls in high or very high lightning-frequency areas.

Figure 18 | **National built-up exposure to different hazards by percentage**



Source: Authors' analysis.

Figure 19 | **National employment exposure to hazards by percentage**



Source: Authors' analysis.

These national percentages establish the scale and relative planning importance of different hazards; however, they are not direct land-use prescriptions. Heat exposure analysis can identify regions requiring detailed heat-risk assessment; analysis of flood and extreme rainfall exposure can help research on drainage, floodplain, transport, and critical infrastructure; and analysis of drought and groundwater exposure can guide water budgeting, recharge, and demand management. State and city agencies should use these national results to select locations for higher-resolution analyses before incorporating evidence into masterplans, development controls, infrastructure appraisals, or emergency planning (Dodman et al. 2022; Ministry of Urban Development 2015; UNDRR 2022). Spatial differentiation at the state and city scales is presented in the next section and Appendix D.

Case studies: States and cities

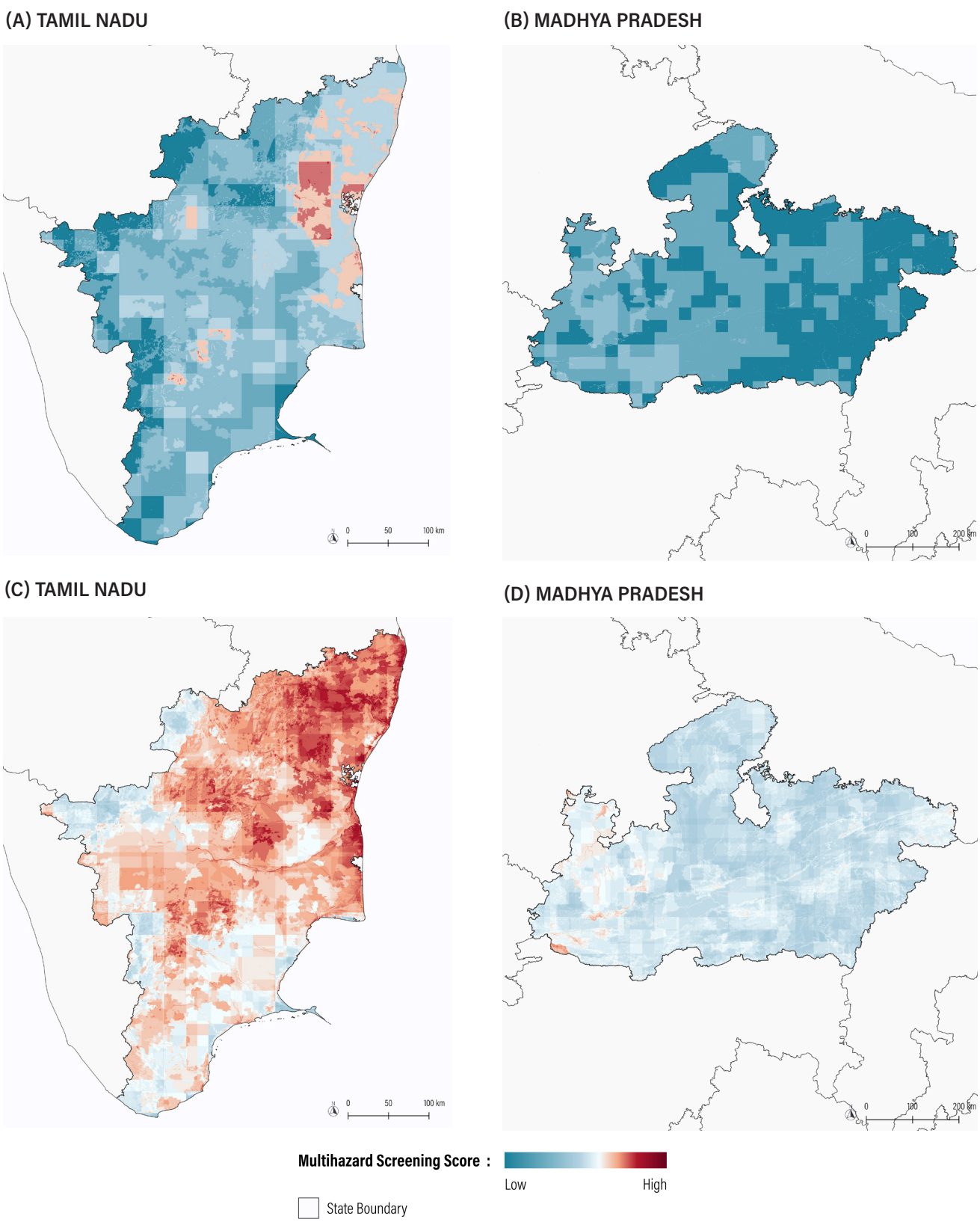
State-level illustrative cases: Tamil Nadu and Madhya Pradesh

Madhya Pradesh and Tamil Nadu illustrate how multi-hazard profiles vary significantly owing to differences in climate, physiography, and hazard interactions. Madhya Pradesh displays mostly a low-to-moderate hazard overlap, with the hazard count and screening scores remaining relatively low (Figures 20(b) and (d)). However, previous studies show that the state is vulnerable to heat, drought, intense rainfall, lightning, forest fires, and moderate seismicity, with the risks amplified by agricultural dependence and recurrent monsoon variability (Madhya Pradesh State Disaster Management Authority; Sharma 2023).

The difference may be caused by the method used: many earlier studies examine individual hazards or sectoral vulnerability, whereas the current analysis focused on spatial overlap and cumulative scores across nationally comparable layers.

Tamil Nadu presents higher hazard counts and screening scores along the eastern coast and northeastern interior, where cyclones, extreme rainfall, low elevation, wind, and heat coincide during the northeast monsoon and cyclone seasons (Figures 20(a) and (c)). Therefore, planning priorities include coastal and flood-sensitive land-use reviews, integrated drainage and retention, protection of wetlands and natural channels, wind- and cyclone-resistant critical facilities, evacuation routes, and reliable power and communication. This contrast illustrates why the same national framework can lead to different state investment portfolios.

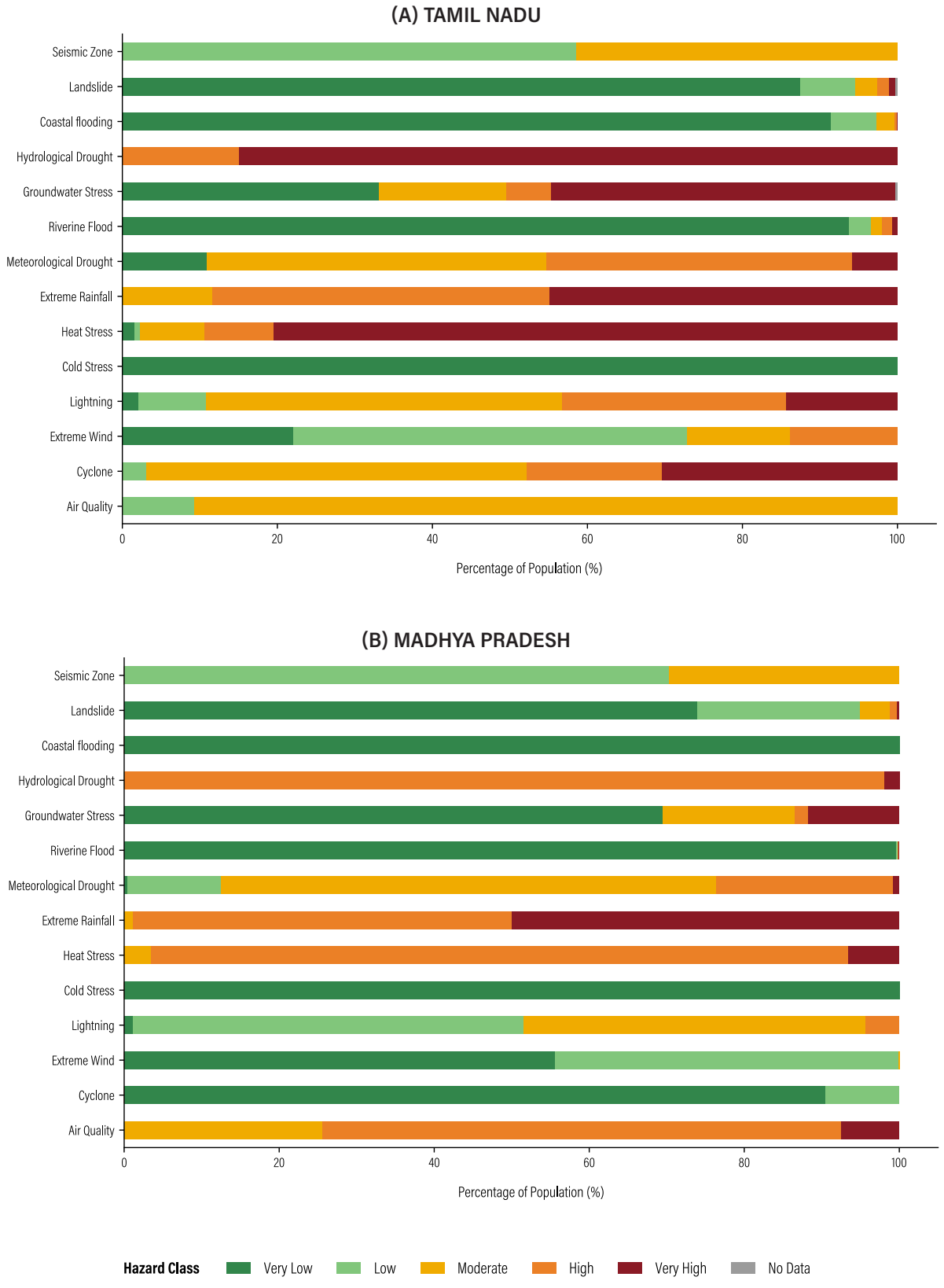
Figure 20 | **Hazard counts of (a) Tamil Nadu and (b) Madhya Pradesh and the multi-hazard screening score of (c) Tamil Nadu and (d) Madhya Pradesh**



Source: Authors' analysis.

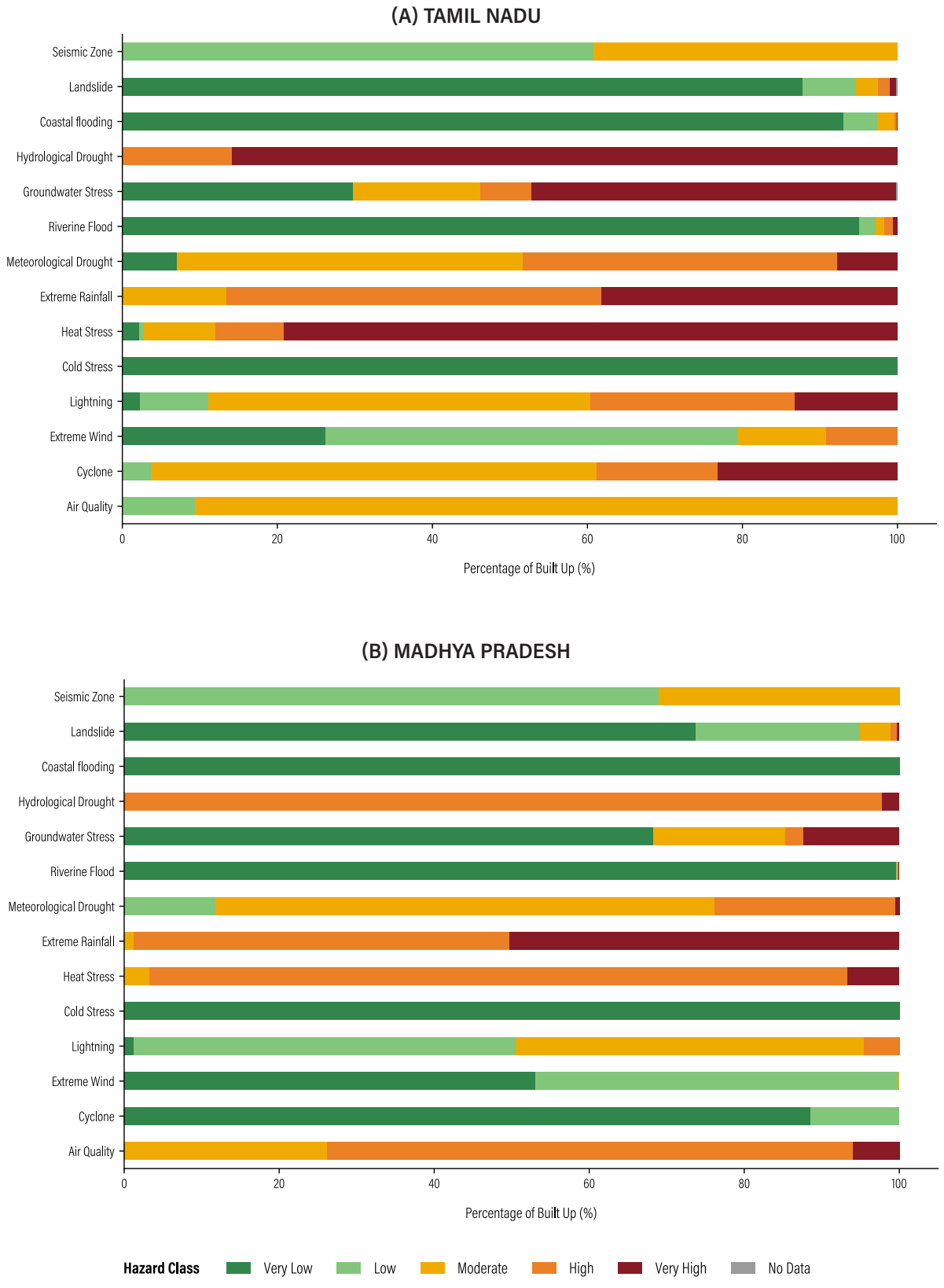
Disclaimer: This map is for illustrative purpose and does not imply the expression of any opinion on the part of WRI India, concerning legal status of any country or territory or concerning the delimitation of frontiers or boundaries.

Figure 21 | **Exposures by hazard class for the population of (a) Tamil Nadu and (b) Madhya Pradesh**



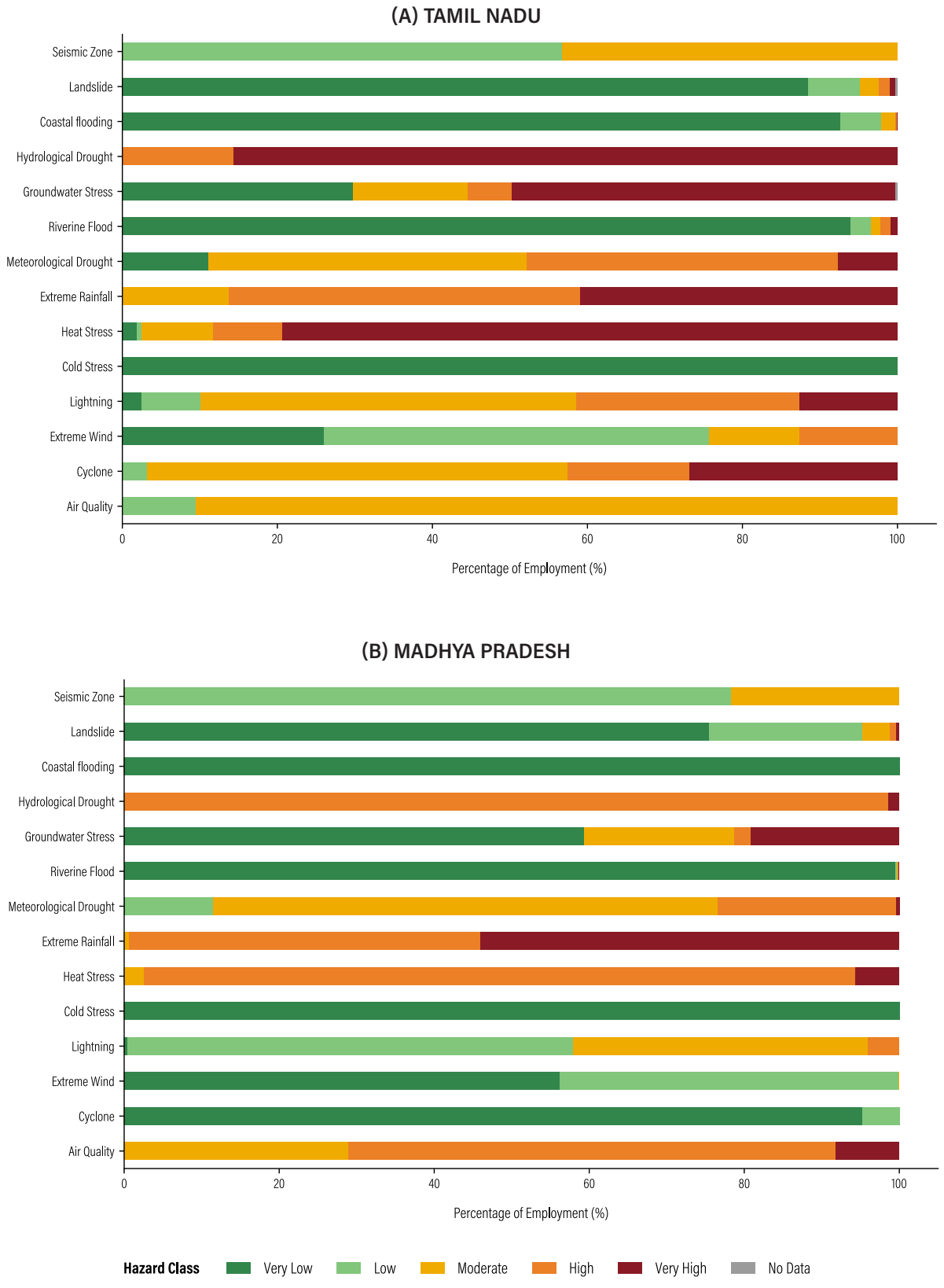
Source: Authors' analysis.

Figure 22 | **Exposures by hazard class for the built-up area of (a) Tamil Nadu and (b) Madhya Pradesh**



Source: Authors' analysis.

Figure 23 | **Exposures by hazard class for the employment (a) Tamil Nadu and (b) Madhya Pradesh**



Source: Authors' analysis.

City-level exposure

The 10 selected cities provide illustrative cases of granular evidence (Appendix D). Bengaluru, Delhi Municipal Corporation, Jodhpur, and Lucknow show extensive exposure to heat, drought, extreme rainfall, and groundwater stress. By contrast, Chennai and Greater Mumbai stand out for their very-high exposure to extreme rainfall, with Chennai also facing cyclone frequency, heat stress, and groundwater pressure. Hilly regions, such as Gangtok, Shimla, and Srinagar, display dominant exposure to seismic hazards, lightning, landslides, and high rainfall. These profiles indicate the need for differential planning based on drainage, wetlands, flood-resilient transport, and service continuity in coastal cities; heat-health preparedness, occupational safeguards, water budgeting, recharge, and reliable utilities in inland cities; and seismic assessment, slope controls, drainage, emergency access, and utility-corridor resilience in mountain cities. They also indicate how a national-scale analysis will vary from a city- or state-specific analysis; therefore, insights from each should be considered as complementary to the others for land-use planning. Applying this framework to cities requires delineated local boundaries, asset inventories, development proposals, and high-resolution hazard evidence. The employment layer adds an economic-location dimension by identifying employment centres requiring occupational protection, infrastructure audits, or business continuity planning; however, it does not estimate productivity loss or comment on the overall economic performance (Hallegatte et al. 2019; International Labour Organization 2019).

Discussion

Interpreting India's multi-hazard prone areas

India's hazard geography reflects deep climatic, geomorphological, and tectonic activities that produce distinct regional hazard profiles (Chamberlain et al. 2024; Khan et al. 2025). These results indicate that India's hazard response requires a differentiated risk-reduction approach (Roy and Matsagar 2021). The Himalayan arc and adjoining hill regions combine high seismicity, landslide susceptibility, intense rainfall, and lightning, requiring seismic compliance, geotechnical and slope-stability assessments, drainage, and slope management (Roy and Matsagar 2021). The coastal region is a cyclone–extreme rainfall–heat stress zone that requires integrated stormwater drainage, retention, and conveyance; protection of wetlands and natural channels; wind- and cyclone-resistant critical facilities; evacuation systems; and continuity planning for major employment locations (Adshead et al. 2024). The Indo-Gangetic Plains combine riverine flooding, extreme rainfall, heat, and air pollution stress, requiring floodplain review, drainage restoration, protection or relocation of critical facilities supported by local evidence, and heat-health preparedness (Roy and Matsagar 2021; Wasson 2018). Semiarid and peninsular interiors combine drought, groundwater stress, and heat, requiring heat-health preparedness, shaded public spaces, water budgeting, aquifer recharge, demand management, and reliable power and water services (Intergovernmental Panel on Climate Change IPCC [2023]). National maps can prioritise these needs, but local modelling and asset data must determine the design and regulations (Dodman et al. 2022; Ministry of Urban Development 2015).[6]

International practice illustrates how such geographic differentiation can be operationalised. Hong Kong's slope-safety system combines the control of new hillside development with slope upgrading, maintenance, rainfall warnings, natural-terrain mitigation, public information, and emergency management (Ho et al. 2016). Similarly, Japan's post-2011 tsunami strategy combines structural protection, land-use measures, warning, and evacuation because physical barriers cannot remove residual risk (Maly and Suppasri 2020).

Potential compounded risks from seasonal and co-occurring hazards

Several hazards can co-occur within the same region and season. In mountainous regions, extreme rainfall can trigger landslides and flooding and seismic exposure further increases structural vulnerability (Chauhan et al. 2025). Coastal cyclones simultaneously generate wind, rainfall, and flooding hazards during a single event. In inland regions, heat stress, drought, and groundwater depletion often occur within the same seasonal cycle, exacerbating water scarcity and agricultural stress. The overlays identify where such combinations require investigation; however, they do not estimate the timing, causation, or cascading failures. Such results require complementary local studies that test event dependence, network interconnections, vulnerability, and recovery pathways (Gill and Malamud 2016; Hallegatte et al. 2019; Zscheischler et al. 2018).

Exposure-level variations across city regions

The results show that the existing population, built-up areas, and employment are exposed to different combinations of hazards across cities, indicating the need for differentiated local assessments and responses. Chennai is exposed to very-high cyclone and extreme-rainfall classes, and Greater Mumbai's exposure lies in the very-high rainfall class, requiring detailed local assessments. Furthermore, Delhi, Bengaluru, Jodhpur, and Lucknow show combinations of heat, drought, groundwater, and rainfall stresses, requiring integrated responses, while Gangtok, Shimla, and Srinagar show seismic and landslide susceptibility, thus requiring slope, drainage, and access corridor assessments. The results also identify where infrastructure dependence may amplify disruption and where future intensification could add exposure if plans do not account for dominant hazards. The exposure analysis represents the demographic and economic characteristics of the region and not the trends of urban growth. Ahmedabad's Heat Action Plan illustrates an operational response to high heat exposure through early warning, public communication, interagency coordination, and health-system preparedness, which were associated with lower heat-season mortality after implementation (Hess et al. 2018). Comparable exposure evidence can help other cities identify where occupational, health service, and neighbourhood-level heat assessments should be prioritised.

The results also show where employment is located within the hazard classes. Similar population and employment shares partly reflect their common concentration in built-up areas as well as the apportionment method used. The actual effects depend on occupation, working conditions, hazard duration, building quality, transport access, utility reliability, and adaptive capacity. Accordingly, exposed employment locations may require heat protection, altered work practices, transport and utility resilience, emergency access, and business continuity assessment, particularly for outdoor and non-air-conditioned work under heat stress and for employment clusters dependent on water, power, or flood-prone transport links (Hallegatte et al. 2019; International Labour Organization 2019).

Applications for spatial planning, infrastructure, and regulation

This study showed that spatial co-occurrence and cumulative screening scores can support differentiated use across planning scales. At the national level, the results can identify recurring hazard combinations that may require a further review of national guidance, standards, and infrastructure development. At the state and regional levels, overlays can identify districts, growth corridors, river basins, coastlines, and infrastructure systems that require higher-resolution studies or cross-boundary coordination. At the city level, screening layers can be combined with proposed land use, development intensity, critical facilities, transport, drainage, power, water, and communication networks. The resulting local evidence can inform master and regional plans, development controls, infrastructure appraisals, disaster management plans, and building permission requirements. However, the national classes should not be converted directly into parcel-level zoning or engineering specifications and local data on hazards, vulnerability, and assets are required (Dodman et al. 2022; UNDRR 2022).

The methodological contribution of this study is the combination of the hazard count and multi-hazard screening score. The hazard count highlights the overlap of the highest classes, and the hazard score captures the accumulation across all classes. Neither metric measures risk, impact, or loss, and neither assumes linear differences between classes. Equal weighting improves reproducibility; however, future research can make the weighting methodology more robust. Furthermore, future sensitivity analyses could test alternative weighting and classification choices.

The value of the current method is to make diverse public datasets sufficiently comparable for national prioritisation while preserving source-specific caveats and providing an auditable bridge to higher-resolution modelling, vulnerability analysis, and regulatory evidence required at local scales.

Conclusion and way forward

India's hazard landscape is spatially structured, and hazard exposure differs across mountainous, coastal, plain, and semiarid settings. The evidence generated at the national scale and illustrative cases of states and cities using the proposed spatial framework for multi-hazard mapping indicates why multi-hazard evidence is more useful when interpreted geographically. However, differences in source data, classification, and resolution as well as the absence of vulnerability and loss modelling prevent the results' direct interpretation to identify local risk or expected impacts. Moving from screening to implementation requires periodically updating the open hazard and exposure layers and testing alternative classifications or weights. Data layers can be updated when the relevant standards or national datasets are revised, and climate- and reanalysis-based layers can also be refreshed when updated baseline periods or materially extended time series become available. Population, built-up areas, and employment exposure layers can also be refreshed in line with the Census, Economic Census, and corresponding GHSL update cycles. National results can be utilised to prioritise state and city studies, microzonation, hydraulic or geotechnical modelling, and infrastructure assessments. Furthermore, differentiated priorities can be addressed via a multi-hazard lens: seismic and slope management in mountain regions; drainage, coastal ecosystems, wind resilience, and evacuation in coastal areas; heat health and water security in inland regions; and floodplain, drainage, and critical-facility protection in riverine areas. Appendix E provides a decision-use matrix linking the national screening outputs to appropriate planning uses, limitations, and higher-resolution data requirements.

Similarly, the spatial evidence can be complemented by local evidence to inform masterplans and regional plans, development controls, building reviews, and disaster management plans. Accordingly, this working paper can inform planning authorities, disaster management agencies, infrastructure providers, urban local bodies, employers, and communities so that the evidence can be co-produced and implemented. For long-term operational use, the framework can be developed as an updatable data service rather than a static atlas—that is, it can be discussed, reviewed, owned, and managed in terms of quality. An open interactive platform can support this screening-to-action pathway, but development of enforceable regulations and project design requires ground truthing based on localised evidence.

Appendix A. Literature review process

1. Review objective and thematic focus: The review was guided by the study's scope of developing a multi-hazard spatial framework for India. It focused on multi-hazard assessment, hazard mapping, climate risk, disaster risk reduction, exposure analysis, and hazard-sensitive planning.
2. Sources and databases reviewed: Academic literature was reviewed using Google Scholar, Scopus, and ScienceDirect. We also reviewed institutional reports and datasets from the IPCC; UNDRR; World Bank; NDMA; BIS; IMD; BMTPC; WRI Aqueduct; NASA; European Centre for Medium-Range Weather Forecasts; Joint Research Centre and Copernicus Emergency Management Service; WRIS; CEEW; Department of Science and Technology; Indian Institute of Technology Guwahati; Indian Institute of Technology Mandi; and Center for Study of Science, Technology and Policy.
3. Keywords used for identification of relevant literature and data sources: The keywords included the following: multi-hazard assessment, compound hazards, hazard mapping, climate risk, disaster risk, exposure analysis, GIS-based hazard mapping, Indian hazard datasets, national policy and planning guidelines, and building codes.
4. Inclusion and exclusion criteria: Studies and datasets were included if they were relevant to India, nationally applicable, publicly accessible, methodologically transparent, and compatible with GIS-based spatial analyses. Duplicates, non-credible sources, blogs, and highly localised studies unsuitable for national-scale analyses were excluded.
5. Research gap identification: Gaps in the existing multi-hazard mapping literature, especially the limited availability of nationally comparable and GIS-based overlays covering multiple hazard types, were identified.
6. Evidence synthesis: Selected studies were reviewed to identify key hazards, datasets, indicators, methodological approaches, limitations, and knowledge gaps.

Appendix B. Hazard indicators, data sources, scale, and preprocessing or classification methods

Table B1 | **Geophysical hazards**

HAZARD CATEGORY	GEOPHYSICAL		
HAZARD INDICATOR	**SEISMIC ZONE**	**LANDSLIDE**	**COASTAL FLOODING**
Data source	BIS seismic zonation map and IS 1893[a]	NASA Global Landslide Susceptibility Map[b,c]	ALOS Global Digital Surface Model and ALOS World 3D – 30m of the Alaska Satellite Facility[d]
Method (pre-processing and classification)	Data obtained from BIS and classification used as per IS 1893: The zonation utilises a deterministic approach based on historical data, isoseismal maps, and seismotectonic features.	Data obtained from NASA and classes used as given in the original source (NASA): The map was generated using data on slope, faults, geology, forest loss, and road networks, which were combined using a heuristic fuzzy approach.	Raw DSM data were obtained, and areas were classified based on sea level rise susceptibility thresholds.
Classes	II = low risk III = medium risk IV = high risk V = very high risk	1 = very low 2 = low 3 = moderate 4 = high 5 = very high	<1 metre (m) 1–2 m 2–5 m 5–10 m >10 m

Notes: ALOS: Advanced Land Observing Satellite; BIS: Bureau of Indian Standards; DSM: digital surface model; GIS: geographic information system; GSI: Geological Survey of India; IS: Indian Standard; NASA: National Aeronautics and Space Administration; NLSM: National Landslide Susceptibility Mapping.

Source: a. BIS website: https://www.bis.gov.in/, b. NASA 2017, c. Stanley and Kirschbaum 2017, d. Earthdata n.d.

Table B1 | **Geophysical hazards (Cont.)**

HAZARD CATEGORY	GEOPHYSICAL		
HAZARD INDICATOR	**SEISMIC ZONE**	**LANDSLIDE**	**COASTAL FLOODING**
Reclassification done (yes or no)	Yes, source-based classification was done. BIS/IS 1893 zones were used directly because they are the nationally recognised seismic hazard categories.	Yes, source-based classification was done. NASA's original five susceptibility classes were used directly because the dataset already provides nationally comparable susceptibility categories.	Yes, threshold-based (Odisha storm) classification was done. Elevation bands were selected to identify progressively higher exposure in very low-lying coastal zones. The thresholds were informed by coastal-screening logic.
Harmonised classification	Zone II = Class 2 or low Zone III = Class 3 or moderate Zone IV = Class 4 or high Zone V = Class 5 or very high (Class 1 was not assigned because BIS seismic zonation for India begins at Zone II.)	Class 1 = very low Class 2 = low Class 3 = moderate Class 4 = high Class 5 = very high	Class 5 = <1 m Class 4 = 1–2 m Class 3 = 2–5 m Class 2 = 5–10 m Class 1 = >10 m or outside the low-elevation coastal band
Unit	No unit	No unit	Metres
Temporal scale	Static map	Static map	Static
Scale or resolution	Regional scale	~1 kilometre	30 m
Selection criteria or rationale for the dataset	The dataset was a government-vetted BIS dataset that was publicly available and nationally consistent and compatible with the GIS overlay.	It was a NASA dataset with adequate national-scale resolution and transparent methodology. The GSI-NLSM was also considered. NASA was retained for its spatially continuous, consistently classified raster suitable for national comparison, while the GSI-NLSM is more appropriate for detailed regional or local assessment.	The dataset had open DSM data, high spatial resolution, suitability for national coastal screening, and GIS compatibility.
Limitation	It is a zonation layer and does not capture local site conditions, soil amplification, or micro zonation within cities. The map does not include recent data and has coarse resolution.	The map is static and does not provide near real-time hazard assessment. It is not suitable for site-specific or local-scale assessments.	This is an elevation-based exposure proxy, not a hydrodynamic coastal-flood model. It does not simulate storm-surge height, tides, waves, coastal defences, drainage, or local flood pathways.

Notes: ALOS: Advanced Land Observing Satellite; BIS: Bureau of Indian Standards; DSM: digital surface model; GIS: geographic information system; GSI: Geological Survey of India; IS: Indian Standard; NASA: National Aeronautics and Space Administration; NLSM: National Landslide Susceptibility Mapping.

Source: a. BIS website: https://www.bis.gov.in/, b. NASA 2017, c. Stanley and Kirschbaum 2017, d. Earthdata n.d.

Table B2 | **Hydrological hazards**

HAZARD CATEGORY	HYDROLOGICAL		
HAZARD INDICATOR	**HYDROLOGICAL DROUGHT**	**GROUNDWATER STRESS (STAGE OF GROUNDWATER EXTRACTION)**	**RIVERINE FLOOD**
Data source	World Resources Institute (WRI) Aqueduct[a,b]	Central Ground Water Board (CGWB), Water Resources Information System (WRIS), 2017 and 2020 assessments[c]	Joint Research Centre and Copernicus Emergency Management Service (JRC/CEMS), Global Flood Awareness System (GloFAS) for 2024 to obtain the 100-year return period flood hazard layer
Method (pre-processing and classification)	Raw data and classes were obtained from WRI Aqueduct. Drought hazard was derived from a non-parametric analysis of historical precipitation deficits at the 0.5-degree resolution; drought exposure was based on a non-parametric aggregation of gridded indicators of population and livestock densities, crop cover, and water stress; and drought vulnerability was computed as the arithmetic composite of high-level factors of social, economic, and infrastructural indicators, collected at both the national and sub-national levels.	The stage of groundwater development compares gross groundwater extraction and annual extractable groundwater resource; it is expressed as a percentage. Two criteria were used to categorise each assessment unit: the stage of groundwater extraction and the long-term trend in groundwater level drop for pre- and post-monsoon records. Data downloaded from WRIS and classes were provided as per CGWB's groundwater assessment methodology.	Riverine flood hazard represents a 100-year return period flood event. The flood inundation maps were created by using the GloFAS and European Flood Awareness System re-analyses to generate flood event hydrographs for different return period events, which were then used as inputs to a two-dimensional hydraulic flood inundation model. The resulting individual small domains with the simulated maximum flood depth for each return period (10, 20, 50, 75, 100, 200 and 500 years) were mosaicked together to create a single gridded dataset.
Classes	0 = low 1–2 = low-medium 2–3 = medium 3–4 = medium-high 4–5 = high	≤70% = safe 70–90% = semi-critical 90–100% = critical >100% = overexploited or saline (assessment units where groundwater is predominantly saline)	0.1–1 metre (m) 1–2 m 2–3 m 3–5 m >5 m
Reclassification done (yes or no)	Yes, source-based classification was conducted. WRI Aqueduct's original risk-score categories were used because the dataset already provides comparable drought-risk classes.	Yes, source-based classification was conducted. The CGWB and WRIS categories were used because they are government-defined categories for groundwater assessment units.	Yes, the continuous modelled flood-depth raster was reclassified into depth bands. Classification was based on histogram review, natural-break logic, and interpretability of flood-depth thresholds.
Harmonised classification	Class 1 = 0 low Class 2 = 1–2 low-medium Class 3 = 2–3 medium Class 4 = 3–4 medium-high Class 5 = 4–5 high	Class 1 = safe Class 3 = semi-critical or saline Class 4 = critical Class 5 = overexploited	Class 1 = 0.1-1 m Class 2 = 1–2 m Class 3 = 2–3 m Class 4 = 3–5 m Class 5 = >5 m
Unit	No unit	No unit	Metres
Temporal scale	2000–14	2017 and 2020 assessments	Static map
Scale or resolution	Basin level	Block-level administrative data	~90 m

Source: a. WRI n.d., b. WRI 2019 c. Ministry of Jal Shakti, Government of India n.d.

Table B2 | **Hydrological hazards (Cont.)**

HAZARD CATEGORY	HYDROLOGICAL		
HAZARD INDICATOR	**HYDROLOGICAL DROUGHT**	**GROUNDWATER STRESS (STAGE OF GROUNDWATER EXTRACTION)**	**RIVERINE FLOOD**
Selection criteria or rationale for the dataset	Public WRI Aqueduct dataset that uses credible global methodology, has basin-scale national coverage, and is suitable for overlay analysis	Government-vetted CGWB and WRIS dataset that is publicly available, has transparent classification, and is compatible with the GIS overlay	Public JRC/CEMS dataset that includes a nationally consistent modelled inundation layer, has adequate resolution, and is GIS compatible
Limitations	The layer is basin level and is intended for strategic screening rather than local drought assessment.	The groundwater stress dataset is available at block or assessment-unit level, and so it may not capture intra-block variations in groundwater extraction, aquifer conditions, or local recharge.	The layer represents modelled riverine inundation and may not capture local drainage, embankment failure, pluvial flooding, or recent flood-protection infrastructure. Moreover, it does not capture pluvial flooding, drainage failure, or other forms of urban flooding.

Source: a. WRI n.d., b. WRI 2019 c. Ministry of Jal Shakti, Government of India n.d.

Table B3 | **Meteorological hazards (Part 1)**

HAZARD CATEGORY	METEOROLOGICAL		
HAZARD INDICATOR	**METEOROLOGICAL DROUGHT**	**EXTREME RAINFALL (HEAVY RAIN DAYS)**	**HEAT STRESS**
Data source	Gridded rainfall data from the India Meteorological Department (IMD)[a]	IMD (2000–21)[a]	ERA5-HEAT and the Universal Thermal Climate Index (UTCI) from World Resources Institute (WRI) India and European Centre for Medium-Range Weather Forecasts (ECMWF)[b]
Method (pre-processing and classification)	Frequency of drought at the pixel level was derived from rainfall data, and classes were determined based on the frequency of events. Initially, annual rainfall for each year was taken (1985–2020), and then the base layer was prepared by taking the mean of all the annual rainfall layers. Annual deficiency percentage (DP) for each year was computed as follows: *DP = [(base layer-each annual layer)/base layer)×100.* Layers with DP≥26 were considered as drought (based on IMD). Frequency of drought at a specific pixel was calculated as follows: *Frequency = count of number of times (≥26) pixel occurred in 36 years/36 years.* (IMD defines meteorological drought as a situation occurring in any area when the seasonal rainfall is deficient by 26% or more of its long-term normal.)	Maximum rainfall in each pixel for each year during 2000–21 was calculated to obtain one raster layer for each per year that represents the maximum daily rainfall within that year. Then, the maximum of these yearly rasters was calculated to obtain the final output, which was visualised in QGIS. The classification was based on that of IMD.	UTCI data for 1991–2021 were downloaded. Units were converted from Kelvin to degree Celsius, and daily maximum UTCI was calculated. The total number of days with maximum UTCI falling under each heat stress category was then computed and exported as a raster. The total number of days under strong-to-extreme heat stress was computed, and frequency of heat stress was calculated as follows: *total no. of days with daily maximum UTCI in the specified category/total number of days.* The raster was then visualised in QGIS, and processing was done in Python. The final layer was then visualised in QGIS.

Notes: ECMWF: European Centre for Medium-Range Weather Forecasts; ERA5: ECMWF Reanalysis version 5; HEAT: Human thermal comfort; QGIS: quantum geographic information system.

Source: a. Climate Prediction Group, India Meteorological Department n.d., b. Di Napoli et al. 2020.

Table B3 | **Meteorological hazards (Part 1) (Cont.)**

HAZARD CATEGORY	METEOROLOGICAL		
HAZARD INDICATOR	**METEOROLOGICAL DROUGHT**	**EXTREME RAINFALL (HEAVY RAIN DAYS)**	**HEAT STRESS**
Classes	0–0.05 0.05–0.1 0.1–0.2 0.2–0.33 >0.33	Extreme rainfall >= 204.5 millimetres (mm) Very heavy rainfall = 115.6–204.4 mm Heavy rainfall = 64.5–115.5 mm Moderate rainfall = 15.6–64.4 mm Light rainfall ≤ 15.5 mm	0–0.2 0.2–0.4 0.4–0.6 0.6–0.8 0.8–1
Reclassification done (yes or no)	Yes, a mixed source-based and statistical classification was conducted. The drought-event threshold was source-based, using IMD's ≥26% rainfall-deficiency definition. The final frequency classes were based on the frequency of events.	Yes, the IMD rainfall-intensity classes were retained and recoded into the common ordinal hazard scale.	Yes, a threshold-based and equal-interval classification was conducted. UTCI heat-stress thresholds were used to identify heat-stress days; the final frequency values were classified into equal intervals from 0 to 1 to make the layer comparable for national overlay.
Harmonised classification	Class 1 = 0–0.05 Class 2 = 0.05–0.1 Class 3 = 0.1–0.20 Class 4 = 0.20–0.33 Class 5 = >0.33	Class 1 = Light rainfall ≤ 15.5 mm Class 2 = Moderate rainfall 15.6–64.4 mm Class 3 = Heavy rainfall 64.5–115.5 mm Class 4 = Very heavy rainfall 115.6–204.4 mm Class 5 = Extreme rainfall ≥204.5 mm	Class 1 = 0–0.20 Class 2 = 0.20–0.40 Class 3 = 0.40–0.60 Class 4 = 0.60–0.80 Class 5 = 0.80–1.00
Unit	No unit	Millimetres	No unit
Temporal scale	Daily: 1985-2020	Daily: 2000–21	Hourly: 1991–2021
Scale or resolution	0.25°	0.25°	0.25°
Selection criteria or rationale for dataset	Public IMD rainfall data with credible long-term observations, adequate resolution for national analysis, and GIS compatibility	Public IMD rainfall data providing transparent IMD rainfall classes, adequate national-scale resolution, and GIS compatibility	Public ERA5-HEAT and ECMWF dataset using the internationally recognised UTCI method and having long-term coverage and GIS compatibility
Limitation	The drought estimate was based only on annual rainfall deficiency against the long-term mean, so it did not capture seasonal rainfall distribution, evapotranspiration, soil moisture, irrigation access, groundwater support, or agricultural drought impacts.	The IMD gridded rainfall dataset has a 0.25° spatial resolution, so it may have smoothed localised extreme rainfall, especially in urban, hilly, and coastal areas.	The ERA5 or ERA5-HEAT heat-stress estimates are reanalysis-based and may not have fully captured local heat extremes influenced by urban heat islands, land cover, elevation, or humidity variations.

Notes: ECMWF: European Centre for Medium-Range Weather Forecasts; ERA5: ECMWF Reanalysis version 5; HEAT: Human thermal comfort; QGIS: quantum geographic information system.

Source: a. Climate Prediction Group, India Meteorological Department n.d., b. Di Napoli et al. 2020.

Table B4 | **Meteorological hazards (Part 2)**

HAZARD CATEGORY	METEOROLOGICAL			
HAZARD INDICATOR	**COLD STRESS**	**LIGHTNING**	**EXTREME WIND**	**CYCLONE**
Data source	ERA5-HEAT (WRI India and ECMWF)[a]	NASA GHRC (1995–2014)[b]	ECMWF ERA5 (2000–24)[c]	IMD E-Atlas with the historical cyclone archive (1891–2020)
Method (pre-processing and classification)	UTCI data for 1991–2021 were downloaded. Units were converted from Kelvin to degree Celsius. Daily minimum UTCI was calculated. The total number of days falling under each cold stress category were then computed and exported as raster. The sum of total days under moderate-to-extreme cold stress was computed. The frequency of cold stress was calculated as follows: total no. of days with daily minimum UTCI in the specified category/ total number of days. The processing was done in Python. The final layer was then visualised in QGIS.	The HRFC_COM_FR is a product from the LIS–OTD gridded climatology dataset. It provides the mean annual flash rate globally. Raw data were downloaded, processed, and clipped to the India boundary.	Instantaneous wind gust data from the ERA5 Reanalysis were imported into GEE. Maximum wind speed over the time period was calculated. For each day, we checked whether the frequency of any pixel value exceeded 25%. Such dates were omitted as data errors. Classification was done using pretty breaks.	The intensity-wise raster files for cyclone for intensity categories (Depression, deep depression, cyclonic storm and severe cyclonic storm) were downloaded from the specified source for 1891–2020. The raster data was then geocoded and converted to polylines using Python. The vector files are then cleaned (arrows and circles removed). Buffers of 100 kilometres were created to represent broad proximity to historical cyclone paths. A uniform buffer was used because the available dataset contains track information only, while the actual affected area varies across cyclone systems and depends on multiple storm characteristics. Therefore, the buffer is a national screening proxy and should not be interpreted as the observed impact footprint of individual cyclones. Furthermore, a new column was added with the value of one assigned to all the buffers. The total number of cyclones (along with buffers) that have occurred at any given location was calculated using the following code in GEE. The downloaded raster was visualised in QGIS, and finally classes were created based on the cyclone count. Classes were chosen based on visual interpretation.
Classes	0–0.05 0.05–0.1 0.1–0.2 0.2–0.33 >0.33	0–5 5–10 10–15 15–20 >20	≤20 20–25 25–30 30–35 35–50	0 1-3 3–8 8–15 >15

Notes: ECMWF: European Centre for Medium-Range Weather Forecasts; ERA5: ECMWF Reanalysis version 5; GEE: Google Earth Engine; GHRC: Global Hydrometeorology Resource Center; HEAT: Human thErmAl comfort; HRFC_COM_FR: High Resolution Full Climatology Combined Flash Rate; IMD: India Meteorological Department; LIS–OTD: Lightning Imaging Sensor–Optical Transient Detector; NASA: National Aeronautics and Space Administration; QGIS: Quantum geographic information system; UTCI: Universal Thermal Climate Index; WRI: World Resources Institute.

Source: a. Di Napoli et al. 2020, b. Cecil 2025, c. Copernicus Climate Change Service, Climate Data Store 2023.

Table B4 | **Meteorological hazards (Part 2) (Cont.)**

HAZARD CATEGORY	METEOROLOGICAL			
HAZARD INDICATOR	**COLD STRESS**	**LIGHTNING**	**EXTREME WIND**	**CYCLONE**
Reclassification done (yes or no)	Yes, a mixed source-threshold and frequency-based classification was conducted. UTCI thresholds defined cold-stress days, while final frequency classes were based on the frequency of events.	Yes, mean annual flash-rate values were reclassified into five equal-interval classes for overlay.	Yes, continuous wind-gust values were reclassified into five wind-speed classes using pretty breaks.	Yes, count-based and histogram-informed classification was conducted. Cyclone incidence was calculated as the number of cyclone-track buffers intersecting a location. Class breaks were selected using the distribution of historical cyclone counts; histogram review; and interpretability of low, moderate, high, and very-high incidence zones.
Harmonised classification	Class 1 = 0–0.05 Class 2 = 0.05–0.1 Class 3 = 0.1–0.20 Class 4 = 0.20–0.33 Class 5 = >0.33	Class 1 = 0–5 flashes per square kilometre per year (flashes/km^2/year) Class 2 = 5–10 flashes/ km^2/year Class 3 = 10–15 flashes/ km^2/year Class 4 = 15–20 flashes/ km^2/year Class 5 is > 20 flashes/ km^2/year	Class 1 ≤ 20 metres per second (m/s) Class 2 = 20–25 m/s Class 3 = 25–30 m/s Class 4 = 30–35 m/s Class 5 = 35–50 m/s	Class 1 = 0 or no recorded cyclone incidence Class 2 = 1–3 Class 3 = 3–8 Class 4 = 8–15 Class 5 is = > 15
Unit	No unit	Flashes/km^2/year	Metres per second	Cyclone count
Temporal scale	Hourly: 1991–2021	Monthly: 1995–2014	Hourly: 2000–24	1891–2020
Scale or resolution	0.25°	0.5°	0.25°	National
Selection criteria or rationale for the dataset	Public ERA5-HEAT and ECMWF dataset with a transparent UTCI framework, adequate national-scale resolution, and GIS compatibility	Public NASA dataset with credible satellite climatology, national coverage, and suitability for overlay analysis	Public ERA5 and ECMWF reanalysis data with long-term national coverage, transparent processing, and GIS compatibility	Official IMD historical archive that is publicly accessible, a credible national source, and compatible with GIS-based incidence mapping
Limitations	ERA5 and ERA5-HEAT are reanalysis based and may not fully capture local microclimatic variations caused by elevation, land cover, urban form, or cold-air drainage.	The LIS–OTD HRFC lightning dataset is based on long-term climatology, so it represents average lightning flash-rate patterns rather than year-wise events or recent changes after 2014.	The data may not fully capture local wind extremes influenced by terrain, urban form, vegetation, or coastal effects.	The IMD Cyclone E-Atlas is a historical track-based archive, and so cyclone incidence reflects recorded cyclone paths rather than direct measurements of local damage, exposure, or intensity at each location.

Notes: ECMWF: European Centre for Medium-Range Weather Forecasts; ERA5: ECMWF Reanalysis version 5; GEE: Google Earth Engine; GHRC: Global Hydrometeorology Resource Center; HEAT: Human thErmAl comfort; HRFC_COM_FR: High Resolution Full Climatology Combined Flash Rate; IMD: India Meteorological Department; LIS–OTD: Lightning Imaging Sensor–Optical Transient Detector; NASA: National Aeronautics and Space Administration; QGIS: Quantum geographic information system; UTCI: Universal Thermal Climate Index; WRI: World Resources Institute.

Source: a. Di Napoli et al. 2020, b. Cecil 2025, c. Copernicus Climate Change Service, Climate Data Store 2023.

Table B5 | **Environmental hazards**

HAZARD CATEGORY	ENVIRONMENTAL
HAZARD INDICATOR	**AIR QUALITY ($PM_{2.5}$)**
Data source	Atmospheric Composition Analysis Group (ACAG), Washington University (1998–2022)[a,b]
Method (pre-processing and classification)	Air pollution was represented using monthly ground-level $PM_{2.5}$ concentration estimates at 0.01° (~1 kilometre [km]) resolution. The mean of maximum yearly concentration of all the years was assigned to each corresponding pixel. Processing was done in GEE. Classes as per the US EPA were used.
Classes	Good = 0–9.0 Moderate = 9.1–35.4 Unhealthy for sensitive groups = 35.5–55.4 Unhealthy = 55.5–125.4 Very unhealthy = 125.5–225.4
Reclassification done (yes or no)	Yes, continuous $PM_{2.5}$ concentration values were reclassified using US EPA concentration breakpoints and then recoded into the common ordinal hazard scale for overlay.
Harmonised classification	Class 1 = 0–9.0 micrograms per cubic metre (µg/m^3): good Class 2 = 9.1–35.4 µg/m^3: moderate Class 3 = 35.5–55.4 µg/m^3: unhealthy for sensitive groups Class 4 = 55.5–125.4 µg/m^3: unhealthy Class 5 = 125.5–225.4 µg/m^3: very unhealthy
Unit	µg/m^3
Temporal scale	Monthly: 1998–2022
Scale or resolution	~1 km
Selection criteria or rationale for the dataset	Public ACAG dataset with high spatial resolution, transparent satellite-model methodology, and suitability for national overlay analysis
Limitations	The $PM_{2.5}$ dataset is satellite-derived and modelled, rather than based solely on ground-monitoring stations, and so local pollution hotspots may not be fully captured.

Notes: EPA: US Environmental Protection Agency; GEE: Google Earth Engine; $PM_{2.5}$: particulate matter finer than 2.5 micrometres in diameter.

Source: a. van Donkelaar et al. 2024, b. Washington University in St. Louis 2026.

Appendix C. Research methodology limitations and caveats (extended)

The extended methodological caveats relevant to interpreting and applying the framework are summarised below.

1. National-scale screening: The proposed framework is intended for national-scale screening and prioritisation. It does not replace statutory hazard maps, seismic microzonation, local hydraulic or hydrological models, geotechnical studies, city-level risk assessments, or project-level engineering assessments. This spatial framework of multi-hazard mapping complements the aforementioned.
2. Indicator and conceptual comparability: The proposed framework combines episodic hazards, climatic stresses, susceptibility indicators, and environmental or resource stresses that represent different physical processes and impact pathways. The indicators were selected individually based on national relevance, literature support, data availability, methodological transparency, and spatial compatibility before being grouped into four domains. Therefore, their integration represents spatial concentration of the selected indicators rather than a common measure of physical hazard magnitude or disaster risk.
3. Classification and Class 5 comparability across indicators: Classification methods differ across indicators, including official standards and statistically derived thresholds. Therefore, Class 5 represents the highest category within each indicator only and does not imply equivalent rarity, probability, or physical intensity across hazards; for example, Class 5 earthquakes are not equivalent to Class 5 floods.
4. Spatial, temporal, and uncertainty indicators: The input datasets differ in terms of native resolution, reference period, and data vintage. Resampling to a common grid is a spatial harmonisation step for multi-hazard overlays and does not create finer-resolution information. The final output is constrained by the coarsest input layer. Comparable quantitative uncertainty measures are also unavailable across all datasets; therefore, a common confidence score was not obtained. The native resolution, temporal coverage, and dataset-specific limitations are reported in Appendix B.
5. Multi-indicator screening score and weighting: The cumulative score sums the ordinal classes using equal-indicator weighting, with each indicator contributing a weight of one. Ordinal classes are not equal-interval measurements, and the score should not be interpreted as an absolute measure of severity, probability, vulnerability, or expected loss. Consequently, domains containing more indicators exerted greater influence because they contained more independently selected nationally relevant indicators, not because additional domain-level weights were assigned.
6. Sensitivity and normalisation: Alternative weighting, classification, indicator selection, and leave-one-indicator-out scenarios were not tested in this first-stage study; therefore, hotspot stability under alternative methodological choices was not quantified (Beccari 2016; OECD et al. 2008). Min–max normalisation only rescaled the observed raw score of 10–54 to 0–1 for presentation and did not change its relative ordering, although the visual range remained dependent on the observed minimum and maximum values.
7. Spatial co-occurrence: The overlays identified where different hazard and stress indicators occur within the same geographical area. They did not establish whether hazards occur simultaneously, share causal drivers, interact physically, trigger cascading effects, or constitute compound events.
8. Exposure and validation: Employment metrics in this study referred to establishment-based employment derived from Economic Census 2013–14. Economic data on employment were taken only as a representative proxy and did not reflect any other parameters such as economic output, productivity, or other economic parameters. Population, built-up area, and employment represented exposure only and did not capture vulnerability, adaptive capacity, livelihoods, productivity, mortality, losses, or service disruptions. Population and employment also relied on GHSL built-up information and were, therefore, not fully independent spatial measures. The screening scores and exposure outputs were not validated against historical mortality, economic losses, crop damage, infrastructure disruption, or relief expenditures.
9. Case-study and city-scale: Tamil Nadu, Madhya Pradesh, and the 10 cities were selected purposively to illustrate contrasting geographical and hazard settings and are not statistically representative of high- and low-hazard cases. City outputs are national screening layers clipped to CBUA boundaries and should not be interpreted as ward-, neighbourhood-, or parcel-level hazard zones.

Appendix D. Case studies of select cities

Figure D1 | **Exposures of the population by hazard class for Bengaluru, Chennai, Delhi Municipal Corporation (DMC), Gangtok, Greater Mumbai, Jodhpur, Kolkata, Lucknow, Shimla, and Srinagar**



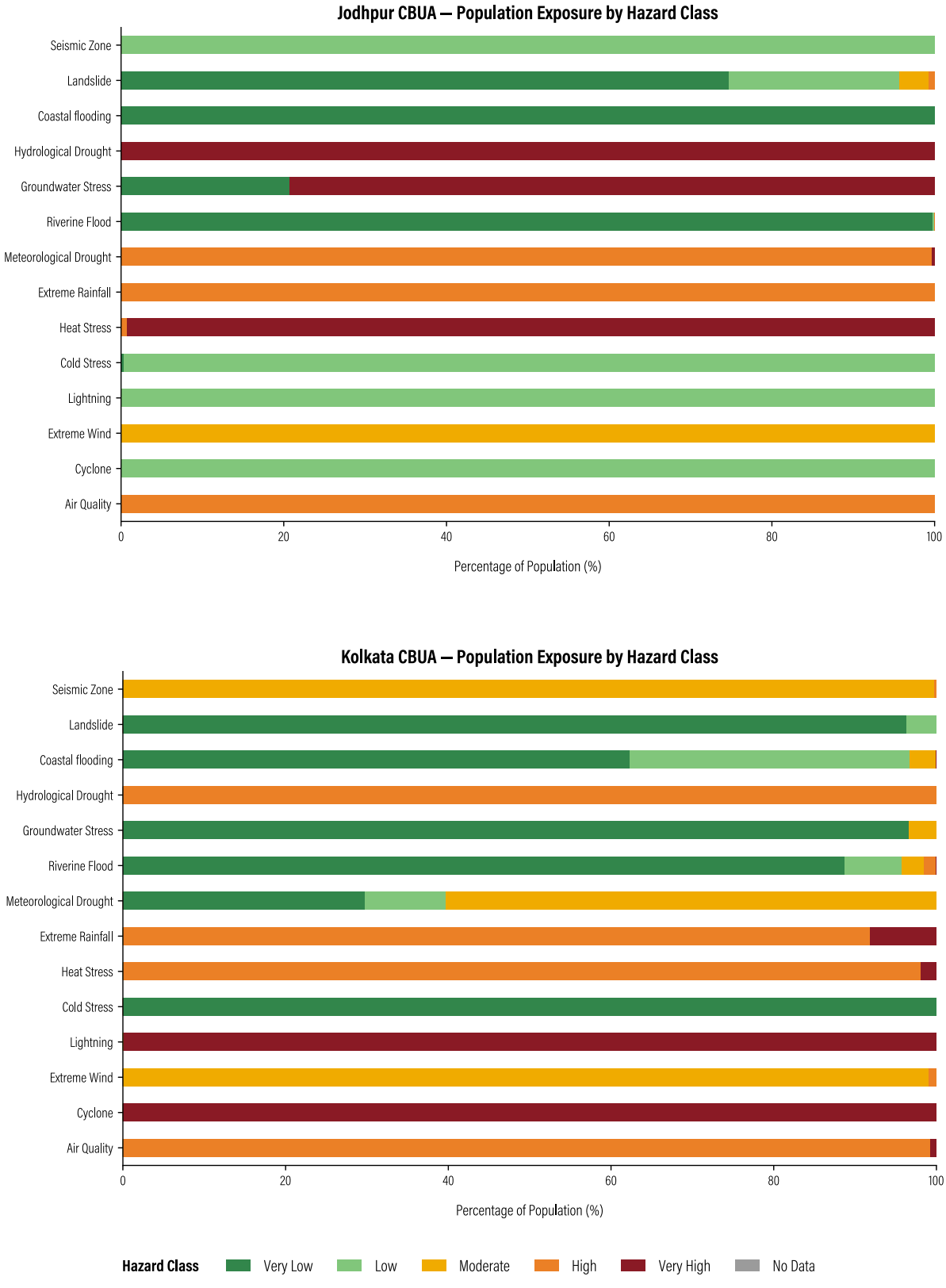
Source: Authors' analysis.

Figure D1 | **Exposures of the population by hazard class for Bengaluru, Chennai, Delhi Municipal Corporation (DMC), Gangtok, Greater Mumbai, Jodhpur, Kolkata, Lucknow, Shimla, and Srinagar (Cont.)**



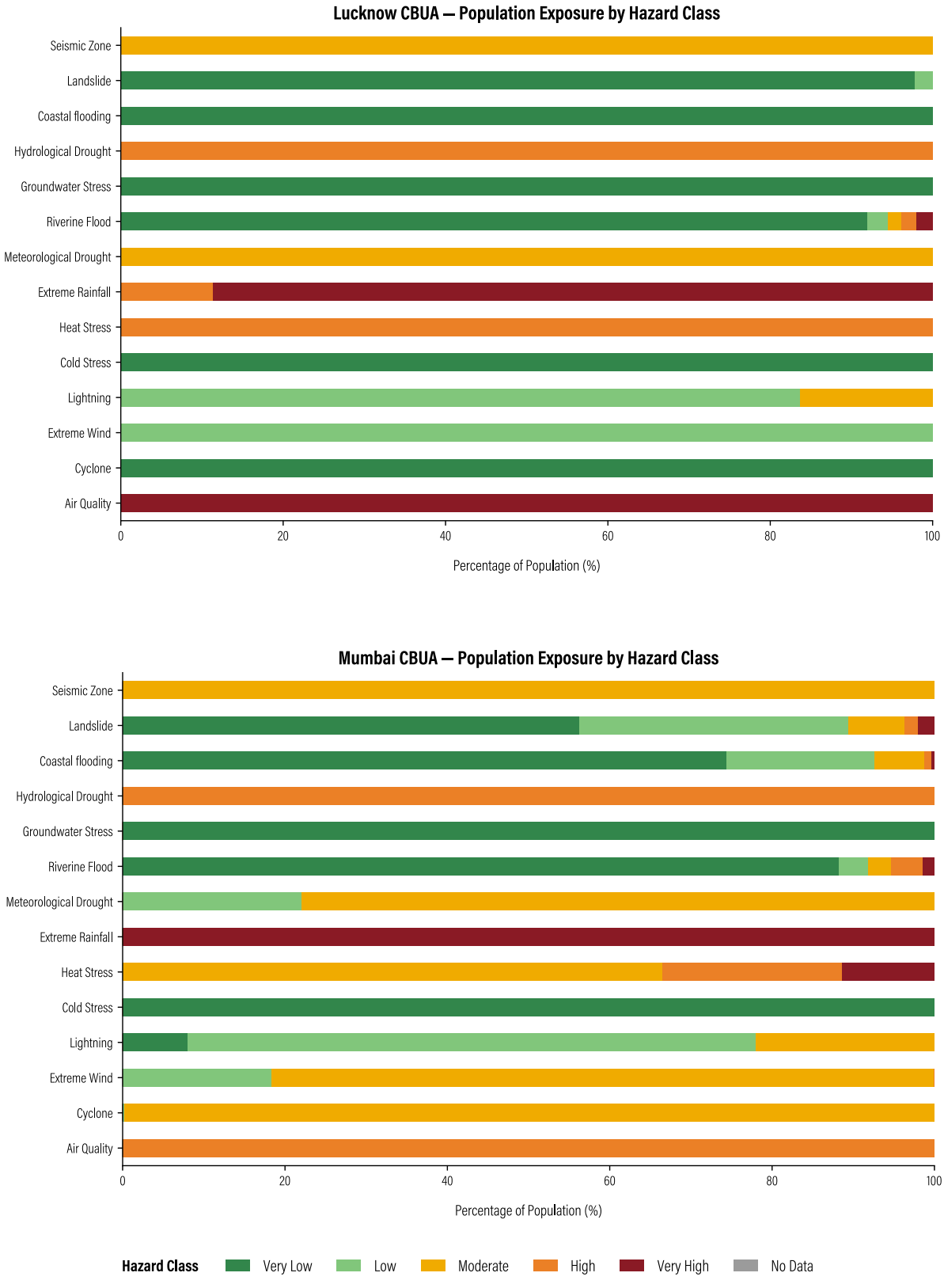
Source: Authors' analysis.

Figure D1 | **Exposures of the population by hazard class for Bengaluru, Chennai, Delhi Municipal Corporation (DMC), Gangtok, Greater Mumbai, Jodhpur, Kolkata, Lucknow, Shimla, and Srinagar (Cont.)**



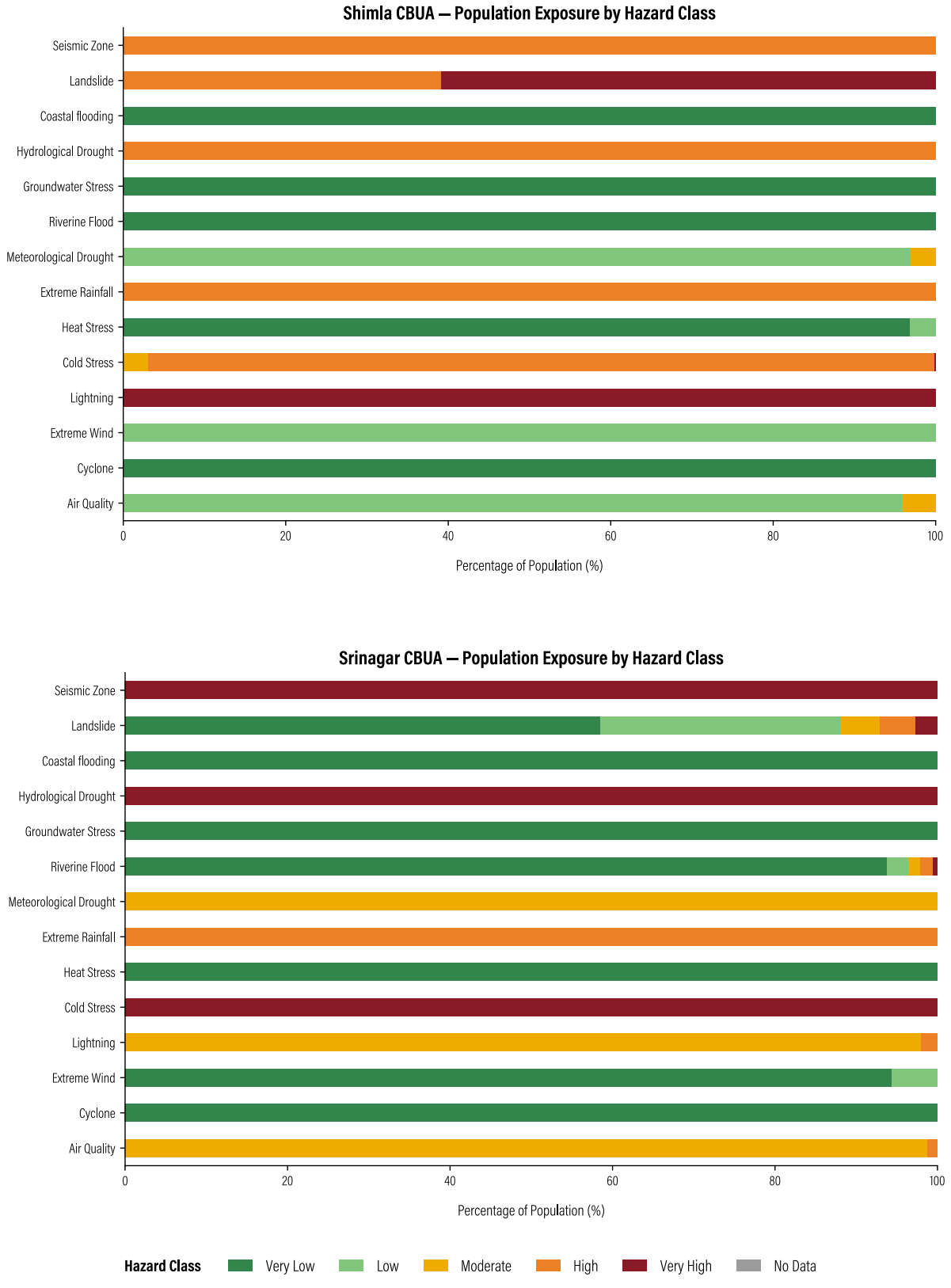
Source: Authors' analysis.

Figure D1 | **Exposures of the population by hazard class for Bengaluru, Chennai, Delhi Municipal Corporation (DMC), Gangtok, Greater Mumbai, Jodhpur, Kolkata, Lucknow, Shimla, and Srinagar (Cont.)**



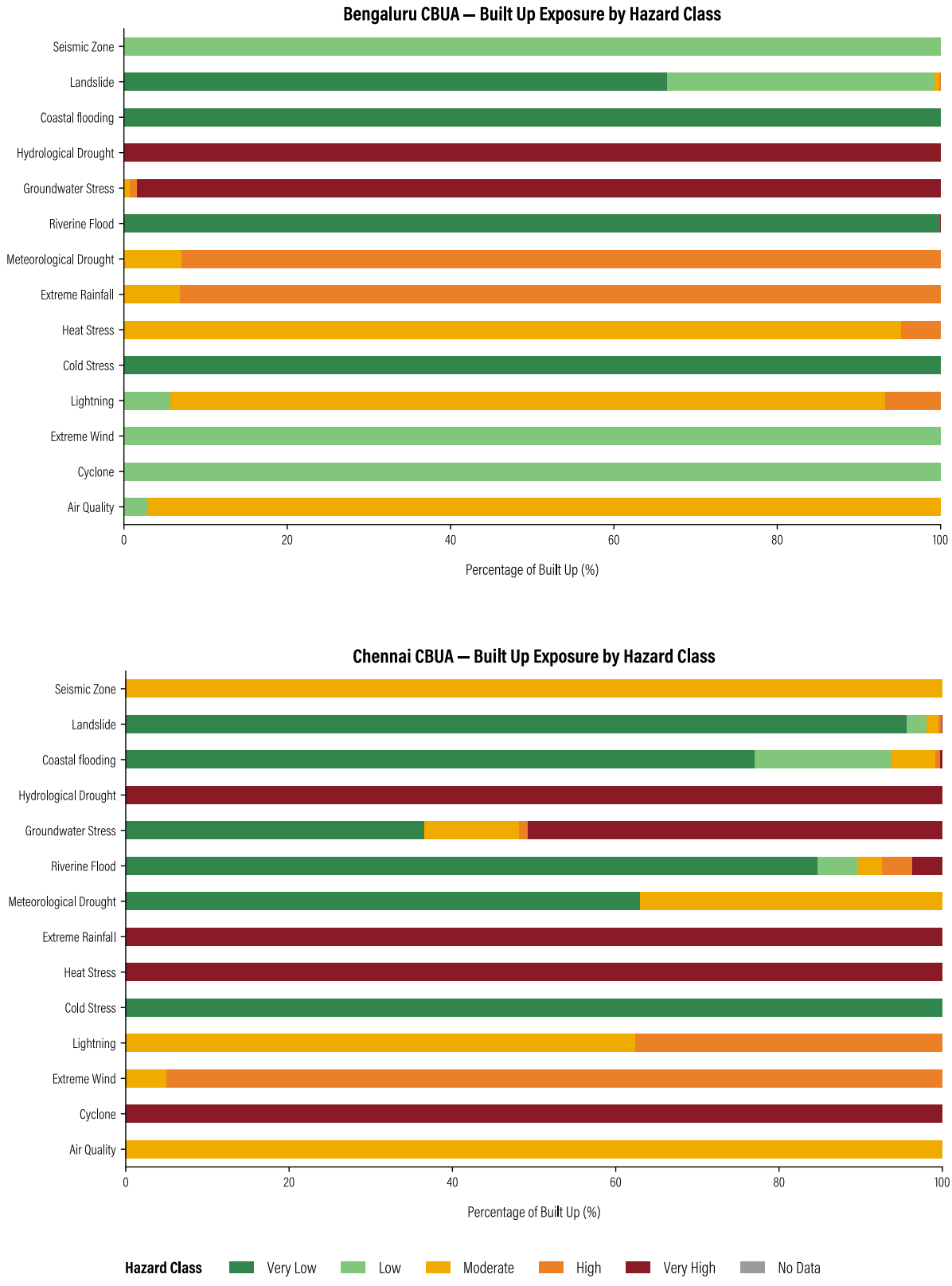
Source: Authors' analysis.

Figure D1 | **Exposures of the population by hazard class for Bengaluru, Chennai, Delhi Municipal Corporation (DMC), Gangtok, Greater Mumbai, Jodhpur, Kolkata, Lucknow, Shimla, and Srinagar (Cont.)**



Source: Authors' analysis.

Figure D2 | **Exposures of the built-up areas by hazard class for Bengaluru, Chennai, Delhi Municipal Corporation (DMC), Gangtok, Greater Mumbai, Jodhpur, Kolkata, Lucknow, Shimla, and Srinagar**



Source: Authors' analysis.

Figure D2 | **Exposures of the built-up areas by hazard class for Bengaluru, Chennai, Delhi Municipal Corporation (DMC), Gangtok, Greater Mumbai, Jodhpur, Kolkata, Lucknow, Shimla, and Srinagar (Cont.)**



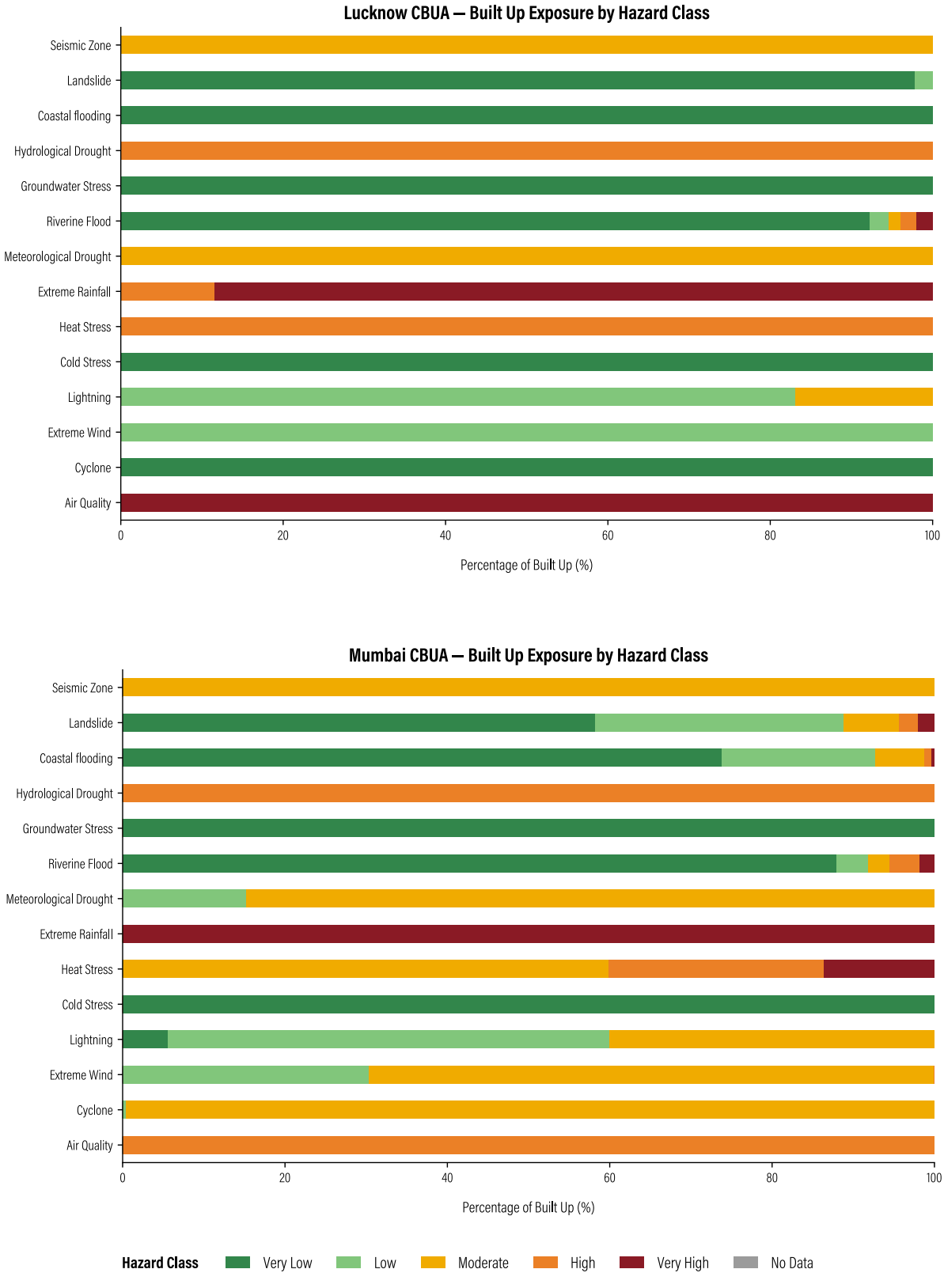
Source: Authors' analysis.

Figure D2 | **Exposures of the built-up areas by hazard class for Bengaluru, Chennai, Delhi Municipal Corporation (DMC), Gangtok, Greater Mumbai, Jodhpur, Kolkata, Lucknow, Shimla, and Srinagar (Cont.)**



Source: Authors' analysis.

Figure D2 | **Exposures of the built-up areas by hazard class for Bengaluru, Chennai, Delhi Municipal Corporation (DMC), Gangtok, Greater Mumbai, Jodhpur, Kolkata, Lucknow, Shimla, and Srinagar (Cont.)**



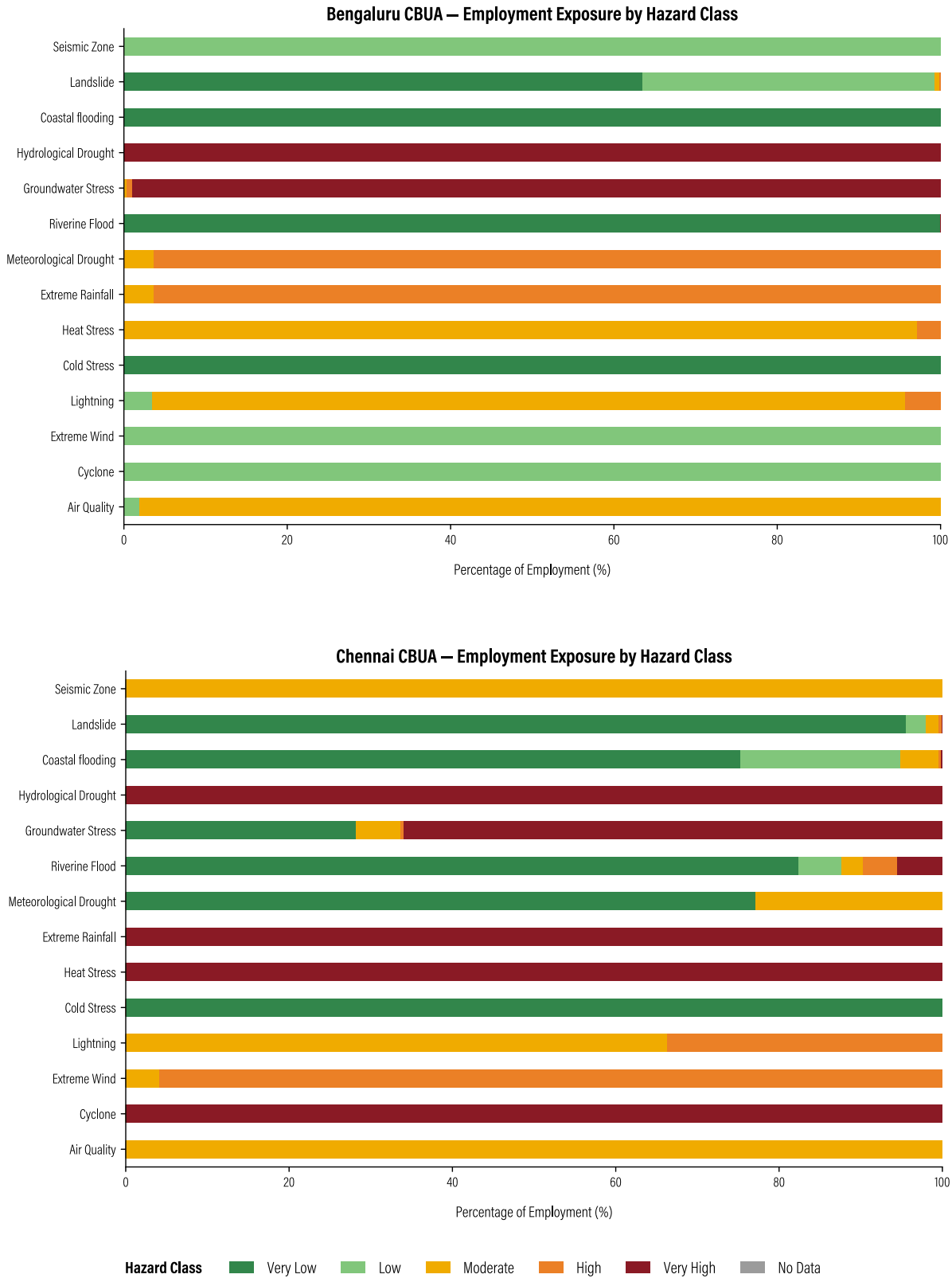
Source: Authors' analysis.

Figure D2 | **Exposures of the built-up areas by hazard class for Bengaluru, Chennai, Delhi Municipal Corporation (DMC), Gangtok, Greater Mumbai, Jodhpur, Kolkata, Lucknow, Shimla, and Srinagar (Cont.)**



Source: Authors' analysis.

Figure D3 | **Exposures of the employment by hazard class for Bengaluru, Chennai, Delhi Municipal Corporation (DMC), Gangtok, Greater Mumbai, Jodhpur, Kolkata, Lucknow, Shimla, and Srinagar**



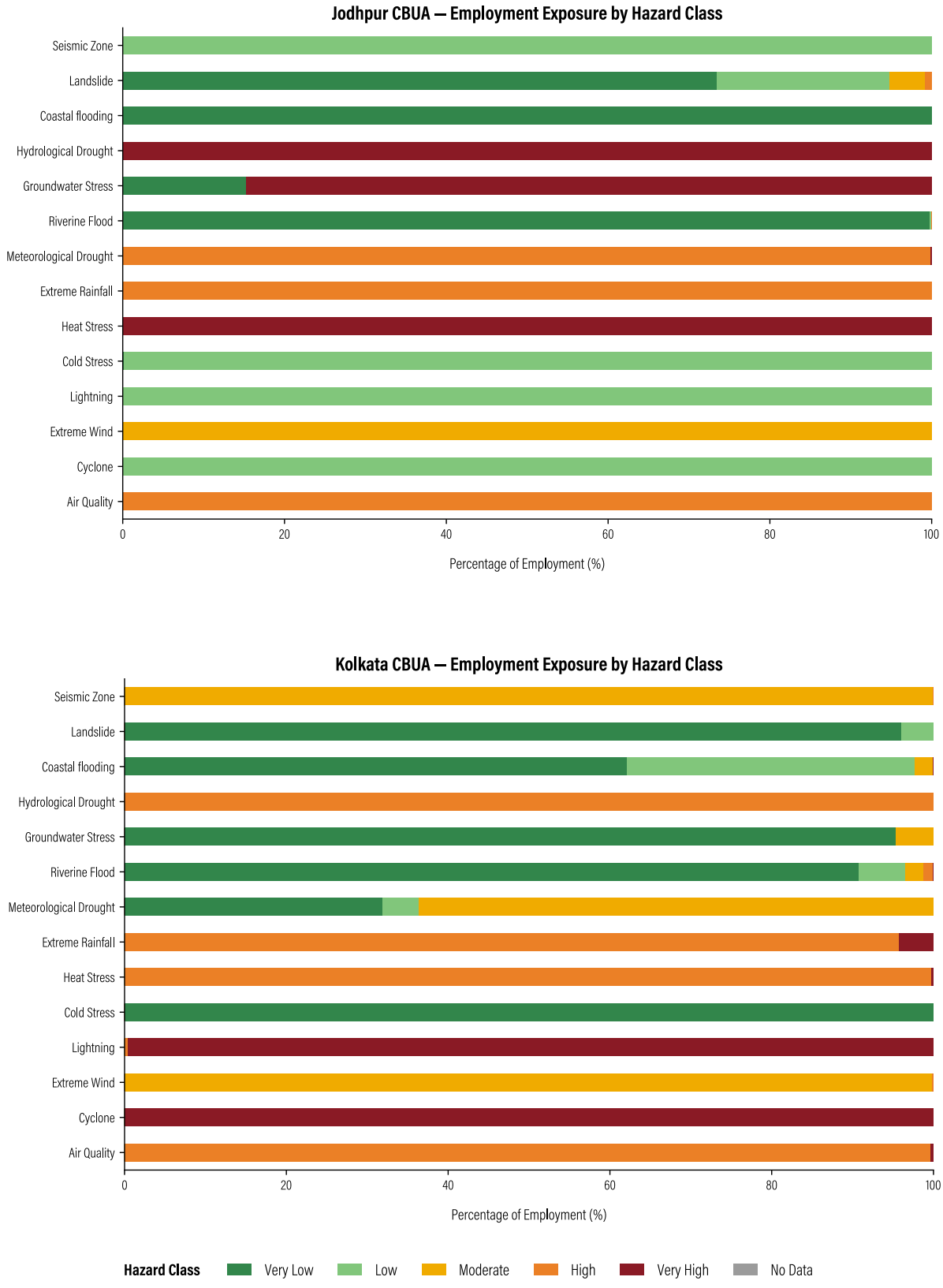
Source: Authors' analysis.

Figure D3 | **Exposures of the employment by hazard class for Bengaluru, Chennai, Delhi Municipal Corporation (DMC), Gangtok, Greater Mumbai, Jodhpur, Kolkata, Lucknow, Shimla, and Srinagar (Cont.)**



Source: Authors' analysis.

Figure D3 | **Exposures of the employment by hazard class for Bengaluru, Chennai, Delhi Municipal Corporation (DMC), Gangtok, Greater Mumbai, Jodhpur, Kolkata, Lucknow, Shimla, and Srinagar (Cont.)**



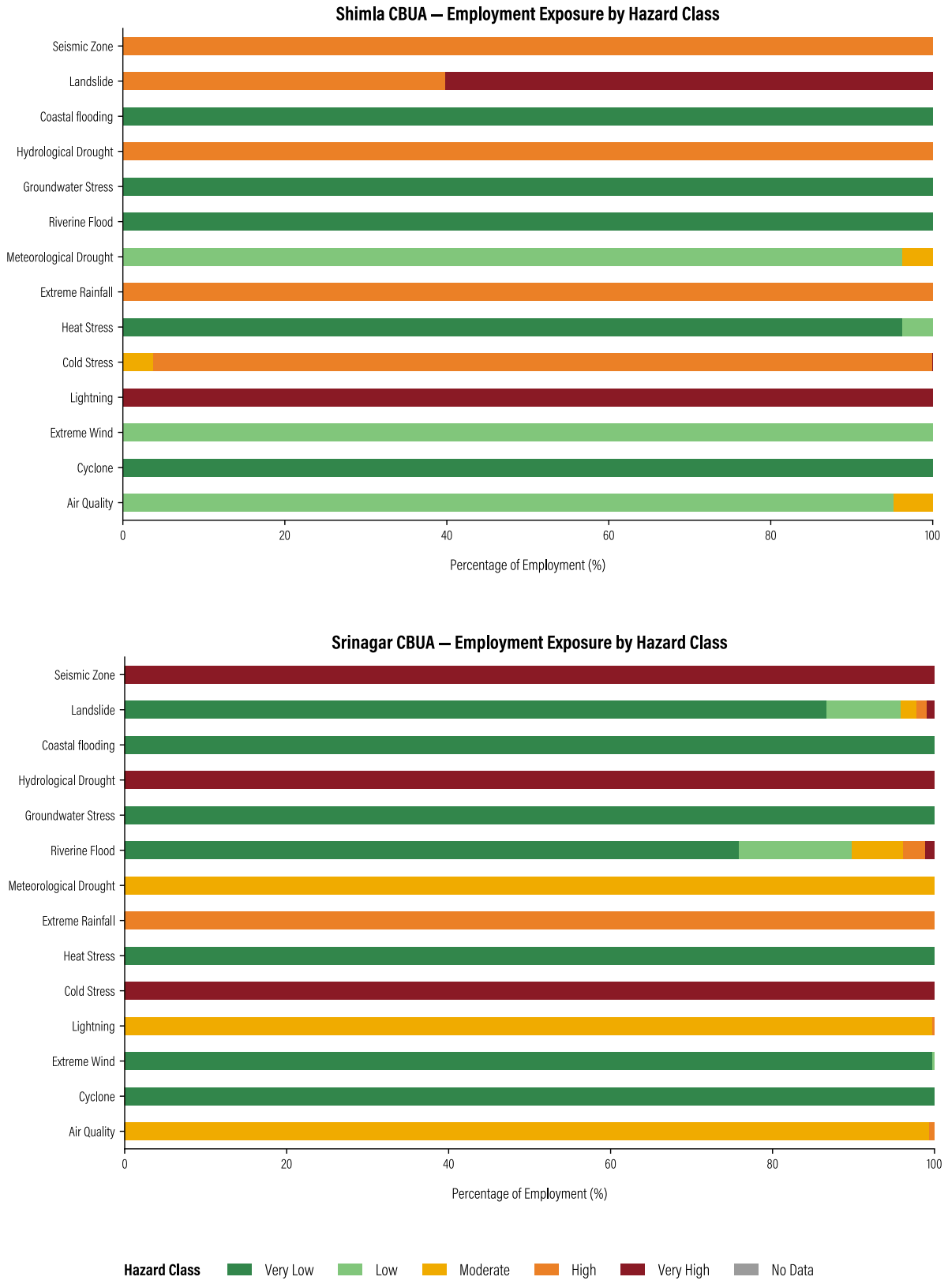
Source: Authors' analysis.

Figure D3 | **Exposures of the employment by hazard class for Bengaluru, Chennai, Delhi Municipal Corporation (DMC), Gangtok, Greater Mumbai, Jodhpur, Kolkata, Lucknow, Shimla, and Srinagar (Cont.)**



Source: Authors' analysis.

Figure D3 | **Exposures of the employment by hazard class for Bengaluru, Chennai, Delhi Municipal Corporation (DMC), Gangtok, Greater Mumbai, Jodhpur, Kolkata, Lucknow, Shimla, and Srinagar (Cont.)**



Source: Authors' analysis.

Appendix E. Decision-use matrix for the national screening framework

Table E1 | **Decision-use matrix for the national screening framework**

DECISION LEVEL	APPROPRIATE USE OF THE NATIONAL FRAMEWORK	USES REQUIRING MORE DETAILED DATA	DATASET PRECEDENCE
National	Comparing broad spatial patterns, identifying hazard and stress indicators requiring policy attention, identifying national data gaps, and prioritising states or regions for further assessment	Statutory zoning, infrastructure design, site selection, or determination of local development assessments	The national screening framework may be used as the primary comparative layer where a more detailed authoritative dataset is not available.
State or regional	Screening districts, development corridors, and infrastructure portfolios, and identifying locations requiring detailed multi-hazard studies	Preparation of regulatory hazard zones, engineering specifications, or project approvals	Official state hazard maps and sector-specific datasets take precedence where available.
City or local	Preliminarily screening growth areas, critical facilities, and service networks, and identifying priorities for local assessment	Master-plan zoning, development controls, floodplain delineation, slope regulation, microzonation, or infrastructure design	Statutory planning datasets, local hydraulic models, seismic microzonation, and officially adopted city or district hazard maps take precedence.

Source: Authors' synthesis based on BMTPC (2019), NDMA (2019), Ministry of Urban Development (2014), Bureau of Indian Standards (2015; 2016a; 2016b; 2016c), and Amarnath et al. (2021).

Abbreviations

ACAG	Atmospheric Composition Analysis Group
ALOS	Advanced Land Observing Satellite
BIS	Bureau of Indian Standards
BMTPC	Building Materials and Technology Promotion Council
CBUA	Contiguously Built Urban Agglomeration
CEEW	Council on Energy, Environment and Water
CGWB	Central Ground Water Board
DSM	Digital surface model
ECMWF	European Centre for Medium-Range Weather Forecasts
ERA5	ECMWF Reanalysis version 5
GEE	Google Earth Engine
GHRC	Global Hydrometeorology Resource Center
GHSL	Global Human Settlement Layer
GIS	Geographic information system
GloFAS	Global Flood Awareness System
GSI	Geological Survey of India
HEAT	Human thermal comfort
HRFC_COM_FR	High Resolution Full Climatology Combined Flash Rate
IMD	India Meteorological Department
IPCC	Intergovernmental Panel on Climate Change
JRC/CEMS	Joint Research Centre and Copernicus Emergency Management Service
LIS-OTD	Lightning Imaging Sensor–Optical Transient Detector
NASA	National Aeronautics and Space Administration
NDMA	National Disaster Management Authority
NLSM	National Landslide Susceptibility Mapping
$PM_{2.5}$	Particulate matter finer than 2.5 micrometres in diameter
QGIS	Quantum Geographic Information System
UNDRR	United Nations Office for Disaster Risk Reduction
USEPA	US Environmental Protection Agency
UTCI	Universal Thermal Climate Index
WRI	World Resources Institute
WRIS	Water Resources Information System

Glossary

Analysis unit: The spatial unit at which harmonised hazard layers are compared in the overlay analysis

Air Quality Index: A composite air-quality measure: If only $PM_{2·5}$ is used, the paper should refer to $PM_{2·5}$ concentration or $PM_{2·5}$-based categories

CBUA: A continuous stretch of built-up area as delineated through satellite imagery that lies within and around a statutory town and transcends both urban and rural local bodies that are spatially connected and form a single agglomerated settlement

Cold stress: Thermal conditions that can cause physiological stress due to low temperature and related atmospheric conditions

Co-occurring hazard: A situation where multiple hazards occur together, sequentially, or interact in ways that can increase impact

Digital elevation model: A spatial dataset representing ground elevation

Employment: Number of jobs within establishments

Exposure: The presence of people, built-up areas, employment, infrastructure, or assets in hazard-prone areas

Extreme class or Class 5: The highest indicator-specific hazard or stress category used in this study: It represents the extreme class for that indicator and does not imply equivalent rarity, probability, or physical intensity across different indicators

GEE: Google Earth Engine, a cloud-based platform used for large-scale geospatial data processing and analysis

GHSL: Global Human Settlement Layer, a global dataset used to estimate built-up areas and population distribution

GIS: Geographic information system, a system used to store, analyse, and map spatial data

Hazard class: A category assigned to a hazard layer, usually ranging from low to very high

Hazard indicator: A measurable variable used to represent a hazard, such as flood depth, seismic zone, heat stress, or $PM_{2·5}$ concentration

Heat stress: Thermal conditions that can cause physiological stress due to high temperature and related atmospheric conditions

Inundation depth: The depth of floodwater above ground level

Min–max normalisation: A method that rescales values to a common 0–1 range using the minimum and maximum observed values

Multi-hazard screening score: A relative composite score created by summing the harmonised ordinal classes of the included hazard indicators to show their spatial overlap: It is a screening measure and does not represent absolute hazard severity, probability, vulnerability, or risk

Nature-based solutions: Actions that protect, sustainably manage, and restore natural or modified ecosystems to address societal challenges while providing benefits for human well-being and biodiversity (Swann et al. 2021)

$PM_{2·5}$: Fine particulate matter with a diameter of 2.5 micrometres or smaller, used as an air pollution indicator

Raster: A grid-based spatial data format made up of pixels, often used for rainfall, temperature, elevation, or hazard layers

Reclassification: The process of converting raw data values into standard categories or classes

Risk-informed planning: Planning that uses hazard and exposure evidence to guide development, infrastructure, and regulatory decisions

Spatial overlay: A GIS method that combines multiple spatial layers to identify overlaps or relationships

Storm surge: Abnormal rise in sea level caused by a storm or cyclone, often leading to coastal flooding

UTCI: Universal Thermal Climate Index, an index that estimates outdoor human thermal stress using air temperature, humidity, wind speed, and radiation

UTCI categories: UTCI thermal-stress categories include extreme cold stress < –40°C; very strong cold stress = –40°C to –27°C; strong cold stress = –27°C to –13°C; moderate cold stress = –13°C to 0°C; slight cold stress = 0°C to 9°C; no thermal stress = 9°C to 26°C; moderate heat stress = 26°C to 32°C; strong heat stress = 32°C to 38°C; very strong heat stress = 38°C to 46°C; and extreme heat stress > 46°C

Vector: A spatial data format representing features as points, lines, or polygons, such as cyclone tracks or administrative boundaries

WRI Aqueduct: A water-risk mapping platform developed by WRI, used in this paper for hydrological drought risk

Endnotes

1. The National Building Code of India (2016) is India's principal code for building planning, design, construction, and safety requirements. It also provides guidance on structural safety, fire protection, disaster resilience, and building services (BIS 2016c).

2. The BIS Standards for Hazard-Resistant Design are a set of technical standards developed by the BIS covering the design and construction of structures resistant to hazards such as earthquakes, wind, and other environmental stresses (BIS 2015, 2016a, 2016b).

3. The BMTPC Vulnerability Atlas of India is a national spatial planning resource that maps district-level vulnerability to earthquakes, cyclones, floods, and other hazards to support safer siting, planning, and construction practices (BMTPC 2019).

4. Disaster management plans by the National Disaster Management Authority (NDMA) constitute national disaster management guidelines and planning frameworks that support disaster risk reduction, preparedness, response, recovery, and resilience building across sectors and government levels (NDMA 2019).

5. The Urban and Regional Development Plan Formulation and Implementation Guidelines provide a framework for integrating land-use planning, infrastructure development, environmental considerations, and disaster risk reduction into urban and regional planning processes (Ministry of Urban Development 2015).

6. For more details on national building codes, structural design, see the BIS website https://www.bis.gov.in/?lang=en.

References

Adil, L., D. Eckstein, V. Künzel, and L. Schäfer. 2025. *Climate Risk Index 2025: Who Suffers Most from Extreme Weather Events?* Bonn: Germanwatch e.V.

Adshead, D., A. Paszkowski, S.S. Gall, A.M. Peard, M.S.G. Adnan, J. Verschuur, and J.W. Hall. 2024. "Climate Threats to Coastal Infrastructure and Sustainable Development Outcomes." *Nature Climate Change* 14 (4): 344–52. https://doi.org/10.1038/s41558-024-01950-2.

Agrawal, N., L. Gupta, J. Dixit, and S.K. Dash. 2021. "An Integrated Assessment of Seismic Hazard Exposure and its Societal Impact in Seven Sister States of North Eastern Region of India for Sustainable Disaster Mitigation Planning." Research Square. https://doi.org/10.21203/rs.3.rs-1003515/v1.

Ahmad, N., and Q. Hassan. 2025. "Ecosystem Services Linked to Nature-Based Solutions for Resilient and Sustainable Cities in India." *Frontiers in Water* 6 (January): 1504492. https://doi.org/10.3389/frwa.2024.1504492.

Alam, M.K., S. Dasgupta, A. Barua, and N.H. Ravindranath. 2022. "Assessing Climate-Relevant Vulnerability of the Indian Himalayan Region (IHR): A District-Level Analysis." *Natural Hazards* 112 (2): 1395–421. https://doi.org/10.1007/s11069-022-05233-x.

Amarnath, G., U.A. Amarasinghe, and N. Alahacoon. 2021. "Disaster Risk Mapping: A Desk Review of Global Best Practices and Evidence for South Asia." *Sustainability* 13 (22): 12779. https://doi.org/10.3390/su132212779.

Bandyopadhyay, S., S. Dasgupta, Z.H. Khan, and D. Wheeler. 2021. "Spatiotemporal Analysis of Tropical Cyclone Landfalls in Northern Bay of Bengal, India and Bangladesh." *Asia-Pacific Journal of Atmospheric Sciences* 57 (4): 799–815. https://doi.org/10.1007/s13143-021-00227-4.

Beccari, Benjamin. 2016. "A Comparative Analysis of Disaster Risk, Vulnerability and Resilience Composite Indicators." *PLoS Currents*, ahead of print. https://doi.org/10.1371/currents.dis.453df025e34b682e9737f95070f9b970.

Boragapu, Raja, Pulak Guhathakurta, and O. P. Sreejith. 2023. "Tropical Cyclone Vulnerability Assessment for India." *Natural Hazards* 117 (3): 3123–43. https://doi.org/10.1007/s11069-023-05980-5.

Building Materials and Technology Promotion Council (BMTPC). 2019. *Vulnerability Atlas of India. 3rd ed.* New Delhi: BMTPC, Ministry of Housing and Urban Affairs, Government of India.

Bureau of Indian Standards (BIS). 2015. *IS 875 (Part 3): 2015: Design Loads (Other than Earthquake) for Buildings and Structures—Code of Practice, Part 3: Wind Loads*. New Delhi: Bureau of Indian Standards.

Bureau of Indian Standards (BIS). 2016a. *IS 1893 (Part 1):2016: Criteria for Earthquake Resistant Design of Structures—Part 1: General Provisions and Buildings.* New Delhi: Bureau of Indian Standards.

Bureau of Indian Standards (BIS). 2016b. *IS 13920:2016: Ductile Design and Detailing of Reinforced Concrete Structures Subjected to Seismic Forces—Code of Practice.* New Delhi: Bureau of Indian Standards.

Bureau of Indian Standards (BIS). 2016c. *National Building Code of India 2016 (SP 7: 2016)*. New Delhi: Bureau of Indian Standards.

Cecil, D. 2025. (Dataset.) LIS/OTD 0.5 *Degree High Resolution Full Climatology (HRFC).* NASA Global Hydrometeorology Resource Center Distributed Active Archive Center. https://doi.org/10.5067/LIS/LIS-OTD/DATA302.

Central Ground Water Board (CGWB). 2021. *National Compilation on Dynamic Ground Water Resources of India, 2020.* Faridabad: Department of Water Resources, River Development and Ganga Rejuvenation, Ministry of Jal Shakti, Government of India.

Chakraborty, R., A. Chakraborty, G. Basha, and M.V. Ratnam. 2021. "Lightning Occurrences and Intensity over the Indian Region: Long-Term Trends and Future Projections." *Atmospheric Chemistry and Physics* 21 (14): 11161–77. https://doi.org/10.5194/acp-21-11161-2021.

Chamberlain, E.L., S.L. Goodbred, M.S. Steckler, J. Wallinga, T. Reimann, S.H. Akhter, R. Bain, G. Muktadir, A. Al Nahian, F.M. Arifur Rahman, M. Rahman, L. Seeber, and C. von Hagke. 2024. "Cascading Hazards of a Major Bengal Basin Earthquake and Abrupt Avulsion of the Ganges River." *Nature Communications* 15 (1): 4975. https://doi.org/10.1038/s41467-024-47786-4.

Chauhan, V., L. Gupta, and J. Dixit. 2025. "Machine Learning and GIS-Based Multi-Hazard Risk Modeling for Uttarakhand: Integrating Seismic, Landslide, and Flood Susceptibility with Socioeconomic Vulnerability." *Environmental and Sustainability Indicators* 26 (June): 100664. https://doi.org/10.1016/j.indic.2025.100664.

Chuphal, D.S., A.P. Kushwaha, S. Aadhar, and V. Mishra. 2024. "Drought Atlas of India, 1901–2020." *Scientific Data* 11 (1): 7. https://doi.org/10.1038/s41597-023-02856-y.

Climate Prediction Group, India Meteorological Department. n.d. "Yearly Gridded Rainfall (0.25 x 0.25) data NetCDF File." https://www.imdpune.gov.in/cmpg/Griddata/Rainfall_25_NetCDF.html. Accessed August 31, 2026.

Copernicus. n.d. "GHSL Datasets Information." https://human-settlement.emergency.copernicus.eu/datasets.php. Accessed August 29, 2026.

Copernicus Climate Change Service, Climate Data Store. 2023. "ERA5 Hourly Data on Single Levels from 1940 to Present." https://doi.org/10.24381/cds.adbb2d47.

Dasgupta, S., A. Barua, I. K. Murthy, P. L. Borgohain, T. Baghel, P. Sankhyayan, Vidya S., et al. 2024. *District-Level Climate Risk Assessment for India: Mapping Flood and Drought Risks Using IPCC Framework*. Department of Science and Technology, Government of India, and Swiss Agency for Development and Cooperation.

Dash, S., T.U. Sreya, and R. Maity. 2024. "Changes in the Spatial Variability of Extreme Precipitation Characteristics across Peninsular India." *Discover Geoscience* 2 (1): 17. https://doi.org/10.1007/s44288-024-00019-z.

Debnath, R., R. Bardhan, and M.L. Bell. 2023. "Lethal Heatwaves are Challenging India's Sustainable Development." *PLOS Climate* 2 (4): e0000156. https://doi.org/10.1371/journal.pclm.0000156.

Dodman, D., B. Hayward, M. Pelling, V. Castan Broto, W. Chow, E. Chu, R. Dawson, L. Khirfan, T. McPhearson, A. Prakash, Y. Zheng, and G. Ziervogel. 2022. "Cities, Settlements and Key Infrastructure." In *Climate Change 2022: Impacts, Adaptation and Vulnerability.* Contribution of Working Group II to the Sixth Assessment Report of the Intergovernmental Panel on Climate Change, edited by H.-O. Pörtner, D.C. Roberts, M. Tignor, E.S. Poloczanska, K. Mintenbeck, A. Alegría, M. Craig, S. Langsdorf, S. Löschke, V. Möller, A. Okem, and B. Rama, 907–1040. Cambridge, UK, and New York: Cambridge University Press. https://doi.org/10.1017/9781009325844.008.

Dutta, D., V.V. Srinivas, and G. Bala. 2025. "Disparity in Spatiotemporal Variability and Risk of Compound Coastal Extremes between India's East-West Coasts." *Npj Climate and Atmospheric Science* 8 (1): 168. https://doi.org/10.1038/s41612-025-01045-5.

Earthdata. n.d. "ASF DAAC: Alaska Satellite Facility Distributed Active Archive Center." https://www.earthdata.nasa.gov/centers/asf-daac. Accessed August 30, 2026.

Gill, J.C., and B.D. Malamud. 2016. "Hazard Interactions and Interaction Networks (Cascades) within Multi-Hazard Methodologies." *Earth System Dynamics* 7 (3): 659–79. https://doi.org/10.5194/esd-7-659-2016.

Hallegatte, S., J. Rentschler, and J. Rozenberg. 2019. *Lifelines: The Resilient Infrastructure Opportunity. Sustainable Infrastructure Series.* Washington, DC: World Bank. https://doi.org/10.1596/978-1-4648-1430-3.

Herrmann Lunecke, M.G. 2015. "Urban Planning and Tsunami Impact Mitigation in Chile after February 27, 2010." *Natural Hazards* 79 (3): 1591–620. https://doi.org/10.1007/s11069-015-1914-4.

Hess, J.J., Sathish L.M., K. Knowlton, S. Saha, P. Dutta, P. Ganguly, A. Tiwari, A. Jaiswal, P. Sheffield, J. Sarkar, S.C. Bhan, A. Begda, T. Shah, B. Solanki, and D. Mavalankar. 2018. "Building Resilience to Climate Change: Pilot Evaluation of the Impact of India's First Heat Action Plan on All-Cause Mortality." *Journal of Environmental and Public Health* 2018 (November): 7973519. https://doi.org/10.1155/2018/7973519.

Ho, K.K.S., R.W.M. Cheung, and C.Y.S. Wong. 2016. "Managing Landslide Risk Systematically Using Engineering Works." *Proceedings of the Institution of Civil Engineers - Civil Engineering* 169 (6): 25–34. https://doi.org/10.1680/jcien.15.00079.

Hofste, Rutger Willem, Samantha Kuzma, Sara Walker, Edwin H. Sutanudjaja, Marc F. P. Bierkens, Marijn J. M. Kuijper, Marta Faneca Sanchez, et al. 2019. Aqueduct 3.0: *Updated Decision-Relevant Global Water Risk Indicators.* Technical Note. Washington, DC: World Resources Institute. DOI 10.46830/writn.18.00146.Hussain, S., E.

Hussain, P. Saxena, A. Sharma, P. Thathola, and S. Sonwani. 2024. "Navigating the Impact of Climate Change in India: A Perspective on Climate Action (SDG13) and Sustainable Cities and Communities (SDG11)." *Frontiers in Sustainable Cities* 5 (January): 1308684. https://doi.org/10.3389/frsc.2023.1308684.

International Labour Organization. 2019. *Working on a Warmer Planet: The Impact of Heat Stress on Labour Productivity and Decent Work.* Geneva: International Labour Organization. https://www.ilo.org/sites/default/files/wcmsp5/groups/public/@dgreports/@dcomm/@publ/documents/publication/wcms_711919.pdf.

India Meteorological Department (IMD). 2022. *Climate Hazards and Vulnerability Atlas of India.* Ministry of Earth Sciences, Government of India.

Indian National Centre for Ocean Information Services (INCOIS). n.d. "Tsunami Modelling." Indian Tsunami Early Warning System, Ministry of Earth Sciences, Government of India. Accessed September 14, 2026.

IPCC (Intergovernmental Panel on Climate Change). 2022. *Climate Change 2022: Mitigation of Climate Change.* Contribution of Working Group III to the Sixth Assessment Report of the Intergovernmental Panel on Climate Change, edited by P.R. Shukla, J. Skea, R. Slade, R. Fradera, M. Pathak, A. Al Khourdajie, M. Belkacemi, R. van Diemen, A. Hasija, G. Lisboa, S. Luz, J. Malley, D. McCollum, S. Some, and P. Vyas. Cambridge, UK, and New York: Cambridge University Press. https://doi.org/10.1017/9781009157926.

IPCC. 2023. *Climate Change 2022: Impacts, Adaptation and Vulnerability.* Contribution of Working Group II to the Sixth Assessment Report of the Intergovernmental Panel on Climate Change, edited by H.-O. Pörtner, D.C. Roberts, M. Tignor, E.S. Poloczanska, K. Mintenbeck, A. Alegría, M. Craig, S. Langsdorf, S. Löschke, V. Möller, A. Okem, and B. Rama. Cambridge, UK, and New York: Cambridge University Press. https://doi.org/10.1017/9781009325844.

Jain, G., and A.B. Bazaz. 2016. "Urban Risks and Resilience in India." *In Urban Policy Dialogues: Operationalising SDGs.* Bengaluru: Indian Institute for Human Settlements. https://doi.org/10.24943/updsdg2016_5.

Jain, S.K., M. Saharia, S.M. Bhallamudi, and L. Philip. 2025. "Climate Resilient Development for Sustainable Water Security for India." *Current Science* 128 (10): 969–86. http://doi.org/10.18520/cs/v128/i10/969-986.

Joshi, R., M. Saharia, I.A. Ahmed, N. Sharma, and G.V. Ramana. 2025. "Mapping Infrastructure Vulnerability to Landslides in India Using High-Resolution Geospatial Data." *Natural Hazards* 121 (10): 11663–93. https://doi.org/10.1007/s11069-025-07256-6.

Kalaiarasi, K.S., K. Singh, and N. Kannangara. 2023. "Mapping India's Exposure to Climate Change: A District Level Study." *Current Science* 125 (2): 124–29. https://doi.org/10.18520/cs/v125/i2/124-129.

Kantamaneni, K., S. Panneer, A. Krishnan, S. Shekhar, L. Bhat, A. K.R., and L. Rice. 2022. "Appraisal of Climate Change and Cyclone Trends in Indian Coastal States: A Systematic Approach towards Climate Action." *Arabian Journal of Geosciences* 15 (9): 814. https://doi.org/10.1007/s12517-022-10076-8.

Kappes, M.S., M. Keiler, K. von Elverfeldt, and T. Glade. 2012. "Challenges of Analyzing Multi-Hazard Risk: A Review." *Natural Hazards* 64 (2): 1925–58. https://doi.org/10.1007/s11069-012-0294-2.

Khan, I., H. Bahuguna, A. Kainthola, R. Ahmed, and M.S. Asgher. 2025. "National-Scale Landslide Susceptibility and Risk Mapping of India Using a Hybrid Data-Driven Approach." *Scientific Reports* 16 (1): 3519. https://doi.org/10.1038/s41598-025-33446-0.

Kodandapani, N. 2021. "Adapting to Climatic Extremes through Climate Resilient Industrial Landscapes: Building Capacities in the Southern Indian States of Telangana and Andhra Pradesh." In *Climate Change in Asia and Africa - Examining the Biophysical and Social Consequences, and Society's Responses,* edited by J.P. Tiefenbacher, Chap. 12. IntechOpen. https://doi.org/10.5772/intechopen.98732.

Kumar, P., and A. Chakraborty. 2025. "Comparative Analysis of Heatwaves and Heat Stress in Six Climatic Zones of India Based on Observed Data." *Results in Earth Sciences* 3 (December): 100076. https://doi.org/10.1016/j.rines.2025.100076.

Mahato, P., S. Srivastava, S. Jogi, and S. Pandey. 2025. "Multi-Hazard Risk Unveiled: Pioneering Techniques for Comprehensive Risk Analysis and Mitigation." *Operations Research Forum* 6 (1): 19. https://doi.org/10.1007/s43069-024-00407-8.

Mahvash Mohammadi, Z., and N. Barakpour. 2024. "Confronting the Effects of Climate Change through Development Plans." *Discover Environment* 2 (1): 84. https://doi.org/10.1007/s44274-024-00124-3.

Maly, E., and A. Suppasri. 2020. "The Sendai Framework for Disaster Risk Reduction at Five: Lessons from the 2011 Great East Japan Earthquake and Tsunami." *International Journal of Disaster Risk Science* 11 (2): 167–78. https://doi.org/10.1007/s13753-020-00268-9.

Mani, S., S. Ghosh, and R. Srinivasan. 2021. "Water Stress and the Effective Management of Water in the Healthcare Sector." *In Climate Change and the Health Sector,* edited by A. Thomas, K.S. Reddy, D. Alexander, and P. Prabhakaran, 149–59. New Delhi: Routledge India. https://doi.org/10.4324/9781003190516-19.

Mathews, Rejeet, Amitabh Kundu, Paramjeet Chawla, Tintu Sebastian, Raj Bhagat Palanichamy, and Madhav Pai. 2023. "Morphology of Delhi National Capital Region's Economic Geography and Its Implications for Planning." World Resources Institute. https://doi.org/10.46830/wrirpt.22.00042.

Mohanty, Abinash, and Shreya Wadhawan. 2021. *Mapping India's Climate Vulnerability: A District-Level Assessment.* New Delhi: Council on Energy, Environment and Water.

Ministry of Jal Shakti, Government of India. n.d. *India Water Resources Information System.* https://web.archive.org/web/20220122172156/https://indiawris.gov.in/wris/. Accessed January 31, 2022.

Ministry of Statistics and Programme Implementation, Government of India. 2019. *Sixth Economic Census 2013-14*, March 26. https://microdata.gov.in/NADA/index.php/catalog/47.

Ministry of Statistics and Programme Implementation, Government of India. 2025. *EnviStats India 2025: Environment Statistics.* https://www.mospi.gov.in/publications-reports/innerpage/414.

Ministry of Urban Development. 2015. *Urban and Regional Development Plans Formulation and Implementation (URDPFI) Guidelines: Volume II A and II B – Appendices to URDPFI Guidelines, 2014.* New Delhi: Town and Country Planning Organisation.

Mishra, J., and A. Verma. 2024. "Balancing Growth and Sustainability: Environmental Diplomacy as the Key to India's Climate Future." *International Journal for Research in Applied Science and Engineering Technology* 12 (3): 1276–84. https://doi.org/10.22214/ijraset.2024.59049.

Mohanty, A. 2020. *Preparing India for Extreme Climate Events: Mapping Hotspots and Response Mechanisms.* New Delhi: Council on Energy, Environment and Water. https://www.ceew.in/publications/preparing-india-for-extreme-climate-change-events-and-weather-conditions.

NASA (National Aeronautics and Space Administration). 2017. "Global Landslide Model." https://web.archive.org/web/20191021064313/https://pmm.nasa.gov/applications/global-landslide-model.

National Disaster Management Authority (NDMA). 2019. *National Disaster Management Plan 2019*. New Delhi: Government of India.

National Remote Sensing Centre (NRSC). 2023. *Glacial Lake Atlas of Indian Himalayan River Basins.* Hyderabad: NRSC, Indian Space Research Organisation.

OECD, European Union, and Joint Research Centre - European Commission. 2008. *Handbook on Constructing Composite Indicators: Methodology and User Guide*. OECD. https://doi.org/10.1787/9789264043466-en.

Pandey, V.V., K.M. Singh, N. Ahmad, and S.K. Srivastava. 2022. "Challenges and Issues of Groundwater Management in India." *Current Science* 123 (7): 856–64. https://doi.org/10.18520/cs/v123/i7/856-864.

Pathak, Lalit, Badri Baral, Kamana Joshi, Dipak Raj Basnet, and Danilo Godone. 2025. "Landslides in the Himalayas: The Role of Conditioning Factors and Their Resolution in Susceptibility Mapping." *Geosciences* 15 (4): 131. https://doi.org/10.3390/geosciences15040131.

Pesaresi, Martino, and Panagiotis Politis. 2023. *GHS-BUILT-S R2023A—GHS Built-up Surface Grid, Derived from Sentinel2 Composite and Landsat, Multitemporal* (1975–2030). European Commission, Joint Research Centre

Pourghasemi, H.R., S. Pouyan, M. Bordbar, and J.J. Clague. 2022. "Environmental Multi-Hazard Assessment and its Importance Role in Land Use Planning and Hazard Management." Research Square, September 7. https://doi.org/10.21203/rs.3.rs-2022191/v1.

Prasad, P., V.J. Loveson, S. Mandal, P. Chandra, and L.C. Kulimushi. 2023. "Multi-Resource Potentiality and Multi-Hazard Susceptibility Assessments of the Central West Coast of India Applying Machine Learning and Geospatial Techniques." *Environmental Earth Sciences* 82 (9): 226. https://doi.org/10.1007/s12665-023-10901-7.

Raduszynski, T., and M. Numada. 2023. "Measure and Spatial Identification of Social Vulnerability, Exposure and Risk to Natural Hazards in Japan Using Open Data." *Scientific Reports* 13 (1): 664. https://doi.org/10.1038/s41598-023-27831-w.

Ranjan, R., and S. Karmakar. 2024. "Compound Hazard Mapping for Tropical Cyclone-Induced Concurrent Wind and Rainfall Extremes over India." *Npj Natural Hazards* 1 (1): 15. https://doi.org/10.1038/s44304-024-00013-y.

Rawat, S., A. Ganapathy, and A. Agarwal. 2022. "Drought Characterization over Indian Sub-Continent Using GRACE-Based Indices." *Scientific Reports* 12 (1): 15432. https://doi.org/10.1038/s41598-022-18511-2.

Ray, K., R.K. Giri, S.S. Ray, A.P. Dimri, and M. Rajeevan. 2021. "An Assessment of Long-Term Changes in Mortalities Due to Extreme Weather Events in India: A Study of 50 Years' Data, 1970–2019." *Weather and Climate Extremes* 32 (June): 100315. https://doi.org/10.1016/j.wace.2021.100315.

Roy, T., and V. Matsagar. 2021. "Multi-Hazard Analysis and Design Guidelines: Recommendations for Structure and Infrastructure Systems in the Indian Context." *Current Science* 121 (1): 44–55. https://doi.org/10.18520/cs/v121/i1/44-55.

Rusk, Jack, Amina Maharjan, Prakash Tiwari, et al. 2022. "Multi-Hazard Susceptibility and Exposure Assessment of the Hindu Kush Himalaya." *Science of The Total Environment* 804 (January): 150039. https://doi.org/10.1016/j.scitotenv.2021.150039.

Sahana, Venkataswamy, and Arpita Mondal. 2023. "Evolution of Multivariate Drought Hazard, Vulnerability and Risk in India under Climate Change." *Natural Hazards and Earth System Sciences* 23 (2): 623–41. https://doi.org/10.5194/nhess-23-623-2023.

Sahoo, B., and P.K. Bhaskaran. 2018. "Multi-Hazard Risk Assessment of Coastal Vulnerability from Tropical Cyclones – A GIS Based Approach for the Odisha Coast." *Journal of Environmental Management* 206 (January): 1166–78. https://doi.org/10.1016/j.jenvman.2017.10.075.

Santra, M., C.S. Dwivedi, and D. Mitra. 2025. "Modeling Coastal Vulnerability in the Indian Sundarban under Possible Shared Socioeconomic Pathways (SSPs)." *Regional Studies in Marine Science* 89 (December): 104273. https://doi.org/10.1016/j.rsma.2025.104273.

Sarif, N., A.H.S.A. Kumar, P. Barman, M.J. Rana, and S. Saha. 2024. "Measuring Hazard-Free Improved Shelter across the Regions of India." *Natural Hazards* 120 (7): 6533–49. https://doi.org/10.1007/s11069-024-06522-3.

Schiavina, Marcello, Sergio Freire, Alessandra Carioli, and Kytt MacManus. 2023. *GHS-POP R2023A—GHS Population Grid Multitemporal* (1975–2030). European Commission, Joint Research Centre.

Sebastian, T., R. Mathews, R.B. Palanichamy, A. S., and P. Chawla. 2026. "Verticality and Horizontal Growth Trends across 3,777 Indian Cities: Examining Built-Up Area Growth in Cities and their Peri-Urban Areas from 1990–2020, its Administrative Realities, and Implications for Planning and Governance." Working Paper. Mumbai: WRI India.

Shahi, N.K., and S. Rai. 2023. "An Increase in Widespread Extreme Precipitation Events during the Northeast Monsoon Season over South Peninsular India." *Scientific Reports* 13 (1): 22757. https://doi.org/10.1038/s41598-023-50324-9.

Singh, G., S. Kumar, R. Karmakar, and A.K. Mishra. 2025. "Rapid Assessment of Landslide Exposure to Elements at Risk for Decision Support in Regional Landslide Forecasting." *Discover Geoscience* 3 (1): 181. https://doi.org/10.1007/s44288-025-00299-z.

Stanley, T., D.B. Kirschbaum. 2017. "A Heuristic Approach to Global Landslide Susceptibility Mapping." *Natural Hazards* 87 (February), 145–64. https://doi.org/10.1007/s11069-017-2757-y.

Swann, S., L. Blandford, S. Cheng, J. Cook, A. Miller, and R. Barr. 2021. "Public International Funding of Nature-Based Solutions for Adaptation: A Landscape Assessment." Working Paper. Washington, DC: World Resources Institute. https://doi.org/10.46830/wriwp.20.00065.

Thomas, V. 2017. *Climate Change and Natural Disasters: Transforming Economics and Policies for a Sustainable Future.* Oxon, UK, and New York: Routledge. https://doi.org/10.4324/9781315081045.

Ul Zaman, M., and B.A. Pandit. 2023. "Assessing the Impact of Climate Variability on Water Resources in Kashmirs Himalayan Landscape." *International Journal for Research in Applied Science and Engineering Technology* 11 (12): 1888–93. https://doi.org/10.22214/ijraset.2023.57734.

UNDRR (United Nations Office for Disaster Risk Reduction). 2022. *Global Assessment Report on Disaster Risk Reduction 2022: Our World at Risk: Transforming Governance for a Resilient Future. Global Assessment Report on Disaster Risk Reduction (GAR) Series.* Geneva: UNDRR. https://www.undrr.org/media/79595/download?startDownload=20260829.

United Nations Economic and Social Commission for Asia and the Pacific (ESCAP). 2019. *The Disaster Riskscape across Asia-Pacific: Pathways for Resilience, Inclusion and Empowerment. Asia-Pacific Disaster Report 2019*. Bangkok: United Nations.

US Environmental Protection Agency (EPA). 2024. *Final Updates to the Air Quality Index (AQI) for Particulate Matter: Fact Sheet and Common Questions*. Washington, DC: EPA.

Van Donkelaar, A., M.S. Hammer, L. Bindle, M. Brauer, J.R. Brook, M.J. Garay, N.C. Hsu, O.V. Kalashnikova, R.A. Kahn, C. Lee, R.C. Levy, A. Lyapustin, A.M. Sawyer, and R.V. Martin. 2024. (Dataset.) *Global Annual PM2.5 Grids from MODIS, MISR, SeaWiFS and VIIRS Aerosol Optical Depth (AOD), 1998-2022, V5.GL.04 (Version 5.04).* Palisades, NY: NASA Socioeconomic Data and Applications Center (SEDAC). https://doi.org/10.7927/AS2R-9P42.

Washington University in St. Louis. 2026. "SatPM2.5 (Satellite-derived PM2.5)." https://sites.wustl.edu/acag/surface-pm2-5/.

Wasson, R.J., V. Jain, A. Katuri, S. Lahiri, S. Parkash, A.K. Singhvi, N. Varma, P. Bansal, and C.J. Chuah. 2018. "Riverine Flood Hazard: Part B. Disaster Risk Reduction in India." *Proceedings of the Indian National Science Academy* 85 (1): 65–76. https://doi.org/10.16943/ptinsa/2018/49502.

Williams, D.S., M.M. Costa, C. Sutherland, L. Celliers, and J. Scheffran. 2019. "Vulnerability of Informal Settlements in the Context of Rapid Urbanization and Climate Change." *Environment and Urbanization* 31 (1): 157–76. https://doi.org/10.1177/0956247818819694.

World Bank. 2011. *Guide to Climate Change Adaptation in Cities.* Washington, DC: World Bank. https://doi.org/10.1596/27396.

World Bank. 2025. *Towards Resilient and Prosperous Cities in India.* Washington, DC: World Bank.

World Economic Forum. 2024. *The Global Risks Report 2024 19th Edition: Insight Report.* Geneva: World Economic Forum. https://www3.weforum.org/docs/WEF_The_Global_Risks_Report_2024.pdf.

WRI (World Resources Institute). n.d. "Aqueduct: Data." https://www.wri.org/aqueduct/data. Accessed August 30, 2026.

WRI. 2019. "Aqueduct 3.0: Updated Decision-Relevant Global Water Risk Indicators," August 6. https://www.wri.org/research/aqueduct-30-updated-decision-relevant-global-water-risk-indicators.

Acknowledgments

We are deeply grateful to all those who contributed to the development of this research. We would first like to thank our colleagues at the World Resources Institute (WRI) who provided valuable insights, guidance and expertise throughout the research and writing process. In particular, we thank Gregory Taff, Sudeshna Chatterjee, Benita Nathania, Ted Wong and Lubaina Rangwala for their review and feedback. We also thank Madhav Pai, Jaya Dhindaw, and Manu V. Mathai for their support and guidance throughout the course of this research.

We are also grateful to our external reviewers, Poonam Pillai (Senior Urban Specialist, World Bank) and Dr. S. M. Kirthiga (Senior Hydromodeler, Integrated Flood Management Centre, TN Disaster Risk Reduction Agency (TNDRRA)), for their detailed internal review and feedback, which helped strengthen the framing, methodology, analysis, and presentation of the working paper. While our reviewers and colleagues were generous with their time, expertise, and feedback, this working paper reflects the views of the authors alone, and any errors or shortcomings remain our own.

We thank Purva Sharma and Robin Infant Raj Devadoss from the Research Integrity (RI) team at WRI. We also thank Aishwarya Murugananthan (Associate, Research [Urban], Centre for Public Policy Research) for her contribution to secondary literature review. We also thank Cactus team for the copyediting support, our colleagues Ankita Rajeshwari, Debarpan Das and, Safa Fathim for the design and layout. We thank Debarpan Das and Romain Warnault at WRI for coordinating the final production review.

About the authors

Sweeta Sumant is Senior Program Associate, Integrated Urban Development, Sustainable Cities & Transport program, at WRI India
Contact: sweeta.sumant@wri.org

Raj Bhagat Palanichamy is Senior Program Manager, Geo Analytics, Sustainable Cities & Transport program at WRI India
Contact: rajbhagat.p@wri.org

Rejeet Mathews is Program Director, Integrated Urban Development, Sustainable Cities & Transport program, at WRI India
Contact: rejeet.mathews@wri.org

Harsha K is Program Associate, Geo Analytics, Sustainable Cities & Transport program at WRI India
Contact: harsha.k@wri.org

Paramjeet Chawla is Senior Program Manager, Integrated Urban Development, Sustainable Cities & Transport program, at WRI India
Contact: paramjeet.chawla@wri.org

Neha Lal is Senior Program Manager, Integrated Urban Development, Sustainable Cities & Transport program, at WRI India
Contact: neha.lal@wri.org

About WRI India

WRI India, an independent knowledge organisation registered as India Resources Trust, provides objective information and practical proposals to foster environmentally sound and socially equitable development. Through research, analysis, and recommendations, WRI India puts ideas into action to build transformative solutions to protect the earth, promote livelihoods, and enhance human well-being.

Know more: wri-india.org

creative commons

Copyright 2026 WRI India. This work is licensed under the Creative Commons Attribution-NonCommercial-NoDerivatives 4.0 International License. To view a copy of this license, visit https://creativecommons.org/licenses/by-nc-nd/4.0/